Deposition of Fine and Coarse Grain Sediments Along Two Reaches of the Northwest Branch Anacostia River

Matthew Kraham

Advisor: Dr. Karen Prestegaard

November 29th, 2021

Geol 394

Abstract.

Stream Sediment transport rates are controlled by both sediment supply and stream hydraulics. Stream channelization can protect banks from erosion, but straight, uniform channels provide few sites for channel or over bank storage. Sediment in alluvial reaches can be stored on point bars, central bars, and on floodplains as water velocity and shear stress are low in these locations. Sediment bars may grow in size and become more stable over time or may be eroded by subsequent high flows. Mobilized sediment will be transported down river. In channelized reaches, sediment is funneled downstream and sediment storage is less likely to occur. Sediment in a channelized reach are typically deposited as overbank deposit only during major flood events when discharge floods out overbank. In this study, data were gathered from two reaches of the lower NW Anacostia River. The upstream alluvial reach is meandering, and the downstream reach is a straightened and leveled flood control channel. The project was designed to evaluate hydraulic conditions for sediment entrainment and deposition. To gather this information, I sampled and analyzed by sieves and pebble counts the grain size of surface and subsurface sediment at three different locations along the sediment bars in each of the two reaches prior to predicted a storm events. Sediment mobilization was determined by marking and tracing surface particles to determine whether particles were transported down river, replaced by new sediment, or buried by new sediment. Sediment tracing was conducted by spray-painting stripes on surface particles on 2 central bars along with 2-point bars in both of the reaches to understand what is occurring. Sediment movement is analyzed along with hydraulic data to determine critical shear stresses for the initiation of movement of sediment. Both reaches showed high mobility of bed sediment, but only the alluvial reach indicated significant bar storage and channel change. From this, I predict that bars in the alluvial reach will grow or maintain their sediment, but the channelized reach will experience replacement of bed material with little to no sediment build-up due to the funneling nature of the river.

The varying grain sizes along the point bars and central bars help us understand what is being transported. For the pebble count we looked at 12 different sizes ranging from < 2 – 90 mm. After gathering the data from both the central bar and point bar we did the same at the other reach. I have collected data from three dates in 2021, March 24th , September 1st, and September 21st . The alluvial reach of the Anacostia River provided early evidence that sediment in that region can be transported at lower shear stresses than that of the channelized reach, but the channelized reach experienced higher shear stresses for the same storm events. If there is a high outflow of sediment in the upper reach of the alluvial but not a high inflow of sediments in the channelized reach, we need to figure out where the missing sediment is deposited. The rapid channel changes in the upstream reaches suggest much of the coarse sediment is going into sediment storage, but significant amounts are settling out of suspension in the downstream estuary.

Table of Contents.

I. Introduction

Significance……..…3

Hypotheses……...4

Previous Work……..4

II. Methodology

Site Locations and Characteristics.....6

Grain Size Masurementss.....7

Particle Tracer Experiments.....8

Selection of Study Sites for Particle Tracer Experiments....10

Particle Tracer.....11

Measurement of flood Flow Depth Over the Top of the Bars at each stripe l*ocation*.....12

Uncertainty.....12

III. Results

Morphological Data.....12

Subsurface Grain Size Distributions.....13

Transported Particle Size Data.....14

Particle Transport Distance Data.....15

Relationship between Di/D50 and t for Each Particle Moved*.....17

Sediment differences between the two reaches.....18

Initiation of Sediment transport of Alluvial and Channelized Reaches.....18

Is Sediment Easier to Transport between Alluvial or Channelized Reach.....19

Does the Complex Nature of the Alluvial Reach Allow for More deposition Compared to the Channelized Reach.....19

IV. Future Work

V. Conclusions

VI. Resources

VII. Appendix

I. Introduction.

Rivers transport sediment of a range of grain sizes. Fine sediment (sand, silt, and clay) is often moved as suspended load. Coarser sediment (sand, gravel, cobbles, and boulders), is transported as bedload and often creates the channel form (cross section and morphology). Sand-sized material can be carried as both bedload and suspended load, depending upon flow discharge and velocity. Recent research indicates that sand in gravel-bed streams can increase the mobility of the gravel fraction and that the transport produced from a bed of mixed grain sizes depends on the population of grains immediately available on the bed surface. (Wilcox et al., 2003). In gravel-bed streams, significant amounts of sand can be stored in the subsurface. The mobility of sand in the subsurface is regulated by the movement of the coarser surface material.

The differential movement of fine and coarse-grained sediment plays a significant role in the ever-changing nature of a river. Urbanization, which increases flood discharges has significant impacts on channel morphology. Many channels adjust to increase peak discharges by widening. Sediment supplied from channel widening or soil erosion can increase the sediment load of rivers. This sediment can be deposited locally or transported downstream.

Significance

The main impetus for this research is to determine where sediment deposition is occurring. A river will change anywhere from daily to annually but with the impacts of human development rivers have been changed to reduce the amount of erosion and flood control. Modifications to a channelized reach include adding boulders to the banks or concrete infrastructure. An example of this can be seen at one of our sites (Fig 1). With the modification of barriers to restrict flow, sediment is carried further downstream and potentially causes problems. A few examples would be clogging sewers, ditches, destroying wildlife, and obstructing waterways. We can see evidence of this near Bladensburg Harbor where they have to dredge the sediments being stored in the harbor. This material is expensive to move.

Figure 1: Channelized stretch of the Anacostia River with riprap placed on edges

Question: is the difference in storage of sand-sized sediment in the alluvial and channelized due to difference in sediment mobility or due to differences in channel morphology?

Hypotheses

a. The bed sediment in the channelized reach is mobilized at lower shear discharges and moves during more flow events than the alluvial reach.

b. In the alluvial reach, sand-sized sediment is deposited in the bed subsurface and on upper surfaces of point bars where it is mobilized only during major flow events. In the channelized reach of the river, sand is stored primarily in the subsurface due to the straightness of the channel and lack of bends where point bars form.

Previous Work

Bedload Transport Theory

Sediment on channel beds will move when the shear stress (force/area) exceeds the grain resisting forces, which is the immersed weight of the particles $(r_s\text{-}r_w)gD^3$ and the frictional resistance with other particles. For uniform channels, the bed stress is: $\underline{t = rg(A/P)\sin a.}$

Where (A/P) is area/perimeter = R (hydraulic radius). In wide channels, R ~ depth (d), and a is the water surface slope angle. Because river gradients are low, sina = tana = gradient. This simplifies the equation for fluid shear stress to:

$\underline{t = rgdS}$ where d can be taken to be the average depth (A/w) of the channel for cross sectional average shear stress or local depth for local shear stress. (Shields, did experiments that defined the ignition of motion for bedload. He defined dimensionless shear stress by setting a ratio of the fluid shear stress to the grain resisting forces. He did experiments with homogeneous sediment and assumed that frictional resistance (angle of internal friction) would constant:

$\underline{t^* = (rgds)/(rs\text{-}rw)gD}$

for flumes with homogeneous sediment, particles moved when the value of t* = 0.06. Shields called this value t*crit, critical dimensionless shear stress. Rivers do not have homogeneous sediment size. Sediment tends to be well-sorted. Gravel streams have a ratio of D_{84}/D_{50} , (std. dev./median) of ~2-2.5. Research on heterogeneous gravel bed streams indicates that the channel bed sediment will move when the D_{84} particle can move, which breaks up the channel bed . Although there is some suggestion "that coarser grains are less mobile than finer grains. The exponent is, however, so small that all sub pavement grain sizes are essentially rendered of equal mobility"(Parker and Klingeman, 1982). Therefore, many gravel-bed streams are stable for a range of flow rates but can move most of the particles on their beds at bankfull and higher flows. Due to the heterogeneity of particles, the critical dimensionless shear stress for the initiation of motion for these gravel beds is 0.045.

Research also indicates that sand in the bed can lower the critical dimensionless shear value required to move sediment (Wilcock,2003). The larger the amount of sand that is the channel bed, the lower the critical dimensionless shear stress required to move the gravel. But the "sand

in the subsurface cannot move until the surface particles move. The gravel bed then regulates the mobility of the subsurface sand" (Parker and Klingeman, 1982).

River channels that have sources of sand may have significantly different t^*_{crit} for gravel sediment for different events. Where the sand is stored also determines whether it will be accessible for transport during future events.

Meandering Rivers

Tight meander bends create eddies where suspended sediment can be deposited, even at high flows. The tightness of a meander bend can be measured as the Rc/width ratio. Sand that is transported as suspended sediment load can be on bank tops in straight reaches and on point bars in meandering reaches, point bar deposits are within the channel. Rivers are defined as meandering when the sinuosity is greater than 1.5. "reaches which have been called meanders are those in which the sinuosity, the ratio of thalweg length to valley length, is equal to or greater than 1.5. This value is an arbitrary one but, in our experience, where the sinuosity is 1.5 or greater, one would readily agree that the stream is a true meander" (Leopold and Wolman, 1957).

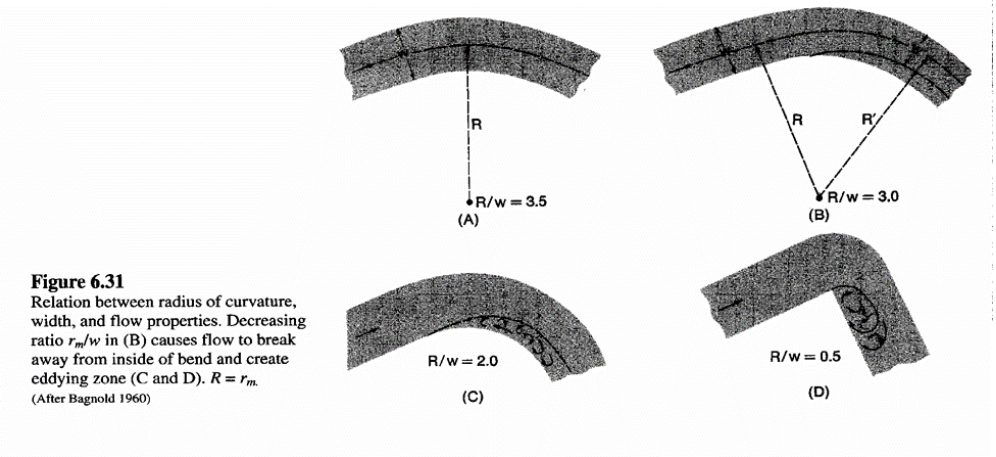

Figure 6.31
Relation between radius of curvature, width, and flow properties. Decreasing ratio r_m/w in (B) causes flow to break away from inside of bend and create eddying zone (C and D). $R = r_m$.
(After Bagnold 1960)

Figure 2: Previous Work on looking at the curvature of the river.

II. Methodology.

Site locations and Characteristics

When searching for the reaches of river that best exemplify a channelized reach and an alluvial reach, several sites were considered. To start, we began at the upper part of the 38th Avenue neighborhood park and then the Adelphi Manor Recreation Center. These two candidates both had the characteristics we were interested in. The 38th Avenue neighborhood park had a channelized reach in which human interference such as levees and flood walls has caused the river to become very straight and broad. The Adelphi Manor Recreation Center is situated along a meandering stretch of river with significant point bars along with central bars. Along these reaches I wanted to choose bars that exhibited similar bar morphologies in both types of reaches. If we chose similar bars, we should see similar data from them if they experience the same amount of rainfall and discharge.

An alluvial (non-channelized) and a nearby channelized reach of the Northwest Branch Anacostia River were selected for study. The alluvial reach is located near the Adelphi Manor Recreation Park and the channelized reach is located near 38th Avenue neighborhood park (Fig. 1). The two reaches have similar drainage basin areas, similar stream gradients, and similar channel widths. They have very different channel morphologies as seen in the pictures below.

Figure 3: Meandering Reach

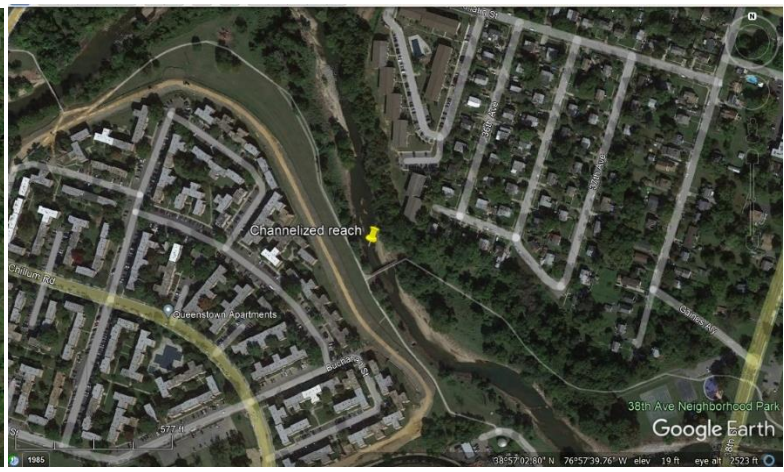

Figure 4: Channelized Reach

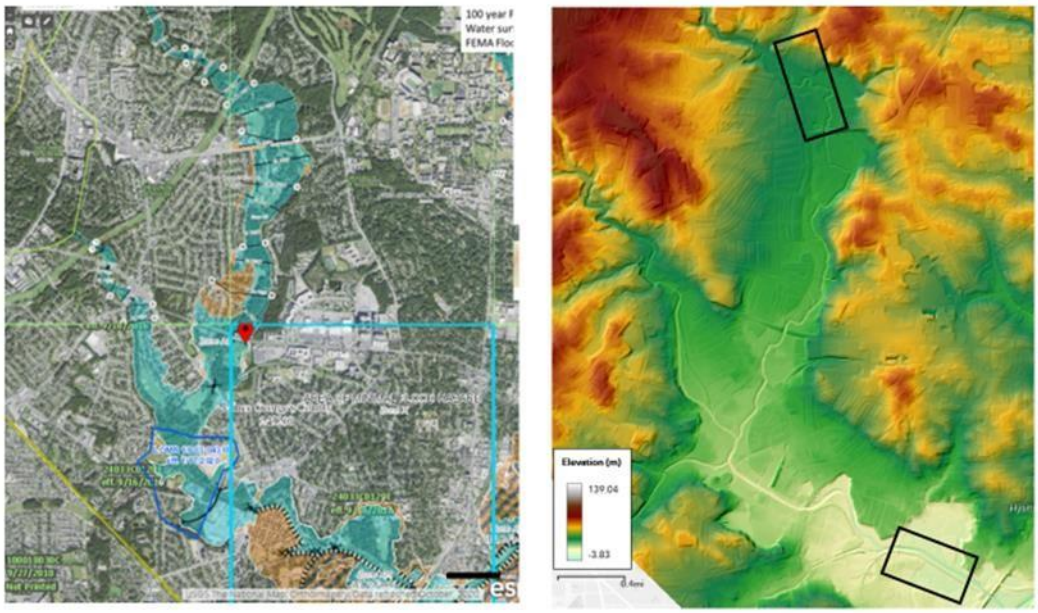

Figure 5: FEMA flood maps (left) and Maryland lidar data image (right) for high flow water surface gradient and bed gradient. FEMA map downloaded from: https://www.fema.gov/flood-maps

Grain Size Measurements:

Pebble counts were conducted in triplicate around a major bar in each location. This helps us understand the sizes of the pebbles around the particle tracers and helps us understand if the same size particles are moving in after a storm. For the pebble count we measured the intermediate width of a pebble and recorded the data. We did this for 100 pebbles along 3 different particle tracer lines. After gathering the data, we can then determine the D50 and D84 (std. deviation above the median) for the samples. With that data we can now calculate the critical shear stress which is the entrainment threshold and compare it to the actual values measured after transport events an example of a grain size distribution for Tree Bar (location on the alluvial reach) in the alluvial reach is shown in fig. 5 as both a histogram and cumulative grain size distribution.

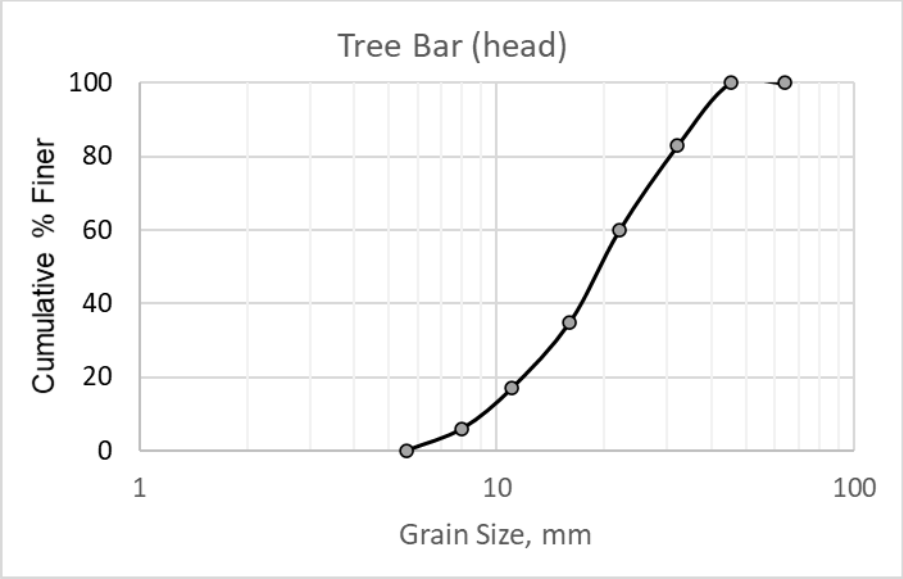

Figure 6: Cumulative graph of pebble count for alluvial reach

The grain sizes for the different reaches are expected to be the same but the systems will have different critical shear stress. Due to the Anacostia River being a straight channel the shear stress events are expected to happen at higher frequencies than the alluvial reach. We can see this in the graphs in the appendix as the graphs tend to have the same bell-shaped curve and 22 mm and 32 mm are the highest present pebble.

After collected data, we can understand what the D50 and D84 were for a storm event. D50 and D84 are the particle size distribution. At D84 is the size distribution of the particles. When D84 happens anything below it should be moved. In Fig 12 we can see that the D84 for is about 22 mm meaning anything below or at 22mm should be displaced.

Particle Tracer Experiments:

The channelized and alluvial reach particle tracers were spray painted onto the ground. At the two reaches two bars were chosen and 3 sites were chosen on each bar. At the three sites, we used spray paint to establish a layer of surface material that could be moved during a storm event. These particles allowed us to monitor if the sediment had stayed where it was, moved, or if new sediment had been deposited on top of it. If the particles have moved, then we can say that the mobility in this area is high during that storm event. If not, then we can say there has not been movement but if new sediment is stored on top of the line, then replacement material is coming from further upstream.

When seeing the movement of sediment, I decided to measure the distance of transport of the sediments from the line, the sizes of those particles, and to measure the new particles that got deposited on the line. I wanted to measure this way given that there might be trend in the amount of sediment moved and the sizes, and/- or the new particles that had moved in.

The particle tracers allow us to understand what the gradient and the depth of the water was during the flood maximum. For instance, on March 24th one of our lines remained untouched

as it was at a higher altitude than the other lines. With that understanding, we could conclude that the flood depth had to be around the height of the line.

Figure 7: Particle Tracers. Orange pebbles are the tracers.

Selection of Study Sites for Particle Tracer Experiments

Some of the criteria followed were that it would be best if we chose bars in which human interference was not likely. Human interference would occur when we painted the rocks, people would pick them up and displace them making it appear that the rocks had moved by natural phenomena but in actuality, they were disturbed due to humans. As a result, we chose bars that were further downstream and deeper in the woods or farther down a trail where the likely hood of someone interacting with our particle tracers is reduced.

The 2nd criterion that we took into consideration is if the bars would be able to show evidence of sediment movement. A bar can be unstable or stable resulting in significant amounts of fine- and coarse-grained material to be lost or gained. On the basis of this we found two bars on the alluvial reach and the channelized reach where this would not be a problem.

The 3rd criterion would be a stretch of river in which we could get discharge data along with criteria shear stress. The channelized stretch of river already had a USGS gauge in which we could gather this data for. However, the upper stretch of the alluvial reach did not have a gauge for us to collect data for. Due to this we decided it would still be a great spot and would get discharge data from subtracting Sligo Creek discharge from the Anacostia River to get the upstream discharge.

With these 3 criteria in place, we settled on a central bar and a point bar at the alluvial reach and the channelized reach. From the Adelphi Manor Recreation Center, we found bars in which human interaction would be minimal as well as bars that could show sediment movement. It is just to the right of the parking lot. At the channelized reach it was a little harder to find a spot in which human interaction would be at a minimum due to the amount of traffic that occurs on the side of the river. Just upstream of the 38th Avenue Neighborhood Park I was able to find a spot in which human interaction would be limited and was fit for sediment movement.

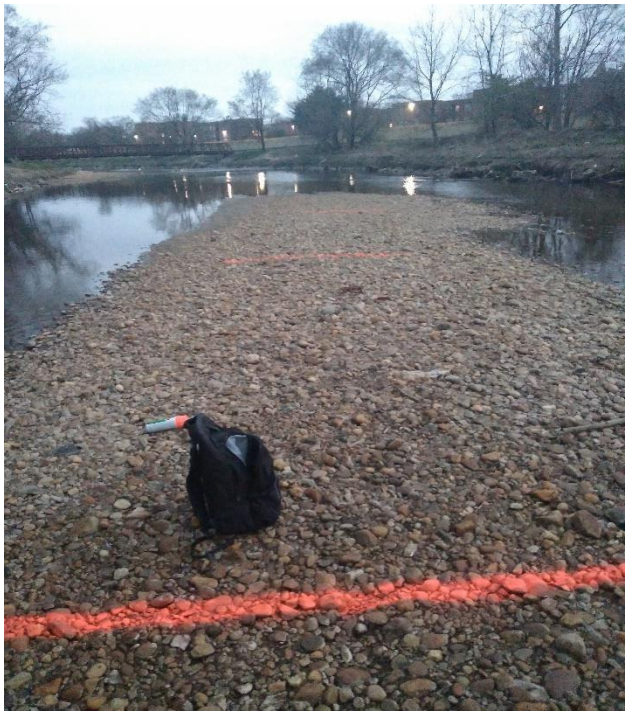

Figure 8: Particle tracer experiments: Left: Northwest Channelized reach, Right: Northwest Alluvial reach. Black circles indicate the other two painted lines

Particle Tracers

Once the bars were found the next step is to spray paint a line. This line plays an important role to help us identify the movement of sediment in the event of a storm. These particle tracers will help us identify the movement and how far they move. They will allow us to understand whether a certain rock size is being moved, whether they are being replaced, or if there is no tracer movement but sediment is being deposited on top of it.

For the 4 bars we selected from the alluvial and the channelized reach, 3 different lines were painted at the bar head, middle, and tail. The movement of particles may not be the same along the gravel bar and the particle tracers allow us to see where the greatest of sediment is moving and where sediment build up is occurring.

After a storm event occurs, I returned to the field to measure the size and distance individual particles moved (Fig. 8). This is used to determine if the sediment in the different reaches move easily and are mobile. We can also identify whether the bars are growing in size by the amount of new material buried on top of the line. These two distinctions will help us understand whether the bars we are looking at are going to stay and grow or whether they will lose sediment and eventually disappear. Once the data are collected, we re-paint the lines for the next transport event.

Figure 9: Particle Tracer Movement

Measurement of Flood Flow Depth Over the Top of the Bars at each Stripe Location

After a flooding event we needed to determine how high the water level had gotten during the flood. To do this, we had to see how far the new sediment had gone up the banks. We analyzed how far the new sediment got deposited and from that point we used a survey rod and level. This can be done with string level and string or with surveying equipment.

The depth and gradient data we were able to calculate from this technique allows us to get the fluid shear stress for the alluvial reach. The channelized reach did not need this technique to be used as a USGS gauge is located downstream allowing us to get data from that.
To get the local shear stress we used the equation $t = rgdS$.

Uncertainty

For the work we have done so far uncertainty is present. The uncertainty comes with the distance of sediment transported, size of the pebbles, and there is uncertainty in the height of the gravel bars we used to calculate the flow depth. The distance of sediment transported has an error of $\pm$ 6 cm for recovered particles. The reason the uncertainty is a high is that we pulled some of the rocks that were a little far from the tape measure which could have swayed the distance travelled. Size of the pebbles has a relatively smaller error as its around $\pm$ .4mm. The calculated flow depth has an error of about $\pm$ 2-4 cm. Water surface gradient is assumed to be the reach gradient, but this might be improved in the future by measuring it at high flow or

III. Results:

The morphological data for the two reaches are compared in Table I. These data indicate significant differences in sinuosity and gradient between the two reaches.

Table I: Morphological data prior to storm event monitoring

site	Ave Width, m	Sinuosity	Rc/W	Ave D50	Ave D84	Gradient
Alluvial	18.5	1.32	4.52	21	28.5	0.0037
Channelized	21.40	1	N.a.	22	31.3	0.0045

From the table above we can see that the 2 reaches have similar widths and median grain size, but different sinuosities. For the alluvial site, the river has an average width of 18.5, this is less than the downstream reach that has an average width of 21.4m. The gradient of the channelized reach is steeper than the alluvial reach. The average grain size of the two reaches is similar., 21-22 mm.

Surface and subsurface grain size distributions were sampled and analyzed after each monitored event. These data are shown in table II.

Table II: Grain size distributions from storm event sampling.

	Event (3/24/2021)	Event (9/1/2021)	Event (9/21/2021)
Site: Meandering			
D50 surface	21 +/- 9.07	19.8 +/- 2.27	18.83 +/- 4.14
D84 surface	30.75 +/- 13.8	32.17 +- 9.17	32.17 +/- 14.86
D50 subsurface	6.22 +/- 2.27	N.a	6.55 +/- 3
D84 subsurface	.79 +/- .37	N.a	1.025 +/- .35
Site: Channelized			
D50 Surface	22 +/- 1.63	18.17 +/- 1.57	18 +/- .58
D84 surface	31.33 +/- 1.6	25.33 +/- 2.75	27.5 +/- 2.63
D50 Subsurface	8 +/- 1.56	N.a	7.35 +/- 1.44
D84 Subsurface	.84 +/- .1	N.a	.89 +/- .12

Subsurface grain size distributions

Subsurface grain size was sampled before the initial event sampling and after each monitored event except for the September 1st storm. When looking at the data in table ll, the D50 and D84 are lower at the alluvial reach. At the alluvial reach for the storm of March 24th, the D50 was 6.22 +/- 2.27 and D84 was .79 +/- .37 this was lower than that of channelized reach of 8 +/- 1.56 and .84 +/- .1. The lower the D50 and D84 the more sand is in the system, since the D50 and D84 were both lower in the subsurface for the March 24th storm and the September 21st storm, then the meandering reach must have more sand particles in the subsurface than that of the channelized reach. In Fig. xx the graph shows the D50 of the surface and subsurface from each location

.

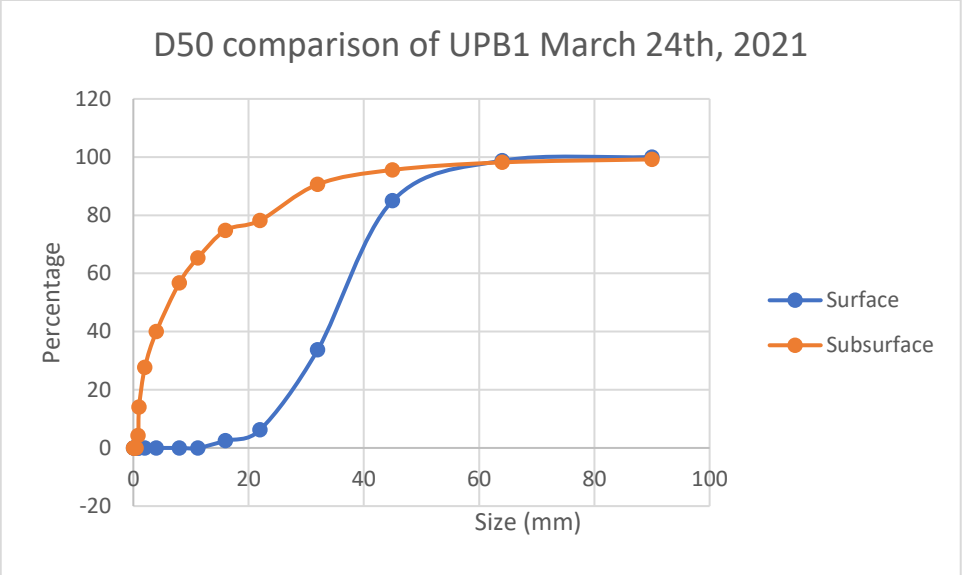

Figure 10: Graph to compare D50 of surface and subsurface for the channelized reach

Transported Particle Size Data

During the March 24th storm varying sizes of sediment moved, some grains moved a several cm while others traveled several meters. To understand what sizes and grains transported we created 2 cumulative percent graph (Fig 10 and Fig 11). When looking at this example from the alluvial site we can see that most of the movement occurred between the grain sizes of 10 – 20mm. With that we can apply it to the pebble counts we did and see if the transported grains are similar in size. From Fig 16 we can see that 3 – 32 mm rocks were transported to a higher degree. This helps us understand what the distribution of the grain sizes were for this particular flood event.

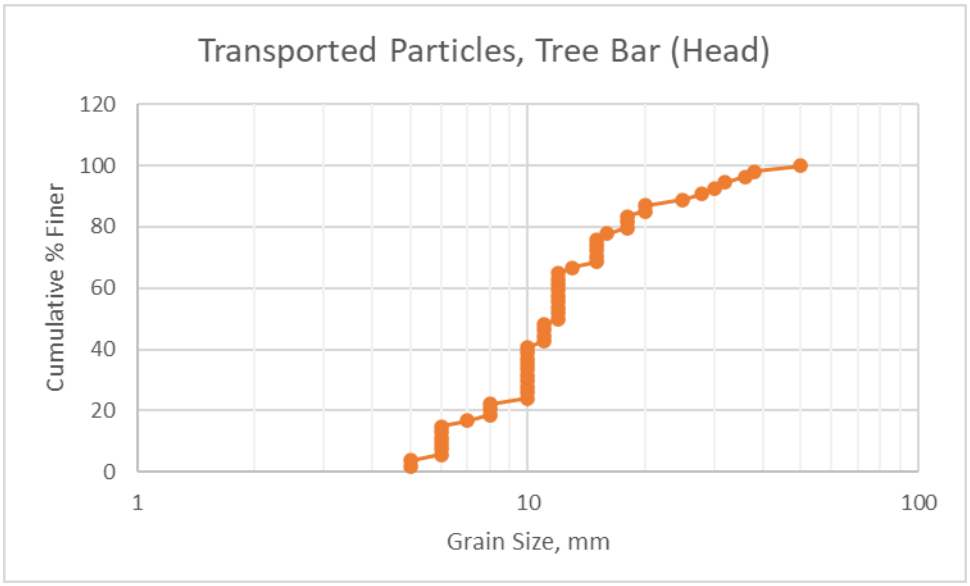

Figure 11: Cumulative Graph of Transported Particles at Alluvial Reach

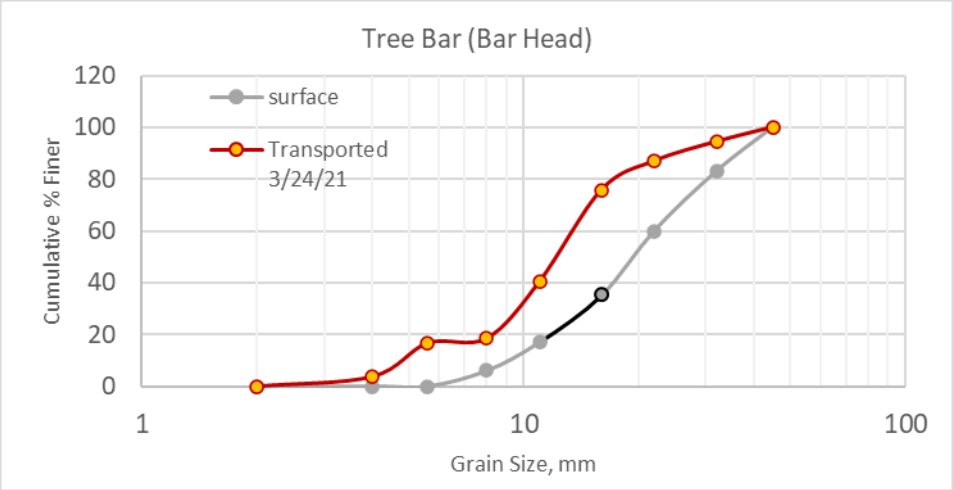

Figure 12: Cumulative grain size distribution of Transported surface particles and initial Surface grain size.

Particle Transport Distance Data

Transported distance as a function of grain size is plotted on Figures 13A and 13B. All particle sizes were observed to move. An envelope curve is used to evaluate the maximum transport distance by grain size. Fig 13A indicates that particles in the 10- 15 mm range moved the furthest at the alluvial site. These particles are also among the most abundant surface grain sizes. A similar range of grain sizes moved in the channelized reach (Fig. 13B), but particles larger than 30 mm moved further. In both reaches, there is not a statistically significant relationship between grain size and transport distance. The envelope curves suggest that smallest and largest particles in a given distribution have the lowest probability of moving significant distances.

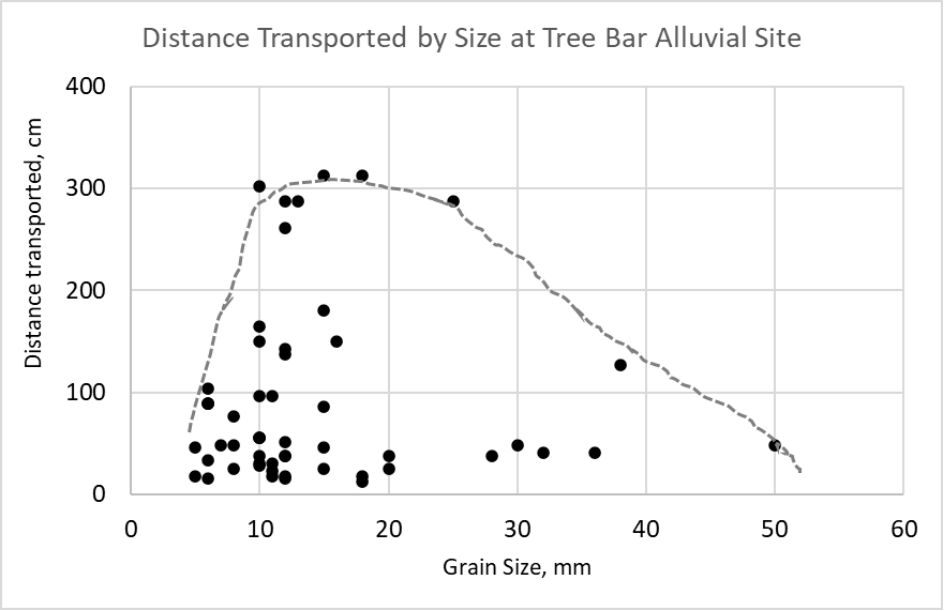

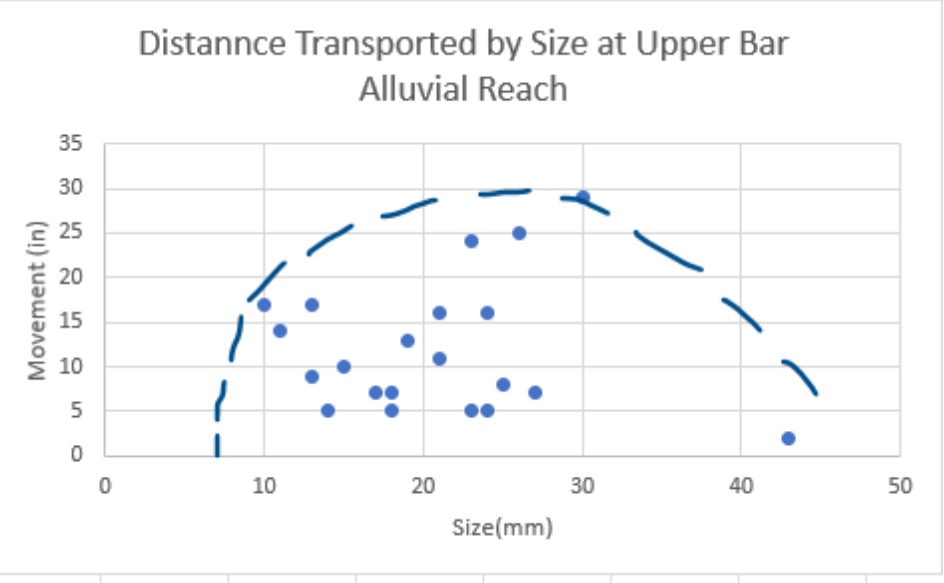

Figure 13: Distance Particles Traveled at: A) Alluvial, and B) Channelized Reach

Relationship between Di/D50 and t for Each Particle Moved*

At each location, I measured flow depth and determined peak event shear stress from depth and gradient data. These data were used to calculate t* and to develop the relationship between Di/D50 (transported particles) and t* . These data indicate that a range of surface sizes were transported during storm events. The dimensionless shear stress, t* for the D_{84} value was taken to be the t^*_{Crit} of the bed (Parker and Klingeman, 1984). If we look at table III on page 19 the t* crit for the March 24th storm was 0.037 for the alluvial reach and for the channelized reach it was approximately 0.051. The graphs below also state that the bed is being mobilized around the t* crit of 0.037 and 0.051. With the t* crit being lower in the alluvial reach the bed is mobilized at a lower flow rate and is moved downstream whereas the channelized reach is mobilized during higher flow rates due to less sand particles being in the surface thus making a higher t* crit value.

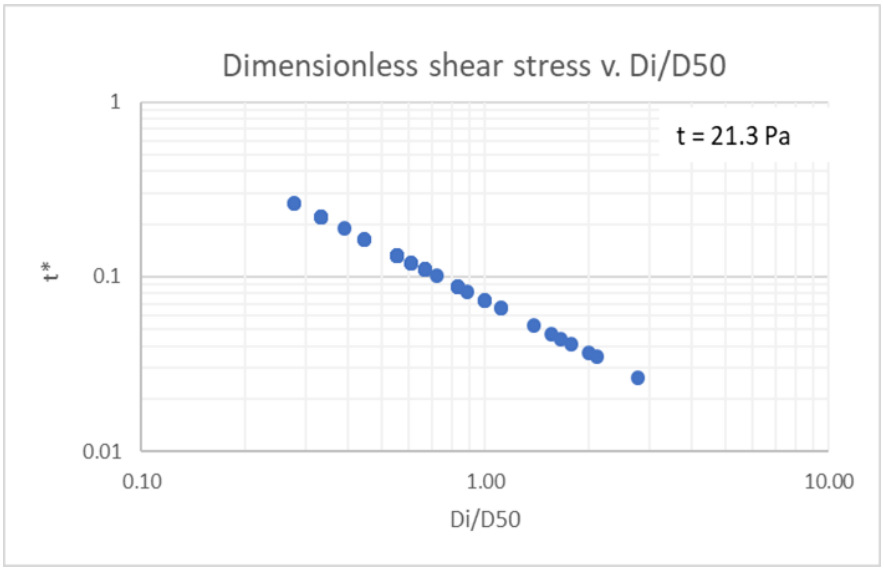

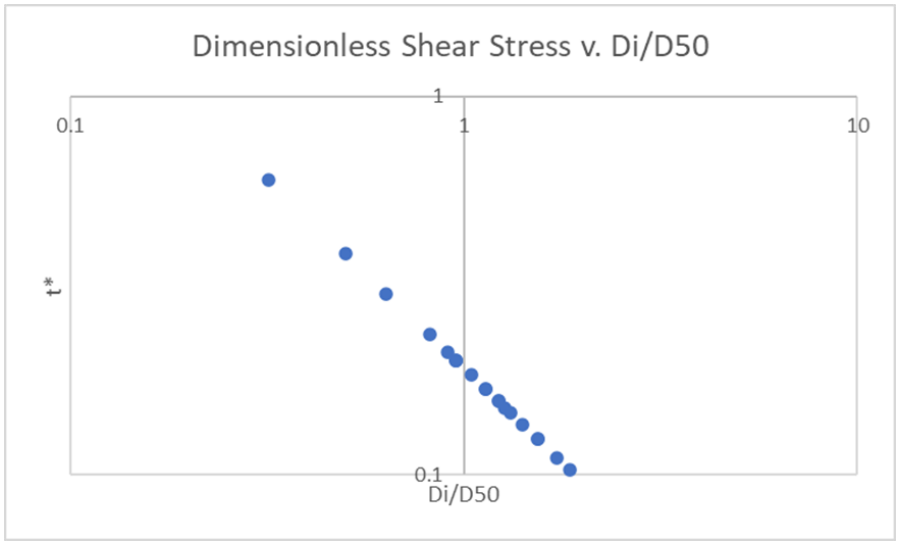

Figure 14: Upper diagram: Alluvial reach: Lower diagram Channelized reach

Sediment differences between the two reaches

At the two reaches, there is differences that contribute to the movement of sediment. The major difference is the amount of sand in the alluvial reach compared to the channelized reach. Using data from table II and table III it shows that in the alluvial reach that there are more sand size particles in the alluvial reach compared to the channelized reach. Sand sized particles allow the bed surface to be mobilized during lower flow events meaning that sediment in the alluvial reach will move during minor events compared to the channelized reach which would move during higher flow rates. The sediment size distribution between the two reaches are relatively the same, if you look at Fig 15 and Fig 16 you can see that the distribution of sediments are very similar.

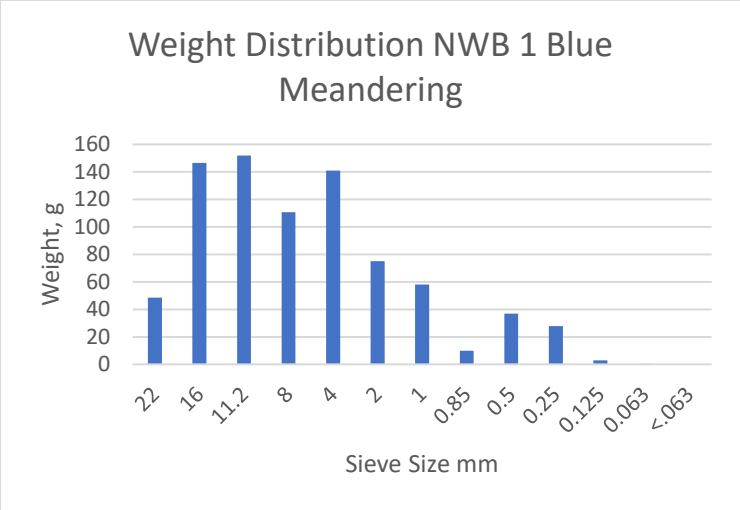

Figure 15: Subsurface distribution of sediment for meandering reach

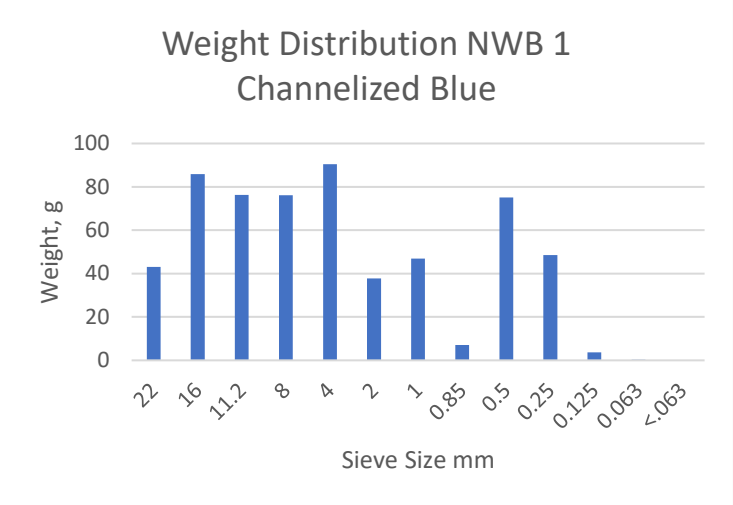

Figure 16: Subsurface distribution of sediment for channelized reach

Initiation of Sediment transport of Alluvial and Channelized Reaches

At the two reaches, I observed that sediment moved during the first measured flow event at both reaches. The distance that particles moved appeared to be different. In the alluvial reach the average of 40 +/- 8.94 particles moved at the 6 monitored sites. In the channelized reach, particles of similar size moved, but a fewer number of particles were recovered. This suggests that additional particles were transported further away from the site. In addition, I also observed sheets of sand and gravel covering painted pebbles at the meandering site. The alluvial reach has spots on the river where the water is lower making for fine sediment and coarse sediment to deposited on the bars.

The surface D_{84} values and the fluid shear stress were used to determine event t^*_{crit} for each event in both the alluvial and channelized reaches. These data are shown in Table III. These data indicate that critical dimensionless shear stresses were higher for the channelized reaches

than the alluvial reaches, even though shear stress values are higher in the channelized reaches for the same event.

Table III: Event grain size, shear stress, and critical t* values

Event	Reach	D_{max} , mm	t fluid, Pa	t*crit
3/24/2021	Alluvial	47.5	28.5	0.037
	Channelized	38	31.3	0.051
9/1/2021	Alluvial	53.1	32.7	0.038
	Channelized	45.1	36	0.049
9/21/2021	Alluvial	46.4	26	0.035
	Channelized	40.7	32.2	0.049

Is Sediment Easier to Transport between Alluvial or Channelized Reach

The sediment in the alluvial and channelized reach are surprisingly mobile at both sites, however, the reason for the mobility may be different. are moving is different. In the alluvial reach we were able to look at photos and the deposition of sand after storm events to understand that sediment moves with relative ease to the sand deposited at these sites. Sand, when in the subsurface can cause a lower shear stress which allows the sediment to move during lower discharges. At the channelized reach the shear stress is higher due to the lack of sand but the discharge at the site downstream is higher than that of the site upstream. Since the discharge is higher downstream with the lack of areas for the sediment to be stored (unless overbank deposit) then the sediment moved will continue downstream and will not be stored compared to the alluvial reach. The two sites then have similar sediment movement but for varying reason of lower shear stress upstream and higher discharge at the channelized reach due to the straightening of the channel.

Does the Complex Nature of the Alluvial Reach Allow for More deposition Compared to the Channelized Reach

For this we, need to understand both of the last two key points of the results. Both the averages for distance traveled and particles moved are greater at the alluvial reach than that of the channelized reach. We can also see that the replacement rates between the two sites are vastly different in figure 26 and 27. This helps us see that although the sediment in the alluvial reach is leaving at a greater rate but that the sediment moving into the reach are being deposited and stored. This is due to the complexity of the alluvial reach. The alluvial reach has many bends and turns that allows for highly variable flow rates along a stretch of river. This allows for the sediments to slowly be deposited along this stretch of river at the many different bars. The same cannot be said about the channelized reach. Along the channelized reach the bars are smaller and further apart. This happens because of the straightening of the river so sediments are not capable of settling along this stretch of river. With the straightness of the channel the sediments do not settle unless they are stored as overbank deposit or in a pocket of lower discharge. For that reason, the alluvial reach is able to store and deposit more sediment than the channelized reach.

IV. Future Work

The data collected is sufficient to understand if sediment is being stored or moved in the river, but work associated with overbank deposits was no takin into consideration. To further understand the sediment deposition in the Anacostia River a gauge placed upstream to accurately get the discharge totals. Also, collecting overbank deposits after each storm would have helped understand how much sand is being stored on the banks and to see for the point bars how deep the sand deposits are. If they are deep we would expect the shear stress for this part of the river to be lower as sand is easily mobilized. If there is a lack of sand the shear stress should be higher as the sediments are harder to move.

V. Conclusions

Looking at the data collected from the storms of March 24th, September 1st, and September 21st, 2021, we are able to say that hypothesis A is incorrect that the channelized reach is able to mobilize the sediment at lower shear discharges and moves during more flow events. When looking at the data collected the channelized reach mobilizes at about the same rate as the alluvial reach but for different reasons. In the alluvial reach the sediment has more sand stored in the subsurface and as a result the shear stress at that site is lower allowing for sediment to move during low discharge events. At the channelized reach the river lacks bars and due to the widening of the river the water moves faster as result. This causes the sediment to not be stored in the channelized reach and is funneled down to the harbor. The only way sediment is stored in the channelized reach is if it becomes overbank deposit. For hypothesis B, the statement is false where the alluvial reach is only able to move during high flow events. With the understanding and finding that sand is in the subsurface at the alluvial reach the sand particles create a lower shear stress thus allowing the sediment to move during lower flow events. At the channelized reach sand is not primarily stored in the subsurface as the flow during a storm event doesn't allow for sand particles to be stored tin the subsurface. Instead, the sand particles are deposited and stored in the overbank of a channelized reach as the flow decreases.

VI. References

How and Why rivers meander? Hydrotopics. (2010, December 5). https://hydrotopics.wordpress.com/2010/10/05/how-and-why-rivers-meander/.

Leopold, L. B., & Wolman, M. G. (1957). River channel patterns: Braided, meandering, and straight. Professional Paper. https://doi.org/10.3133/pp282b

Parker, G., & Klingeman, P. C. (1982). On why gravel bed streams are paved. Water Resources Research, 18(5), 1409-1423. doi:10.1029/wr018i005p01409

Wilcock, P. R., & Crowe, J. C. (2003). Surface-based Transport Model for Mixed-Size Sediment. Journal of Hydraulic Engineering, 129(2), 120–128. https://doi.org/10.1061/(asce)0733-9429(2003)129:2(120)

VII. Appendix

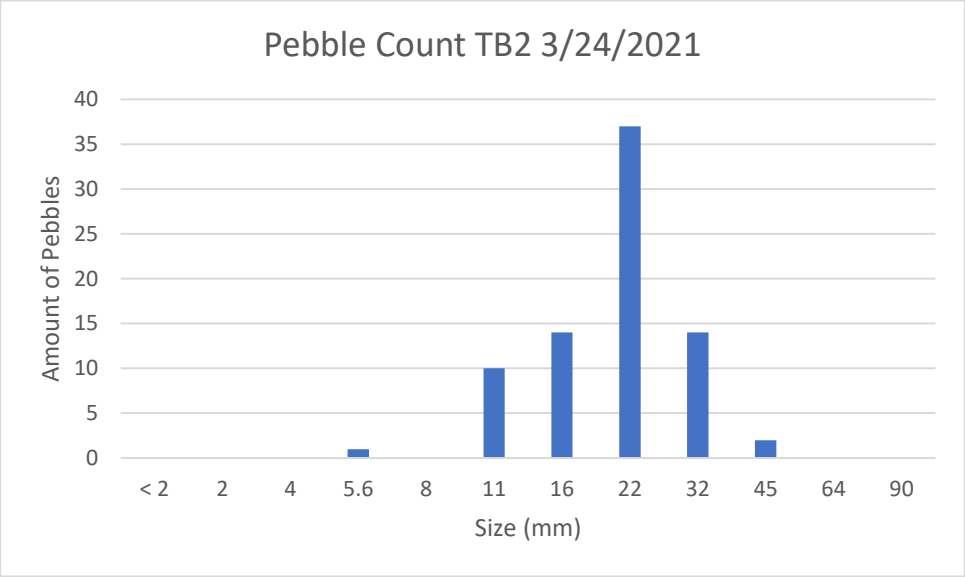

Figure 18: Pebble Count for Tree Bar 2

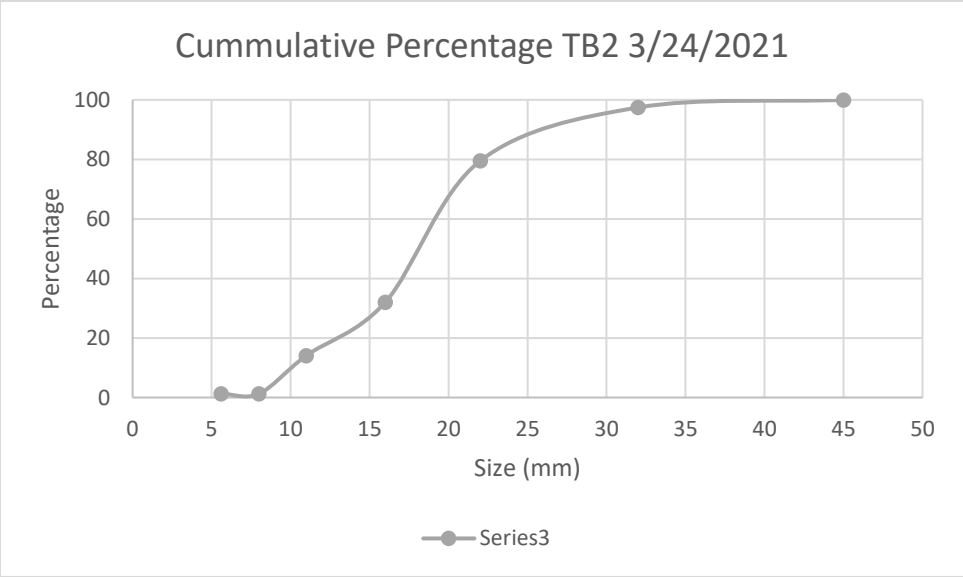

Figure 19: Cumulative Percentage for Tree Bar 2

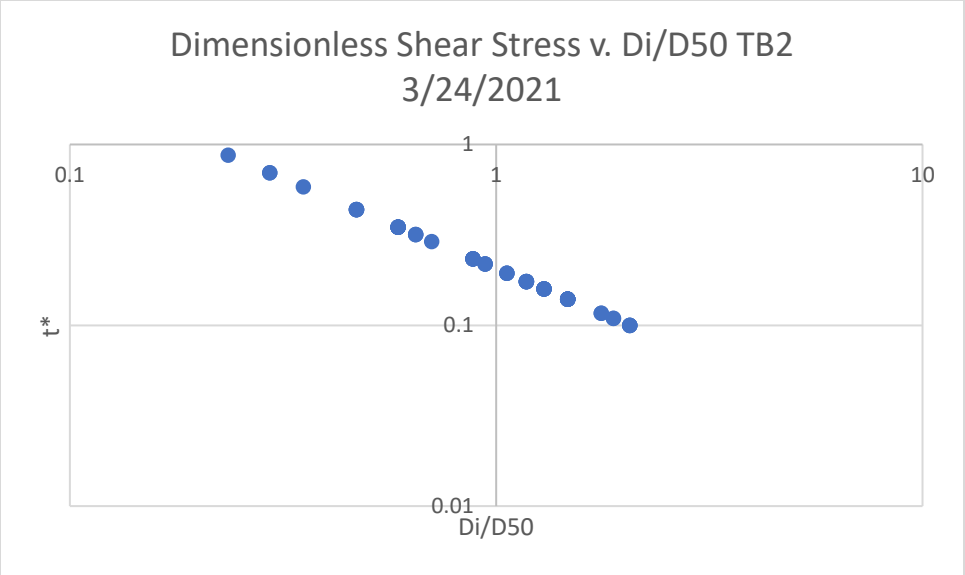

Figure 20: Dimensionless shear stress and Di/D50 of Tree Bar 2

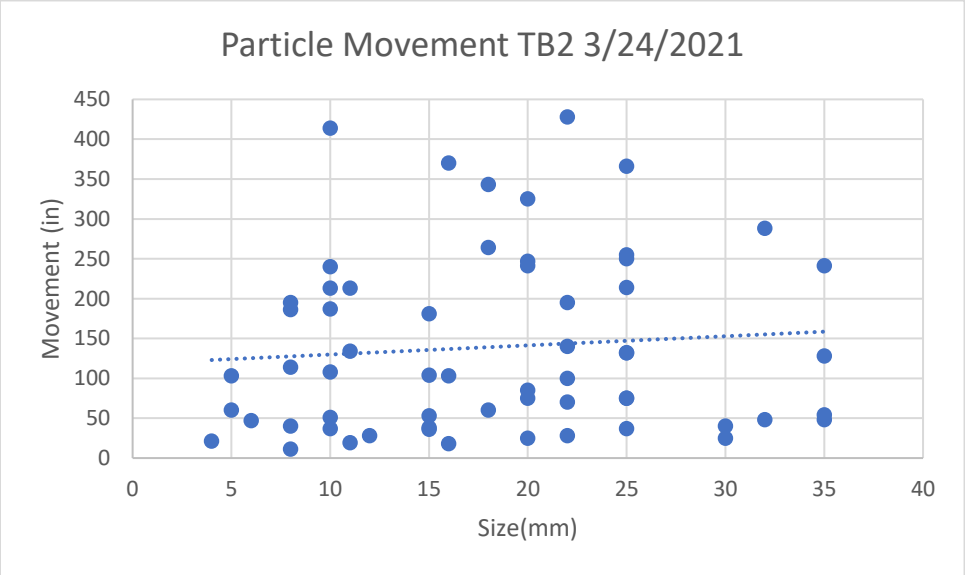

Figure 21: Particle Movement at Tree Bar 2 after Storm Event

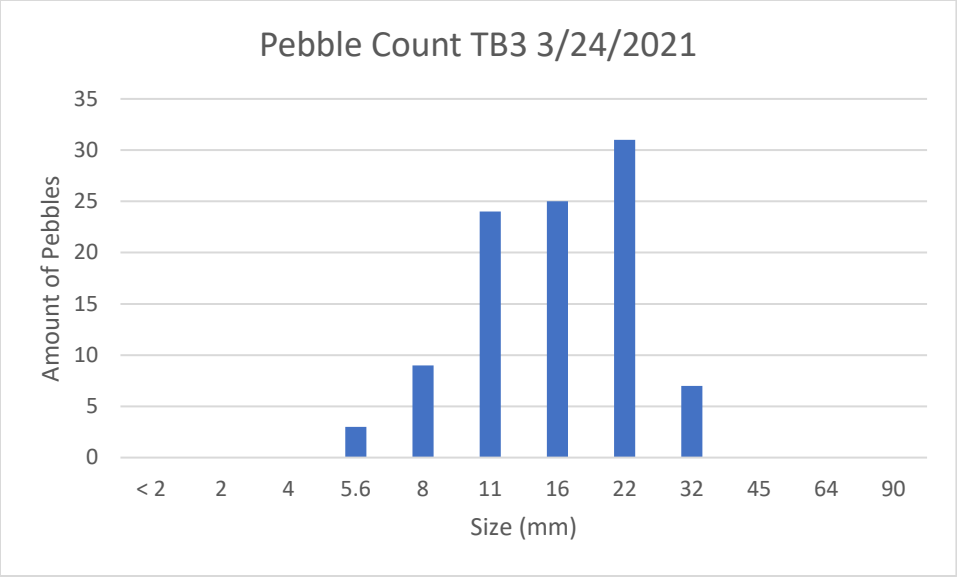

Figure 22: Pebble Count of Tree Bar 2 on Alluvial Reach

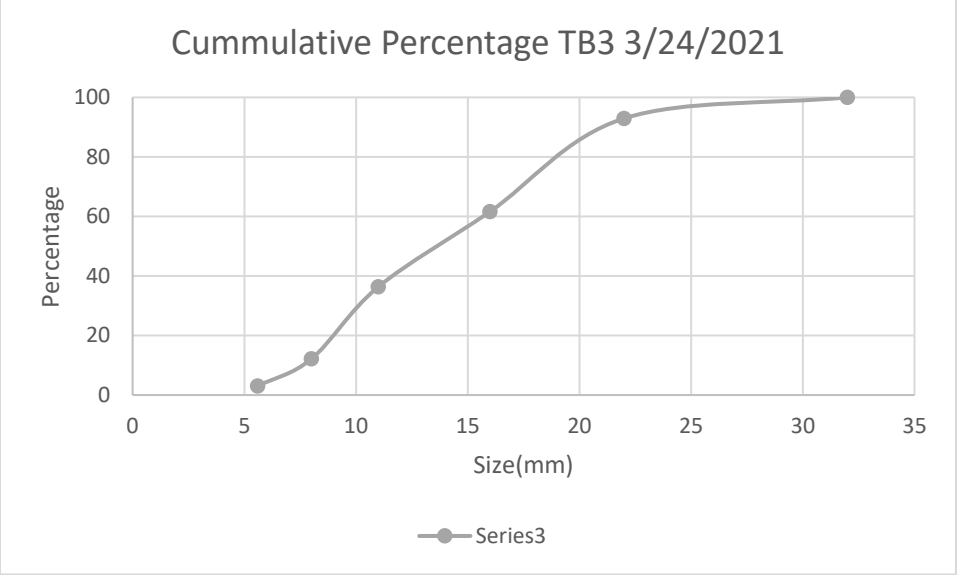

Figure 23: Cumulative Percentage of Tree Bar 2

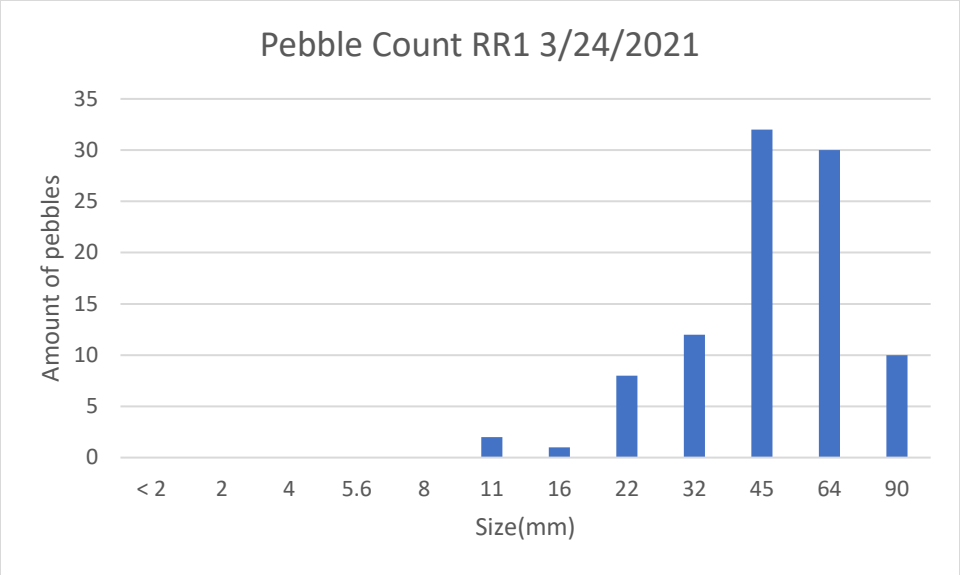

Figure 24: Pebble Count of Rift Rap 1 on Alluvial Reach

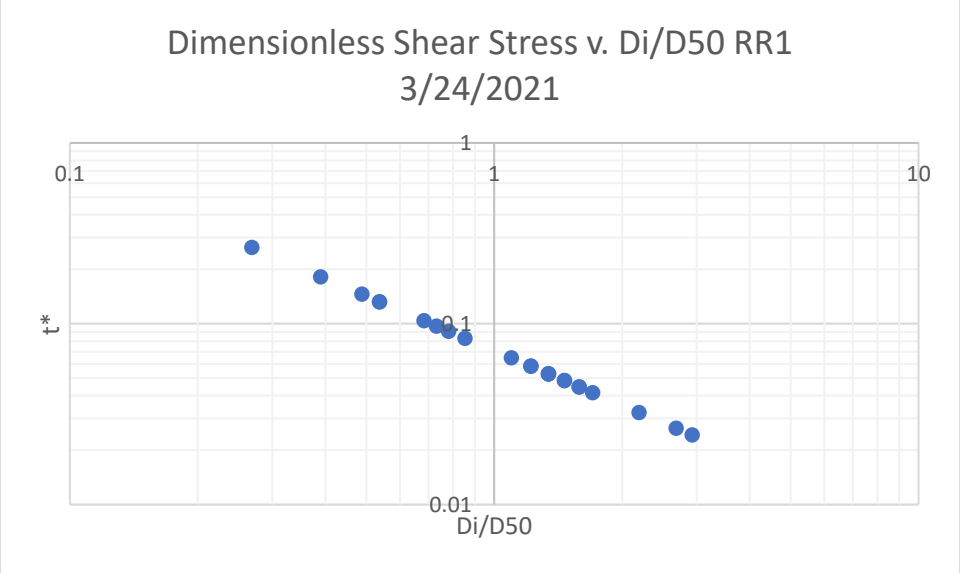

Figure 25: Dimensionless Shear Stress of Rift Rap 1

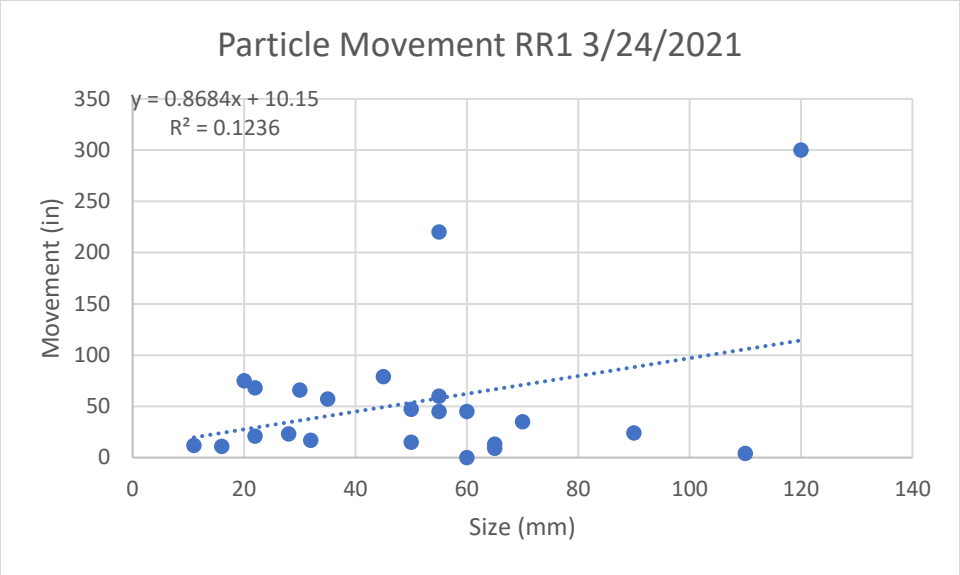

Figure 26: Particle Movement of Rift Rap 1 after Storm

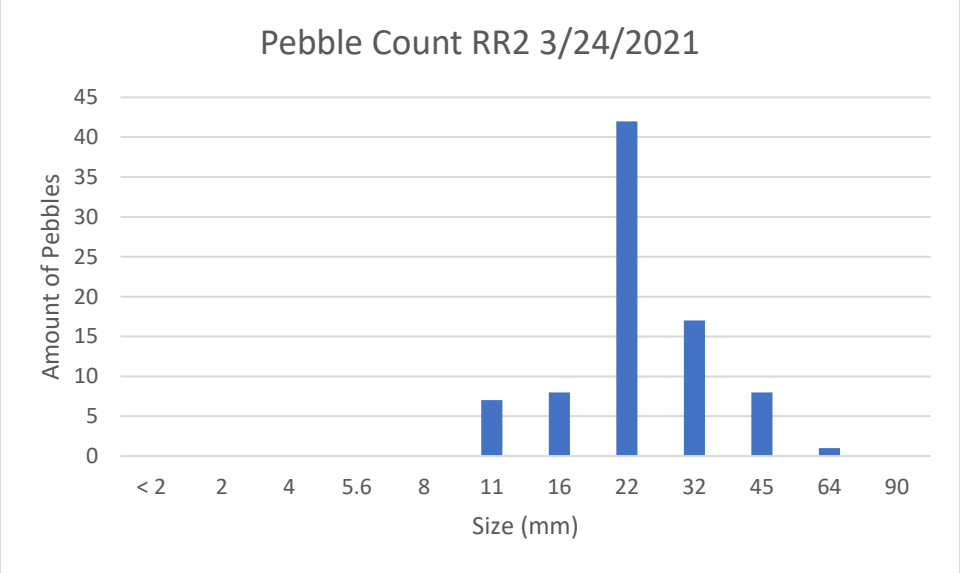

Figure 27: Pebble Count of Rift Rap 2 on the Alluvial Reach

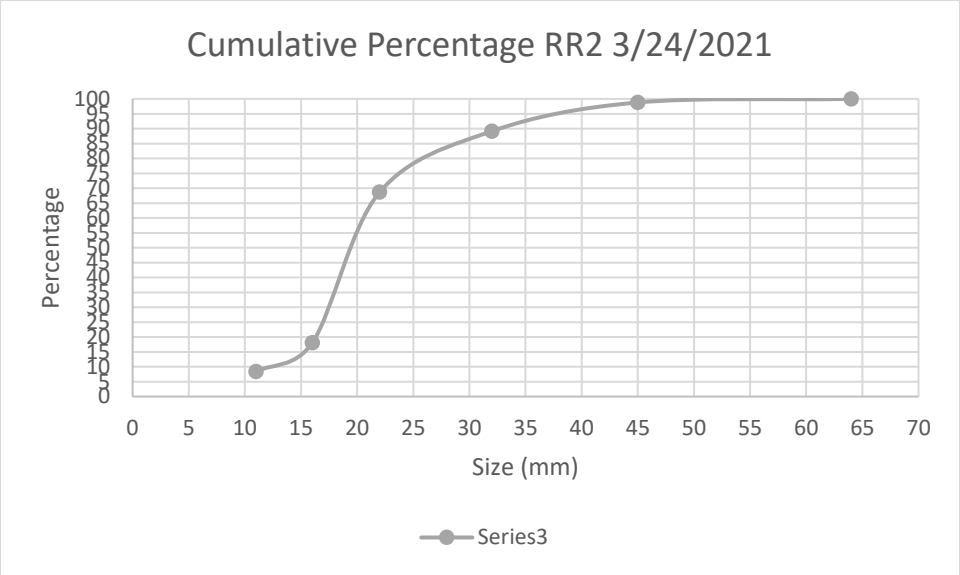

Figure 28: Cumulative Percentage of Rift Rap 2

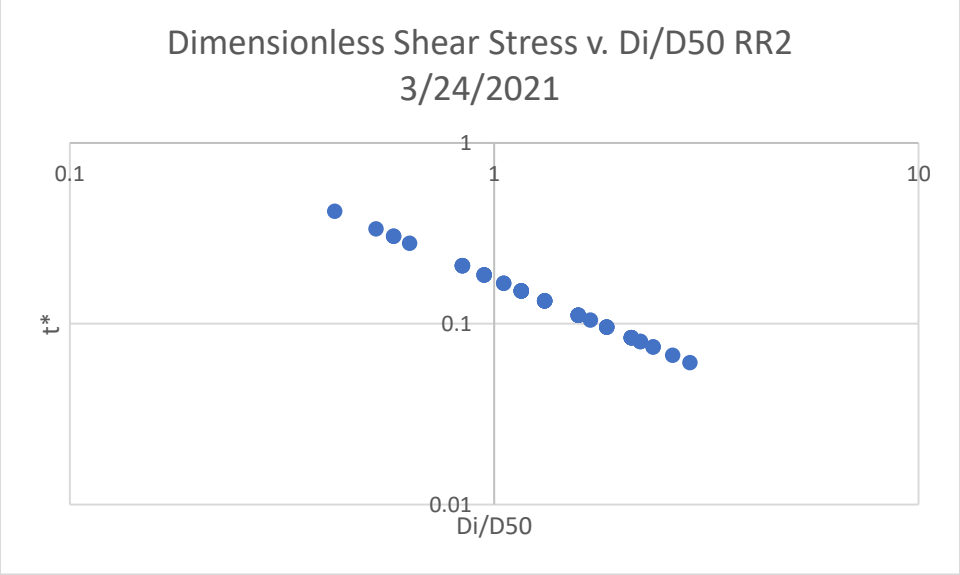

Figure 29: Dimensionless Shear Stress of Rift Rap 2

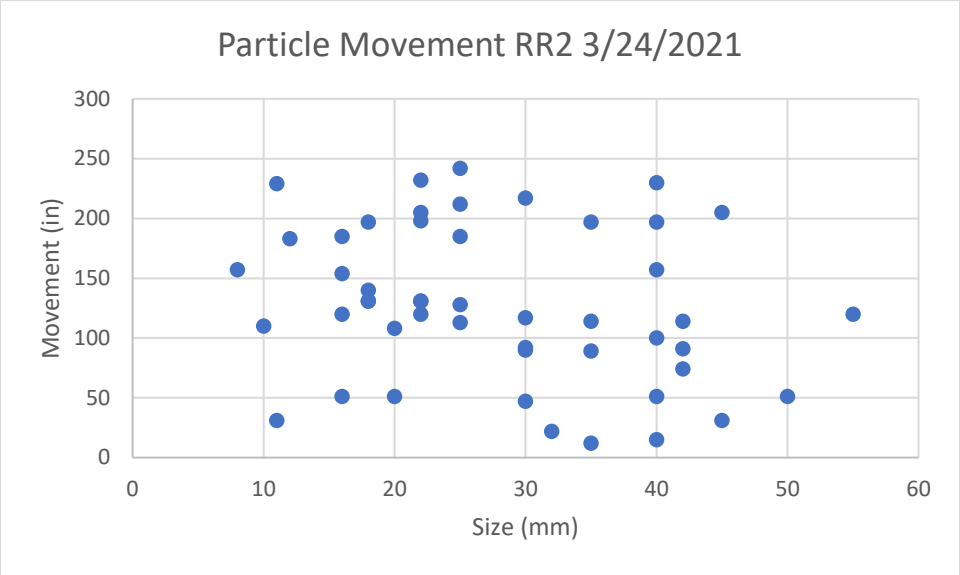

Figure 30: Particle Movement of Rift Rap 2 after Storm

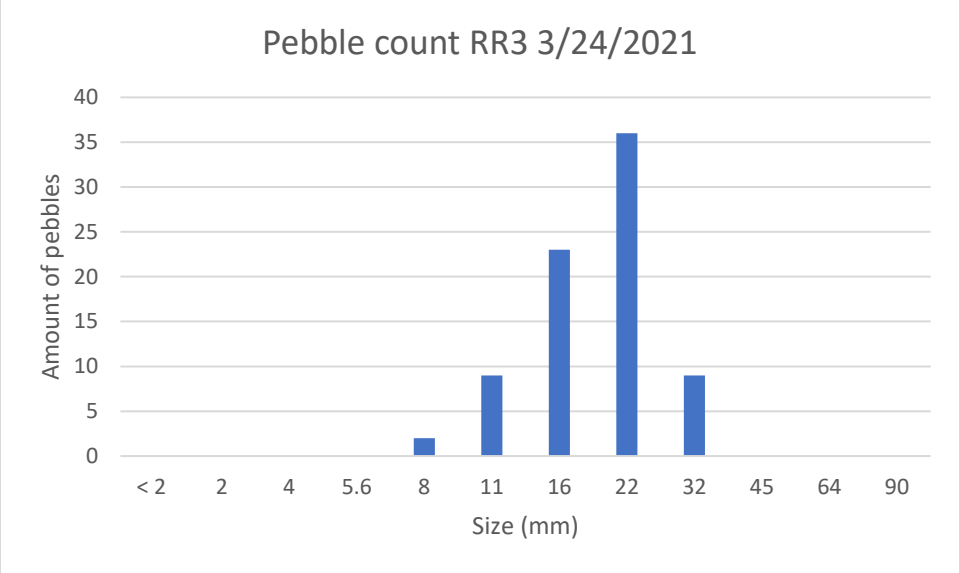

Figure 31: Pebble Count of Rift Rap 3

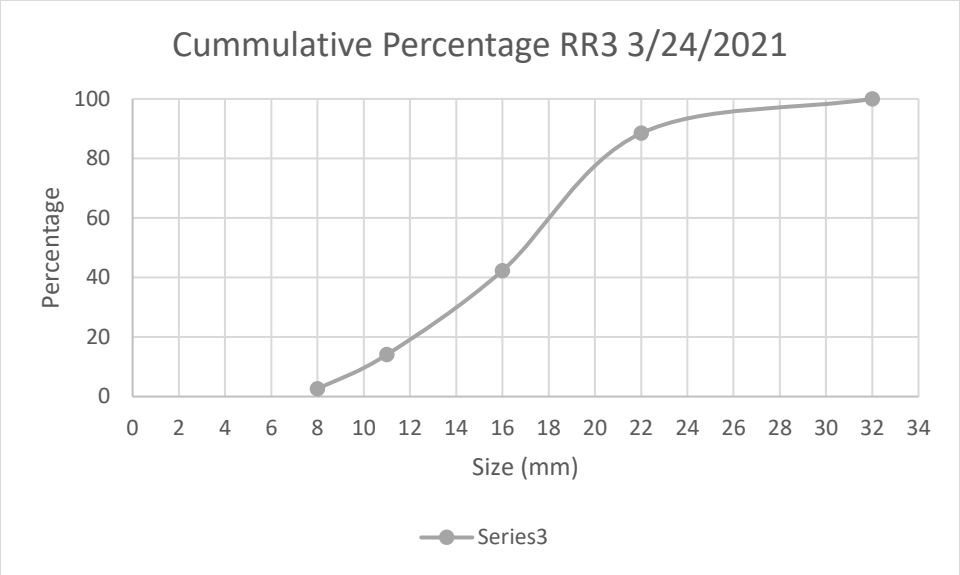

Figure 32: Cumulative Percentage of Rift Rap 3

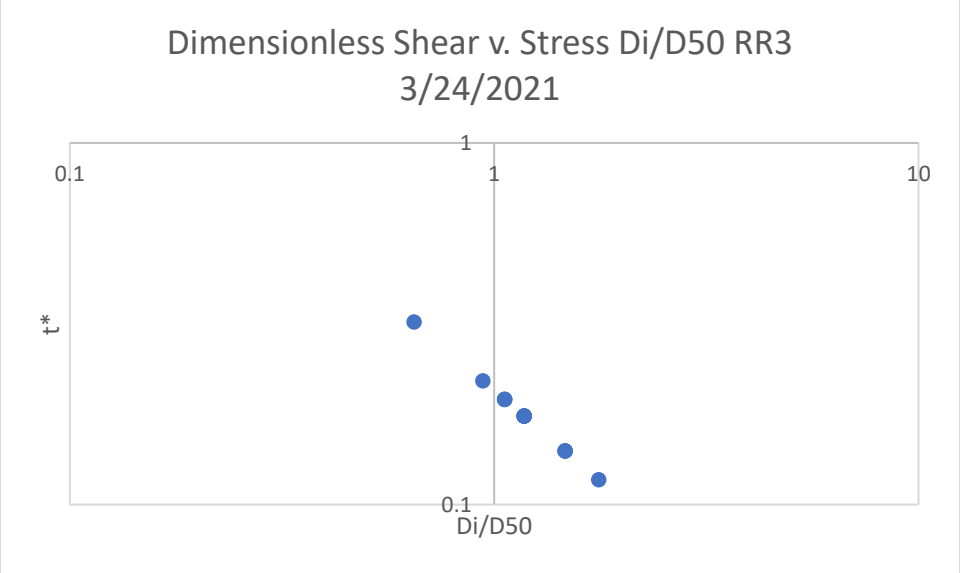

Figure 33: Dimensionless Shear Stress of Rift Rap 3

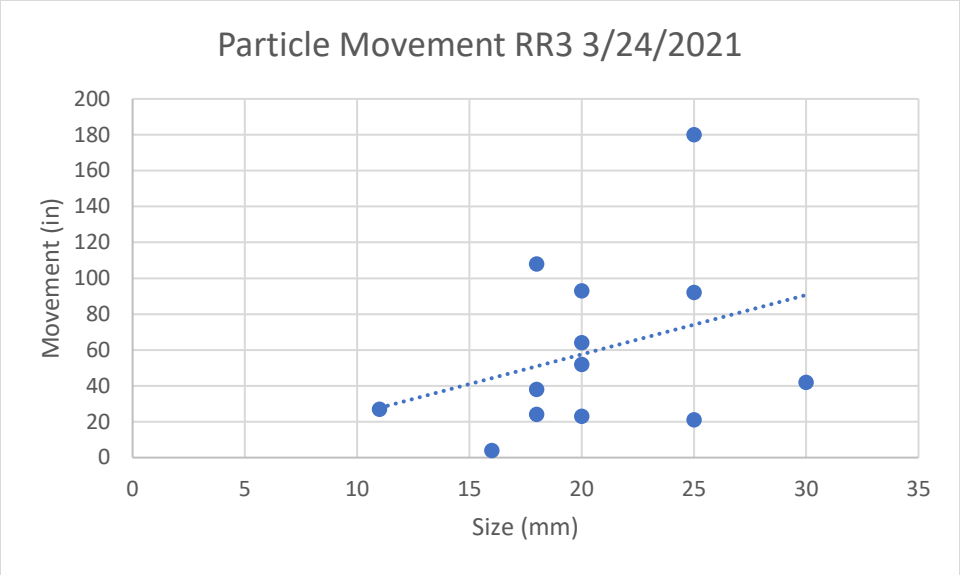

Figure 34: Particle Movement of Rift Rap 3 after Storm

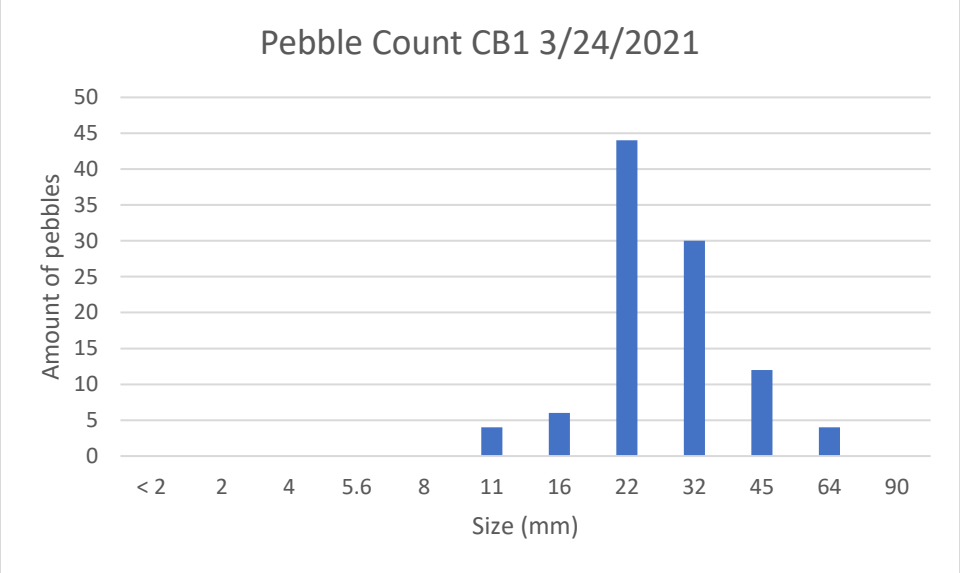

Figure 35: Pebble Count of Central Bar for Channelized Reach

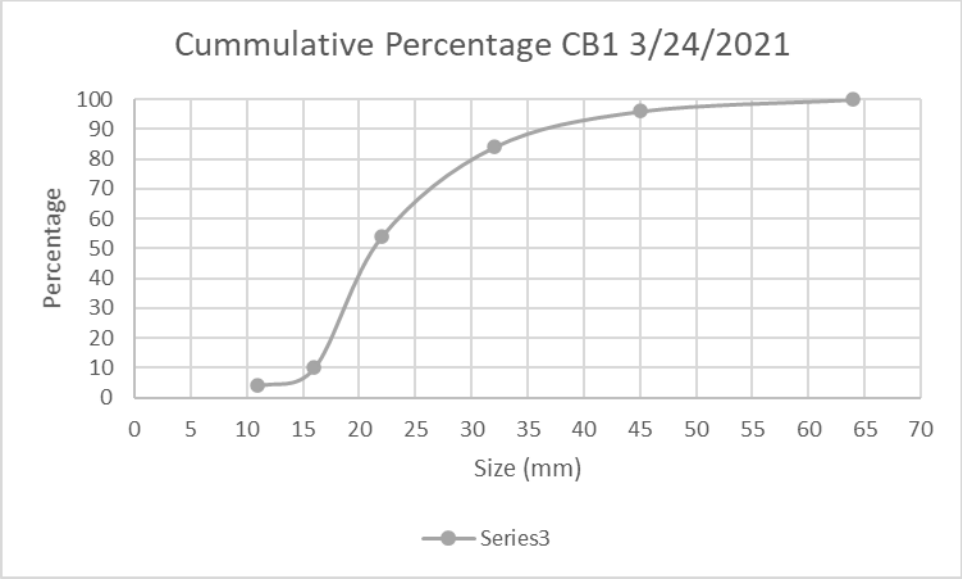

Figure 36: Cumulative Percentage of Central Bar 1

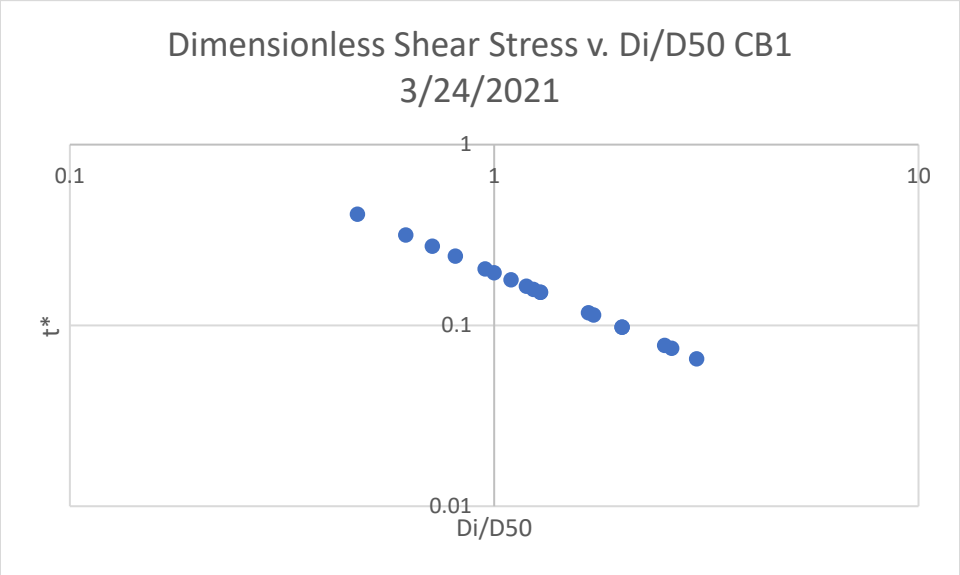

Figure 37: Dimensionless Shear Stress of Central Bar 1

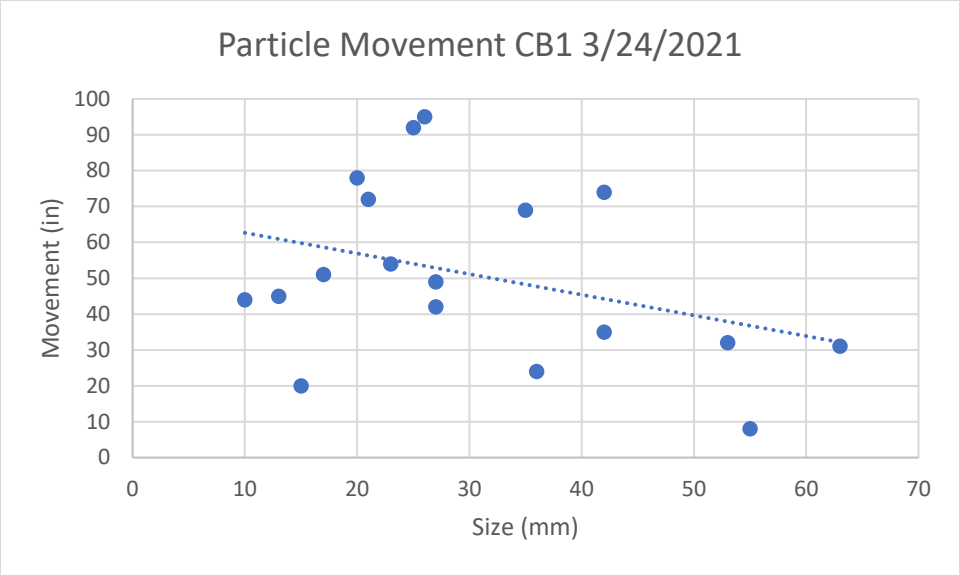

Figure 38: Particle Movement of Central Bar after Storm

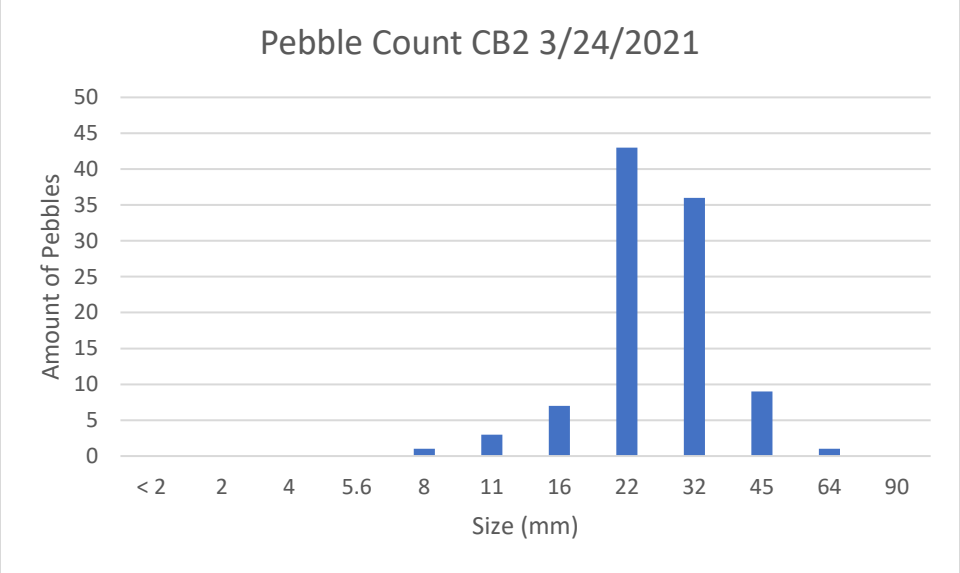

Figure 39: Pebble Count of Central Bar 2 on Channelized Reach

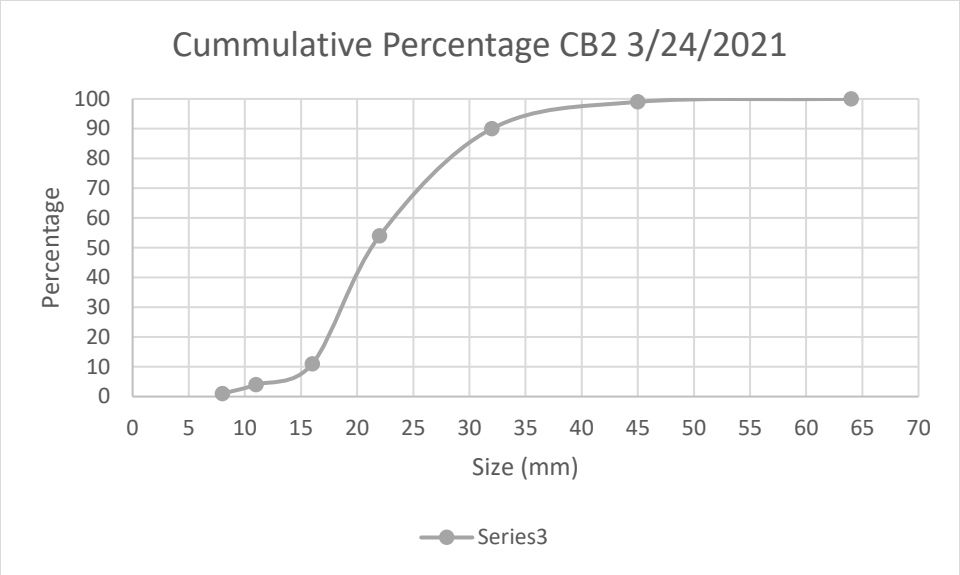

Figure 40: Cumulative Percentage of Central Bar 2

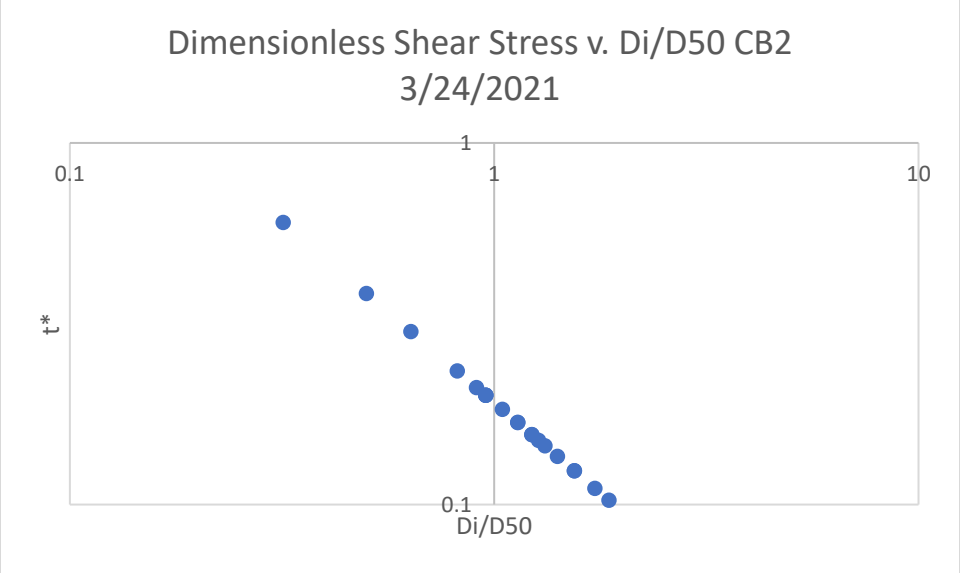

Figure 41: Dimensionless Shear Stress of Central Bar 2

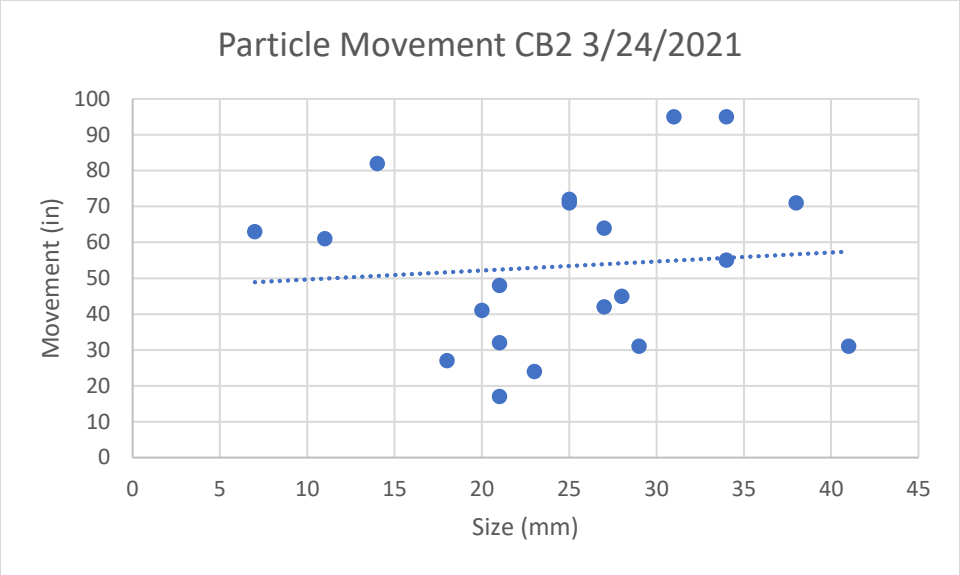

Figure 42: Particle Movement of Central Bar 2 after Storm

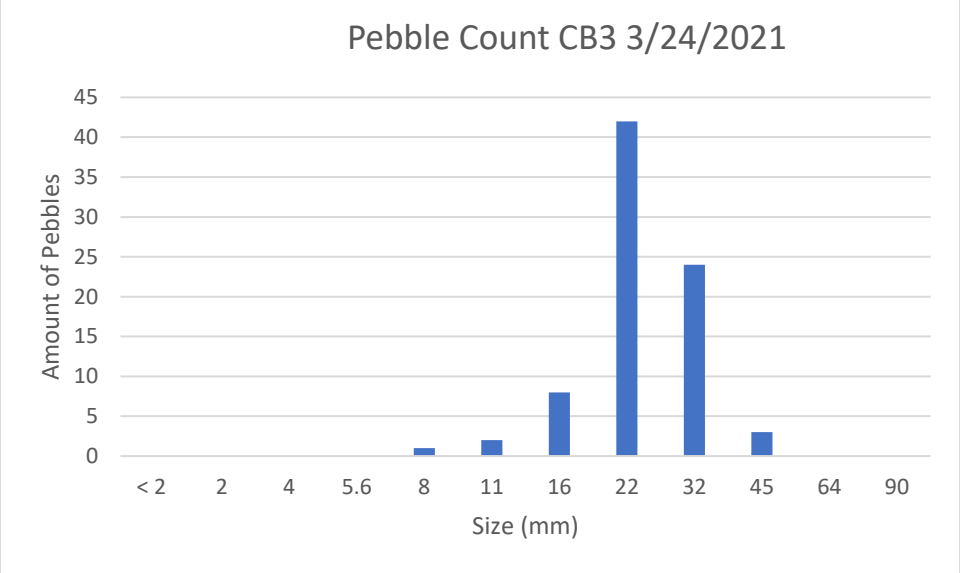

Figure 43: Pebble Count of Central Bar 3 on Channelized Reach

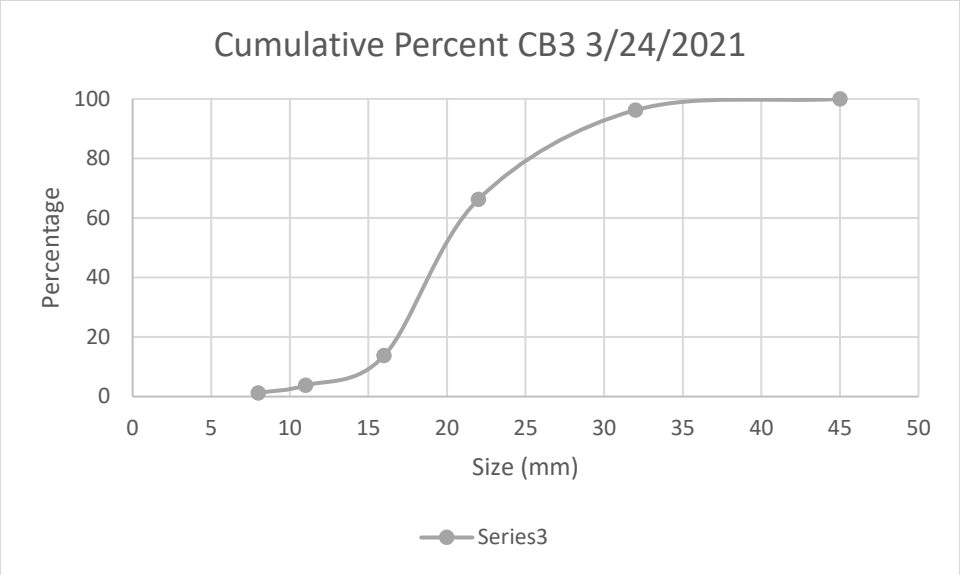

Figure 44: Cumulative Percentage of Central Bar 3

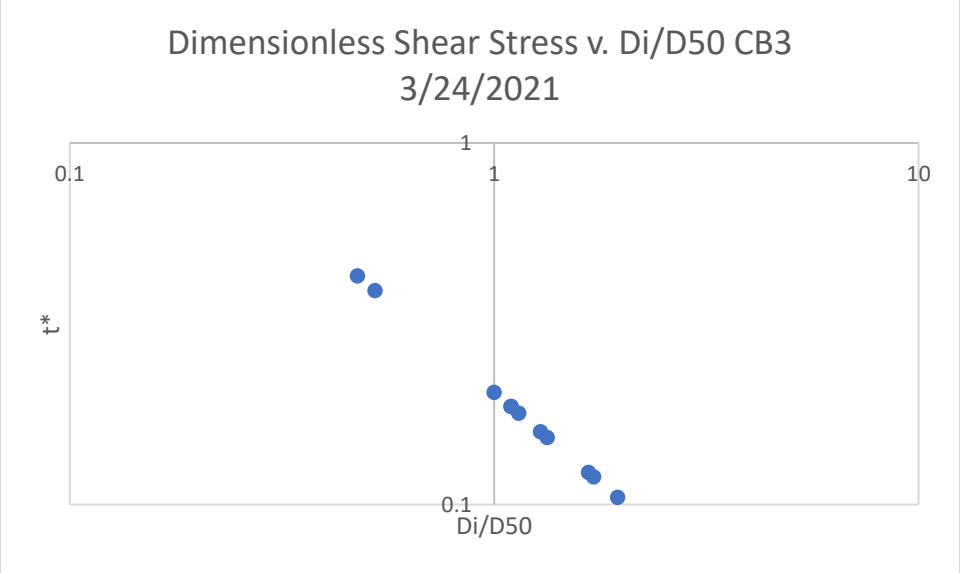

Figure 45: Dimensionless Shear Stress of Central Bar 3

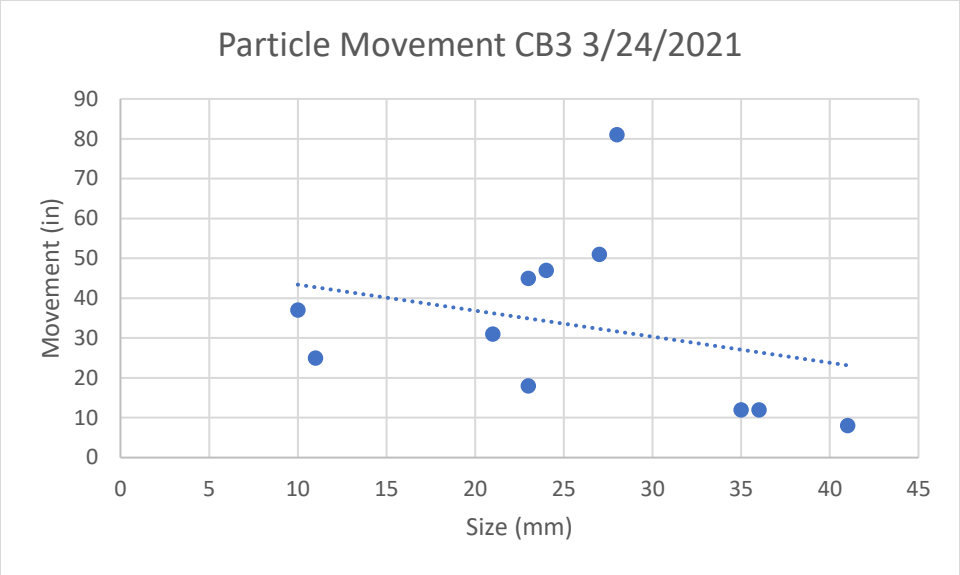

Figure 46: Particle Movement of Central Bar 3 after Storm

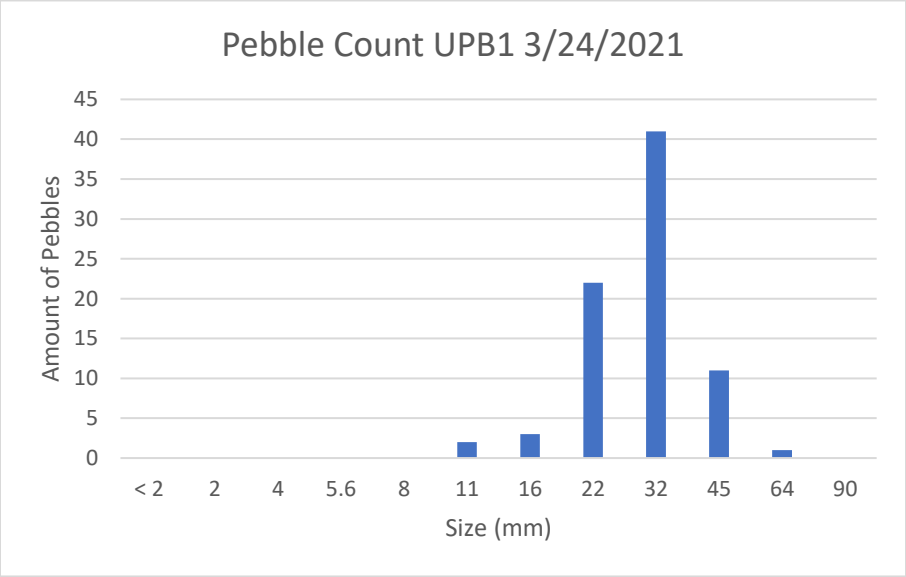

Figure 47: Pebble Count of Upper Point Bar 1 on Channelized Reach

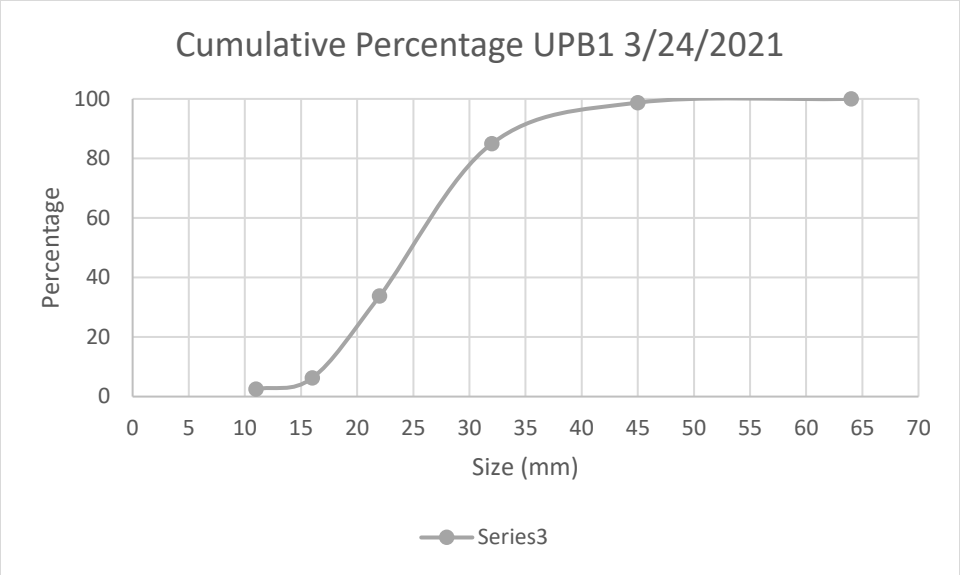

Figure 48: Cumulative Percentage of Upper Point Bar 1

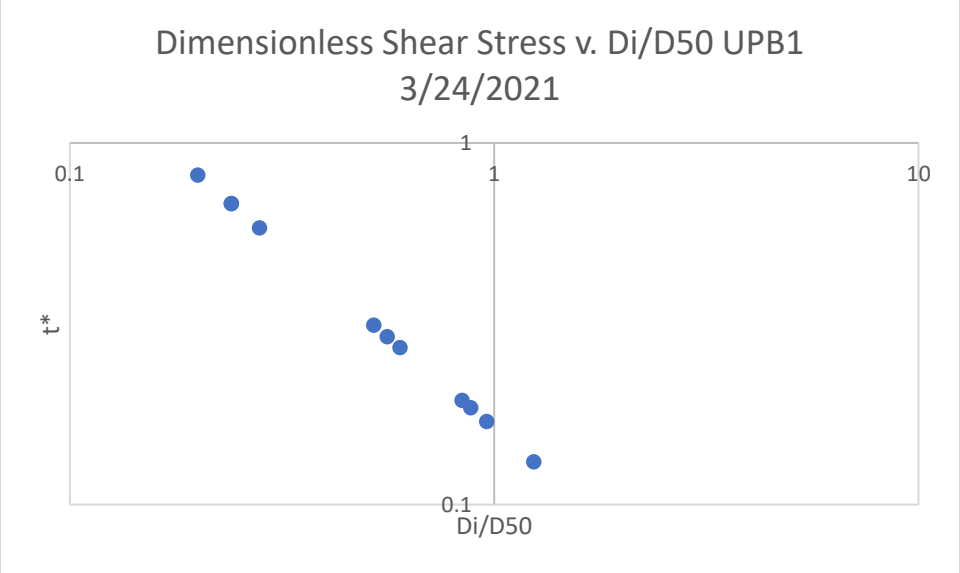

Figure 49: Dimensionless Shear Stress of Upper Point Bar 1

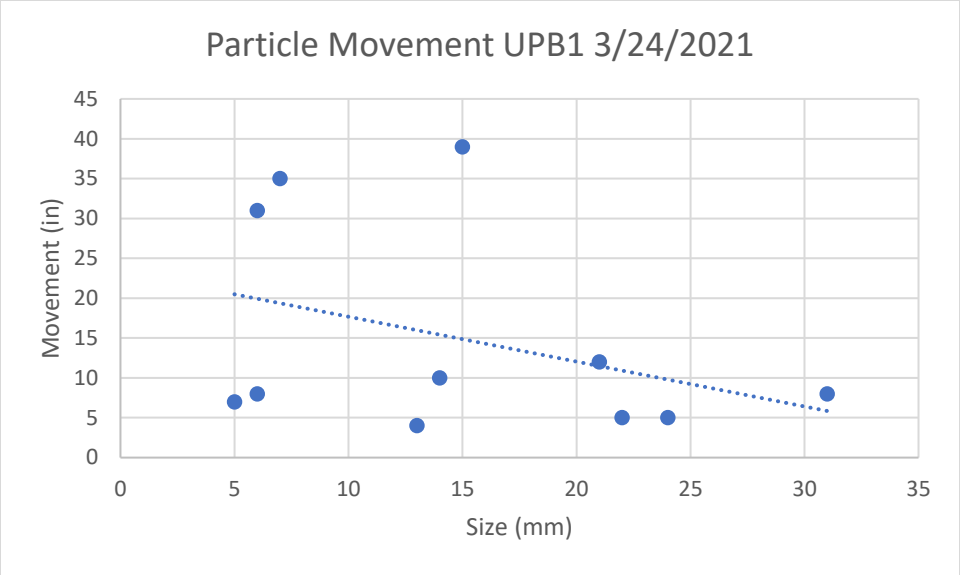

Figure 50: Particle Movement of Upper Point Bar 1 after Storm

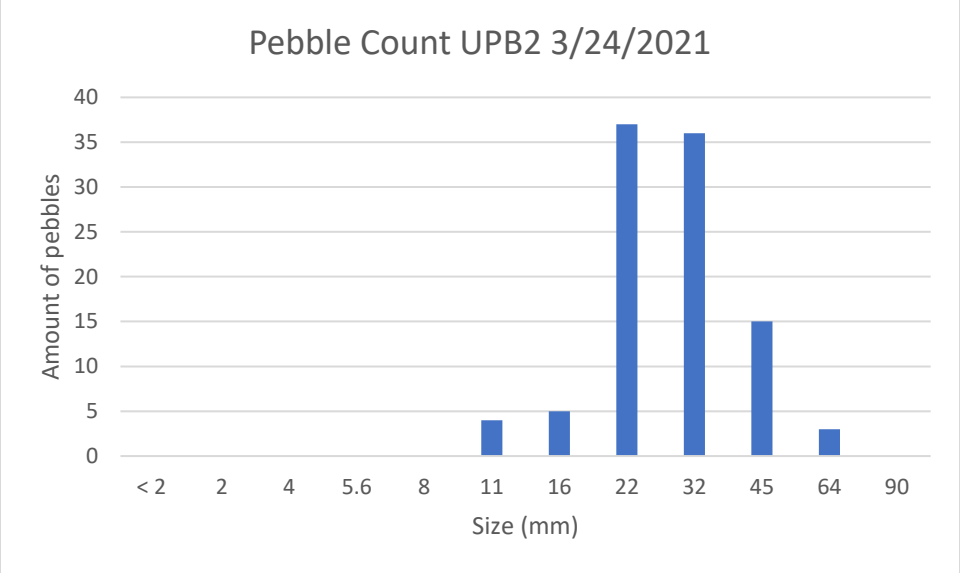

Figure 51: Pebble Count of Upper Point Bar 2

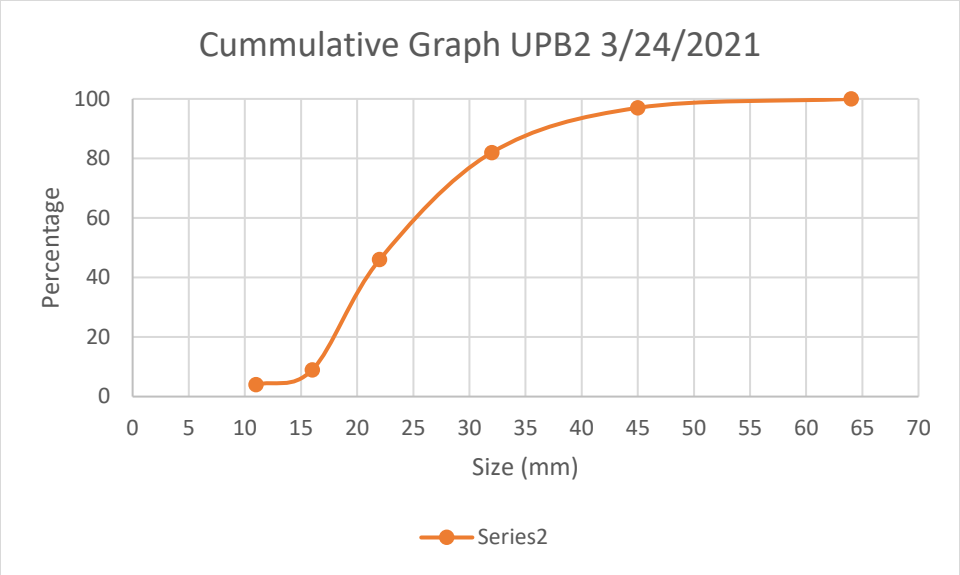

Figure 52: Cumulative Graph of Upper Point Bar 2

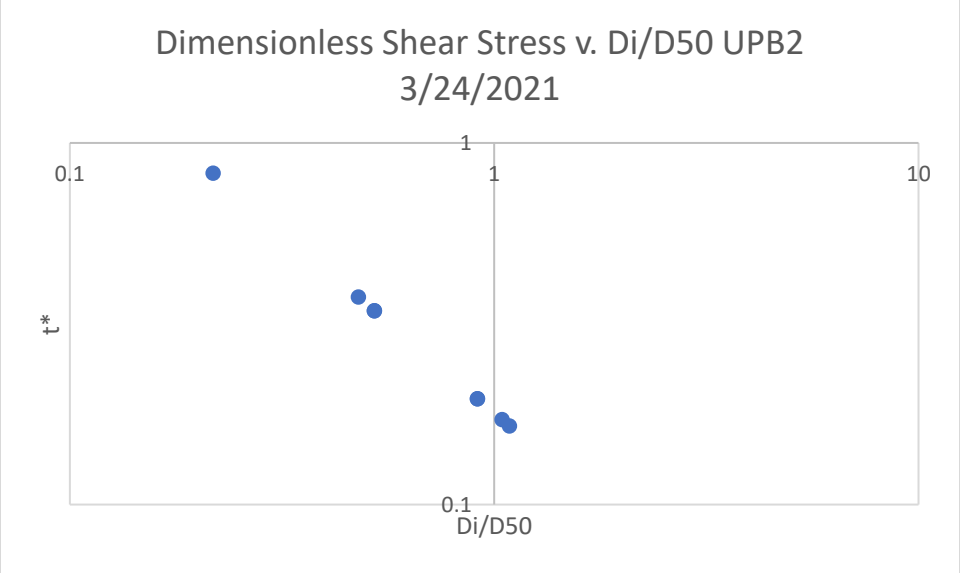

Figure 53: Dimensionless Shear Stress of Upper Point Bar 2

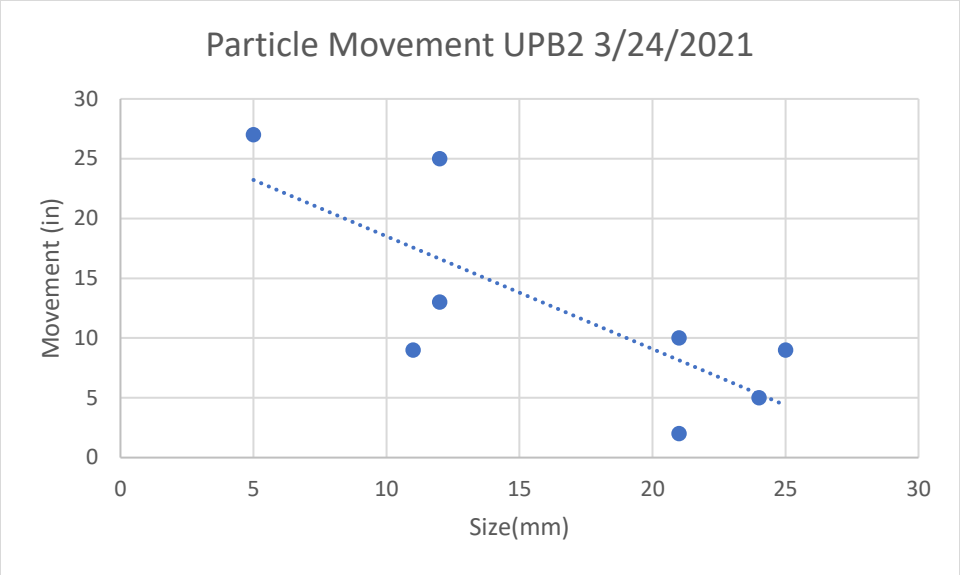

Figure 54: Particle Movement of Upper Point Bar 2 after Storm

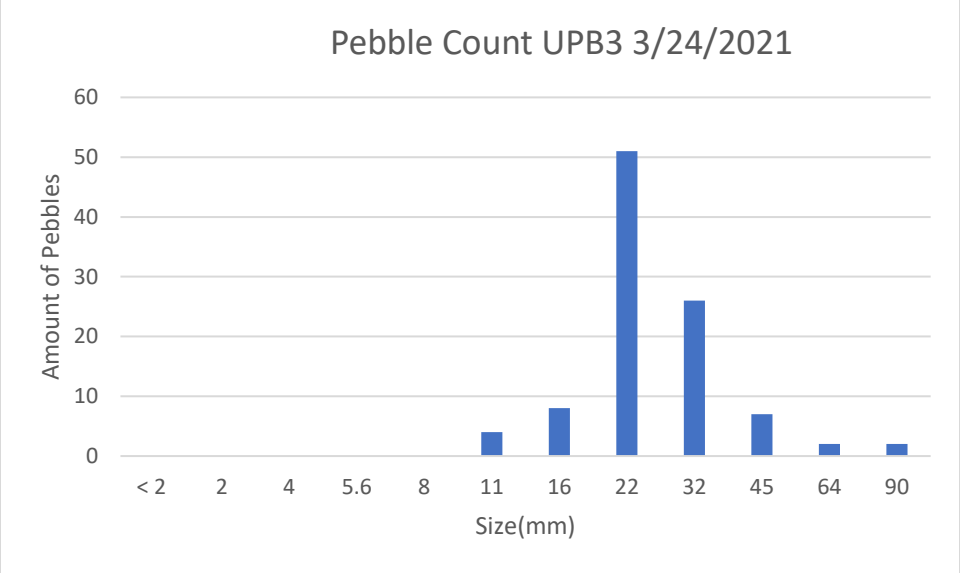

Figure 55: Pebble Count of Upper Point Bar 3

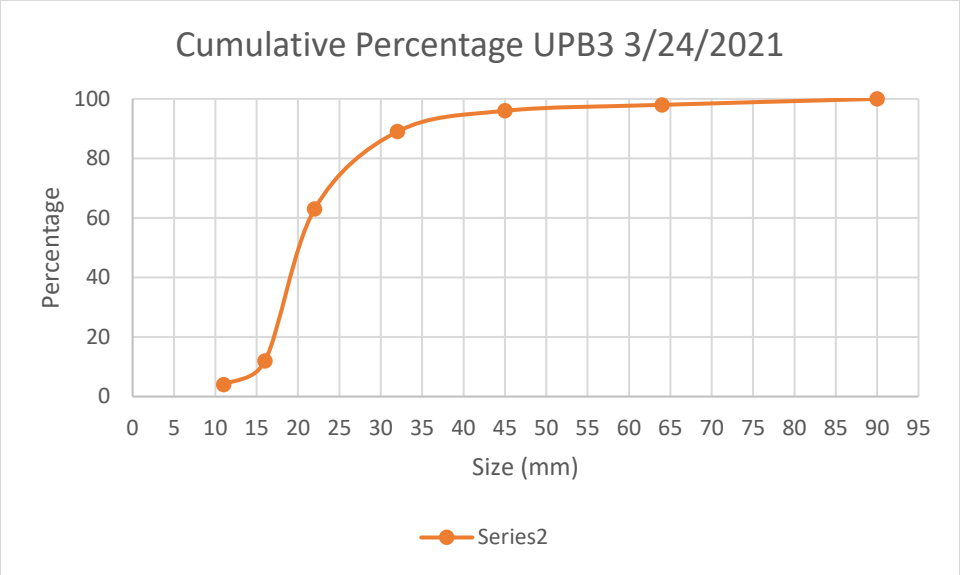

Figure 56: Cumulative Percentage of Upper Point Bar 3

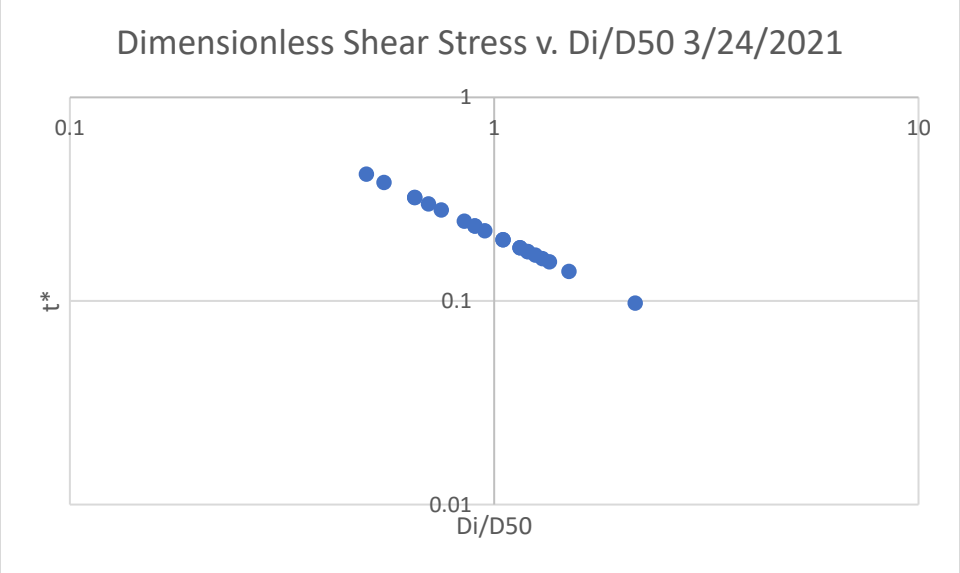

Figure 57: Dimensionless Shear Stress of Upper Point Bar 3

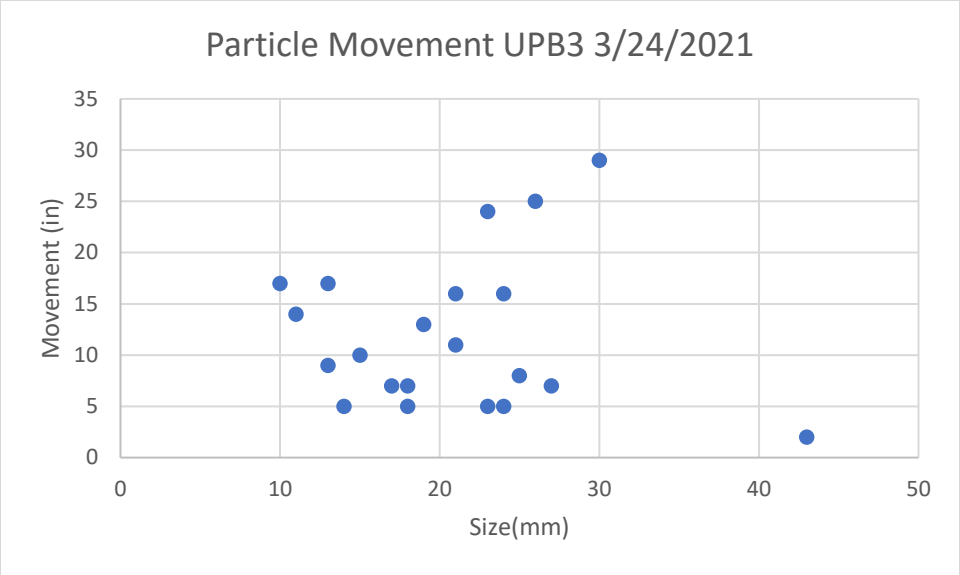

Figure 58: Particle Movement of Upper Point Bar 3 after Storm

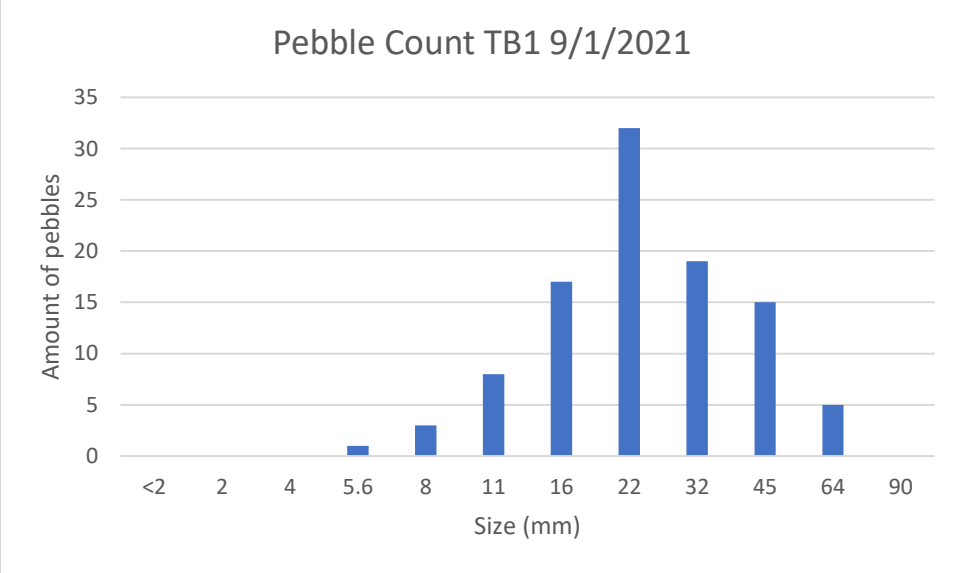

Figure 59: Pebble Count of Tree Bar 1 of Alluvial Reach

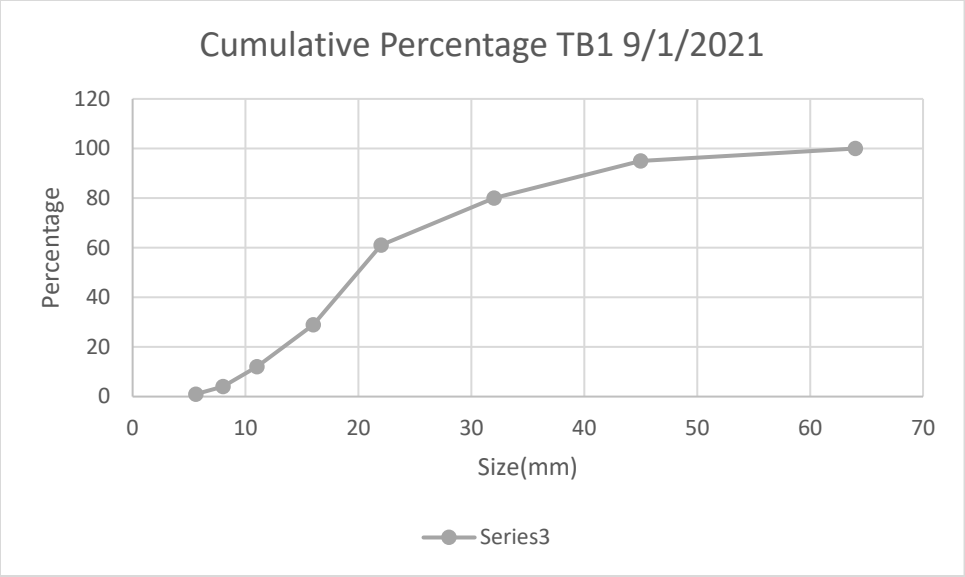

Figure 60: Cumulative Percentage of Tree Bar 1

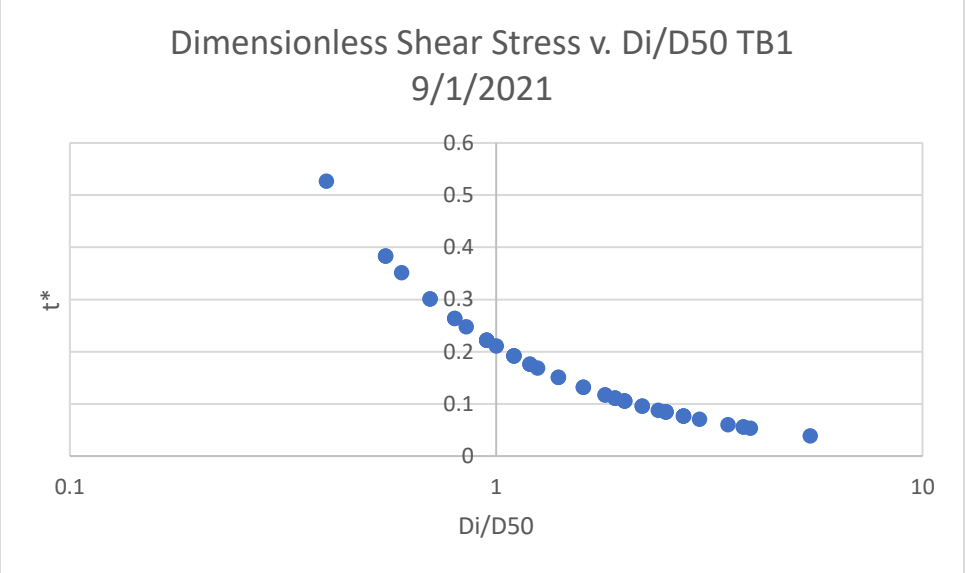

Figure 61: Dimensionless Shear Stress of Tree Bar 1

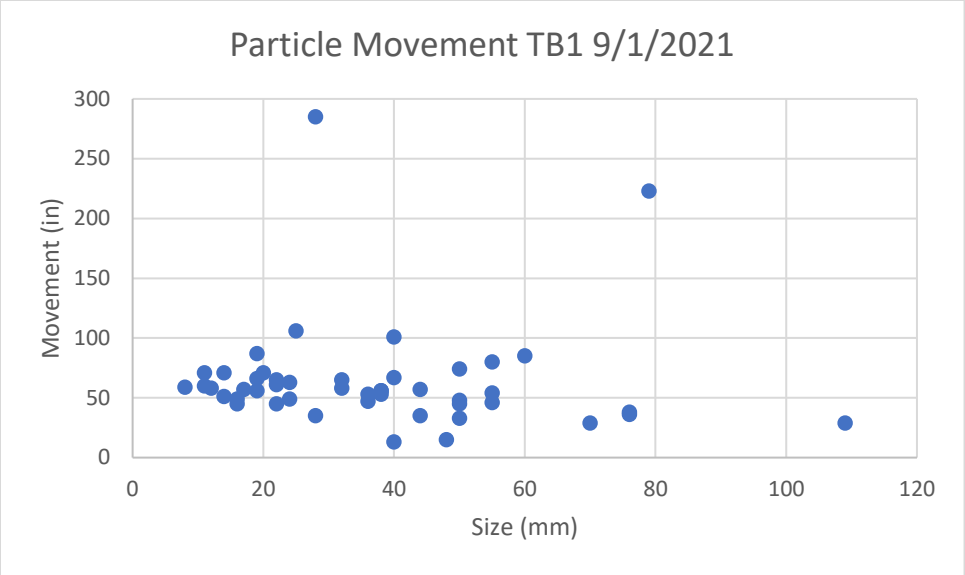

Figure 62: Particle Movement of Tree Bar 1 after Storm

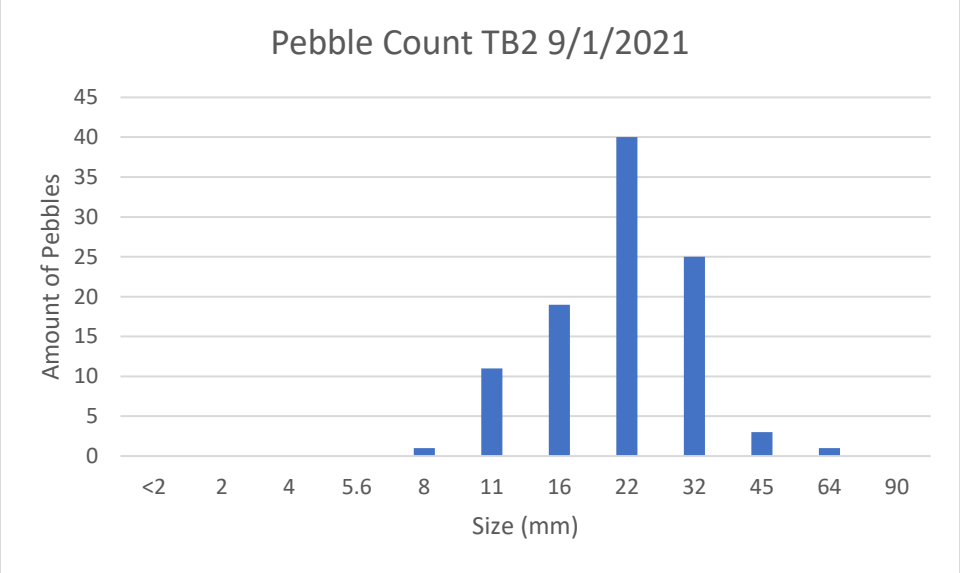

Figure 63: Pebble Count of Tree Bar 2

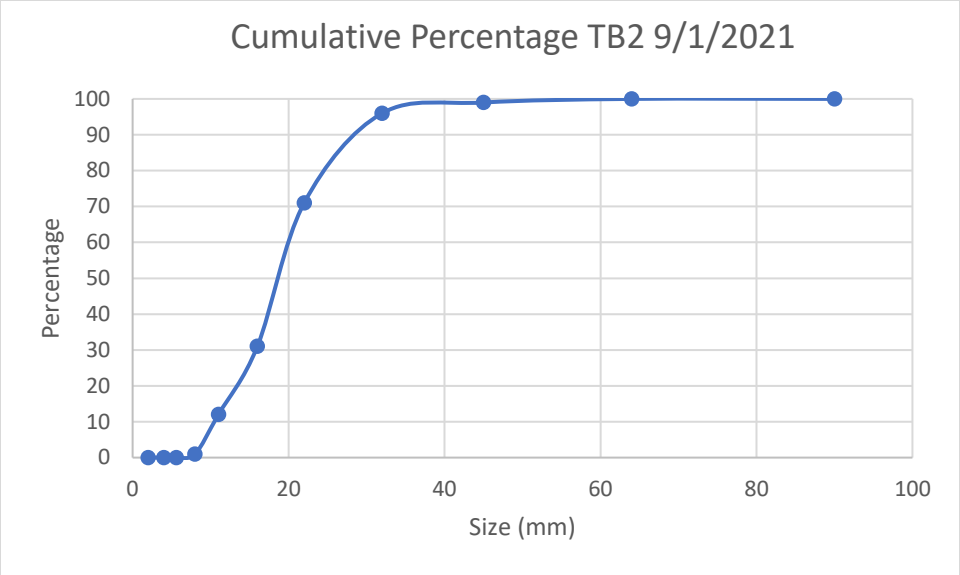

Figure 64: Cumulative Percentage of Tree Bar 2

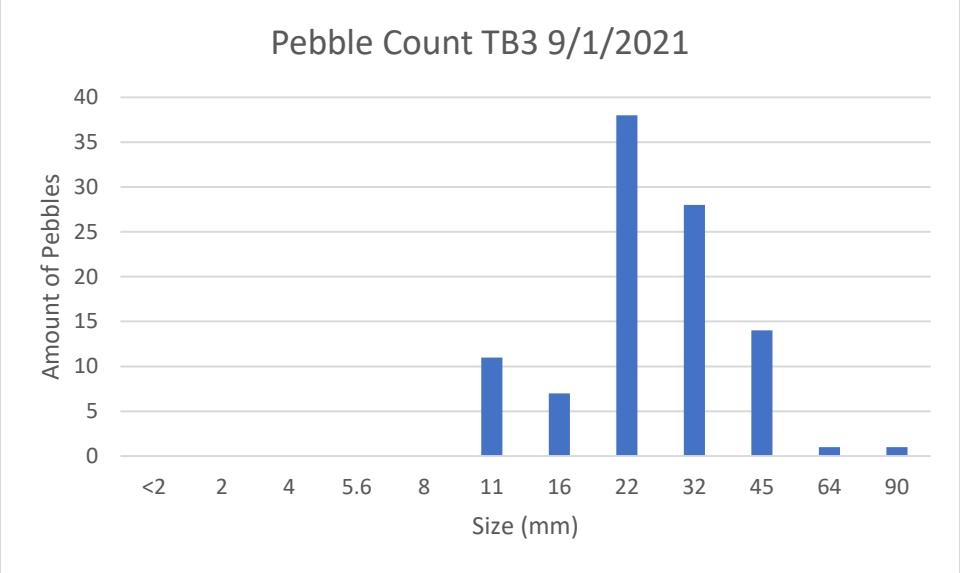

Figure 65: Pebble Count of Tree Bar 3

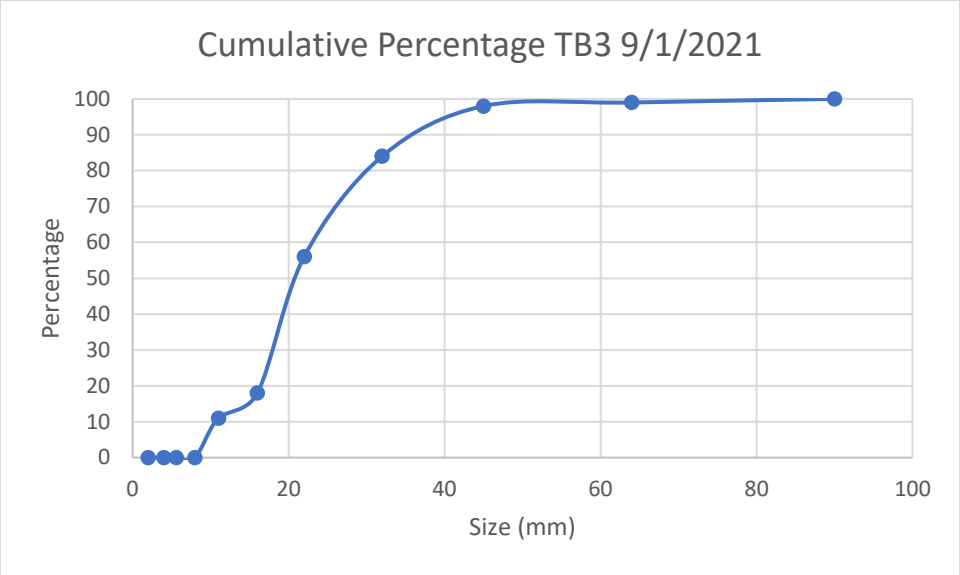

Figure 66: Cumulative Percentage of Tree Bar 3

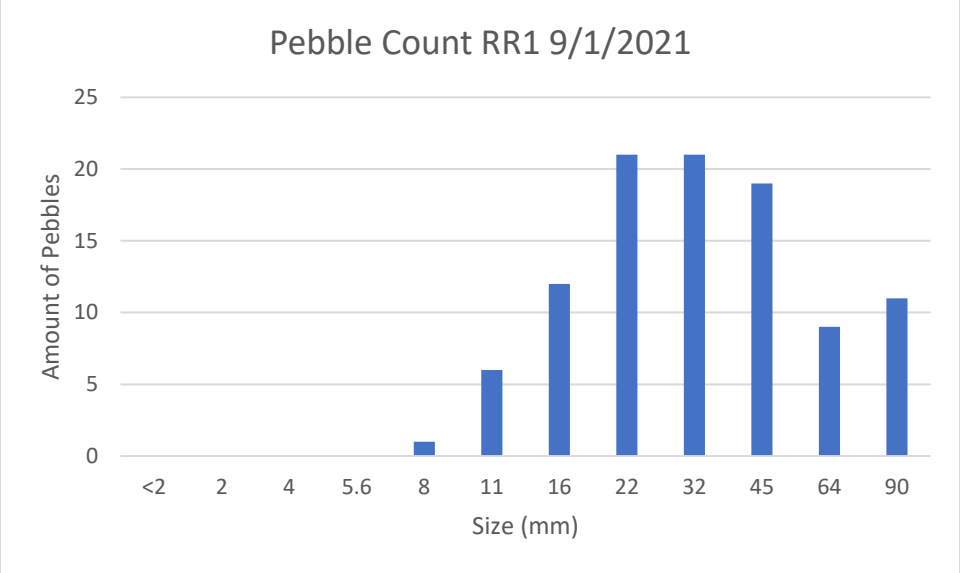

Figure 67: Pebble Count of Rift Rap 1 of the Alluvial Reach

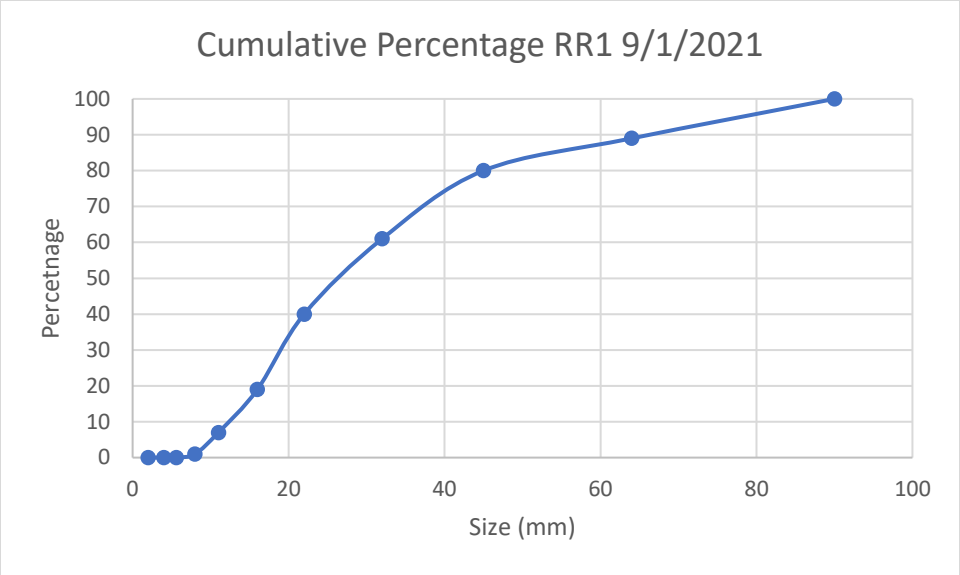

Figure 68: Cumulative Percentage of Rift Rap 1

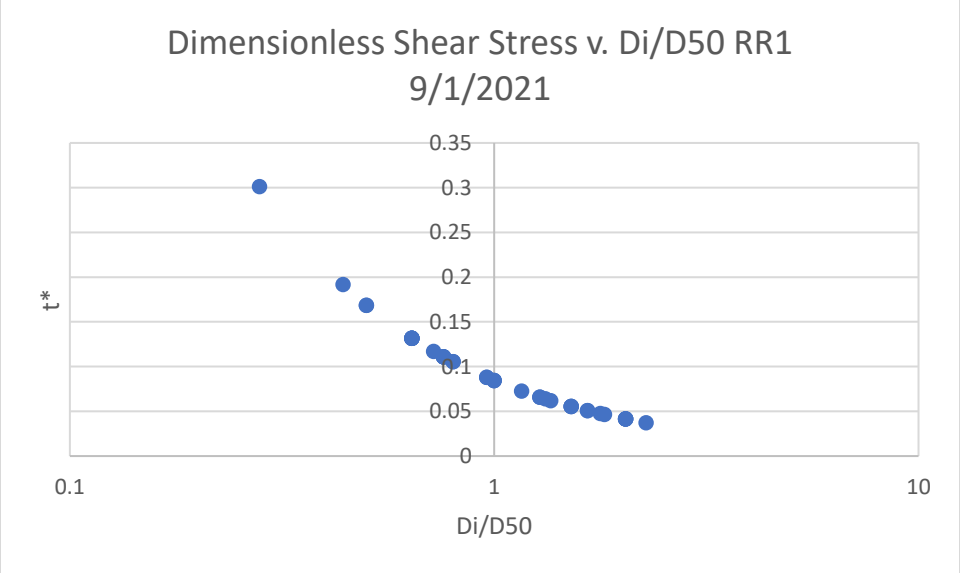

Figure 69: Dimensionless Shear Stress of Rift Rap 1

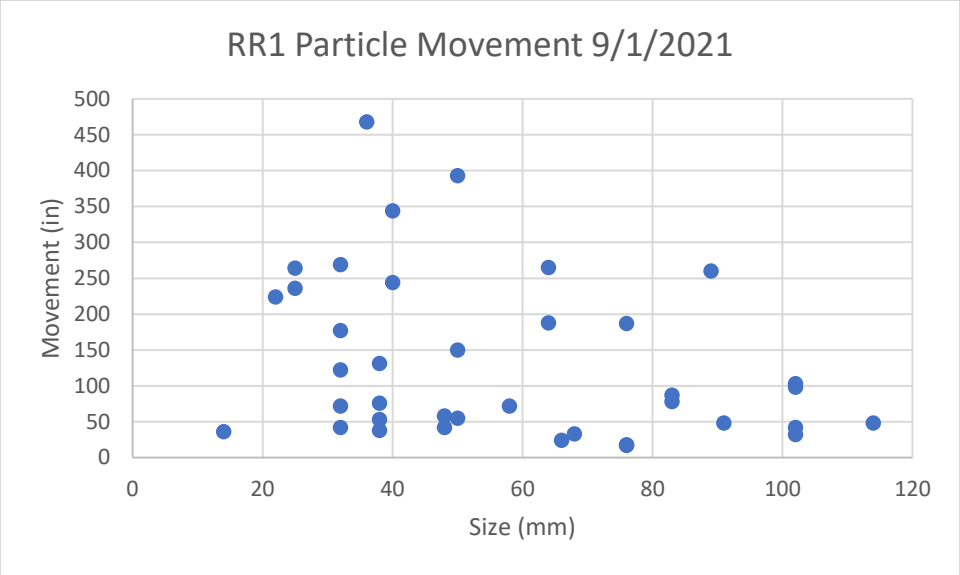

Figure 70: Particle Movement of Rift Rap after Storm

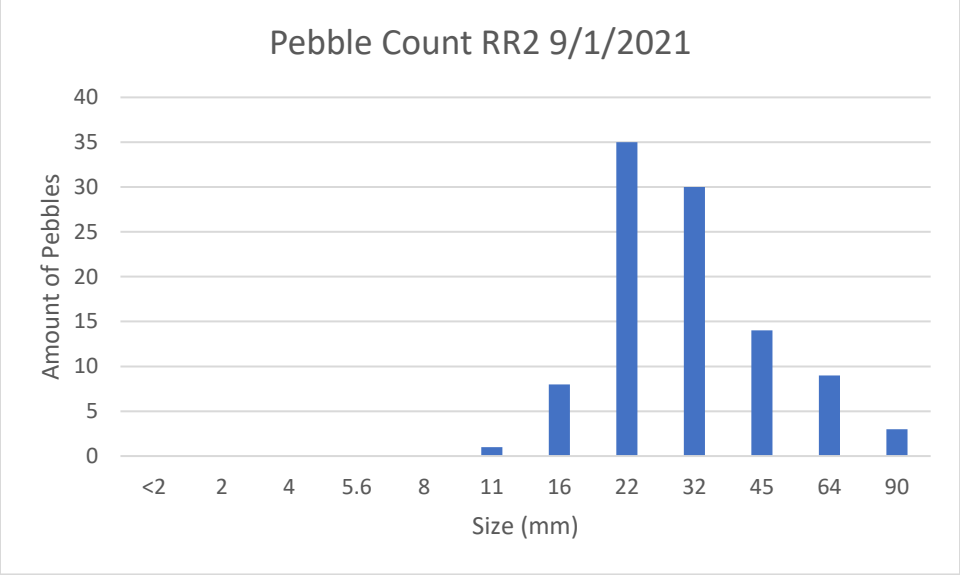

Figure 71: Pebble Count of Rift Rap 2

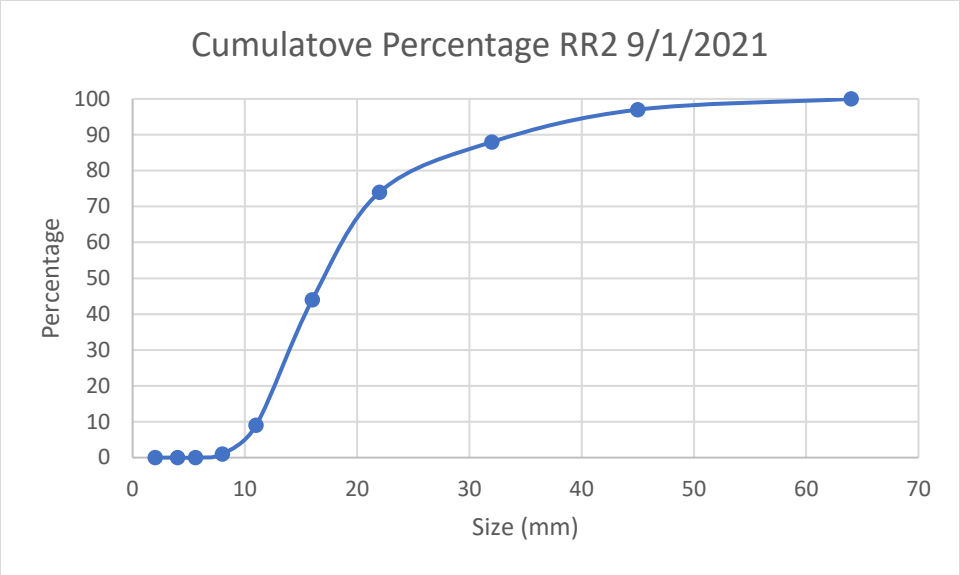

Figure 72: Cumulative Percentage of Rift Rap 2

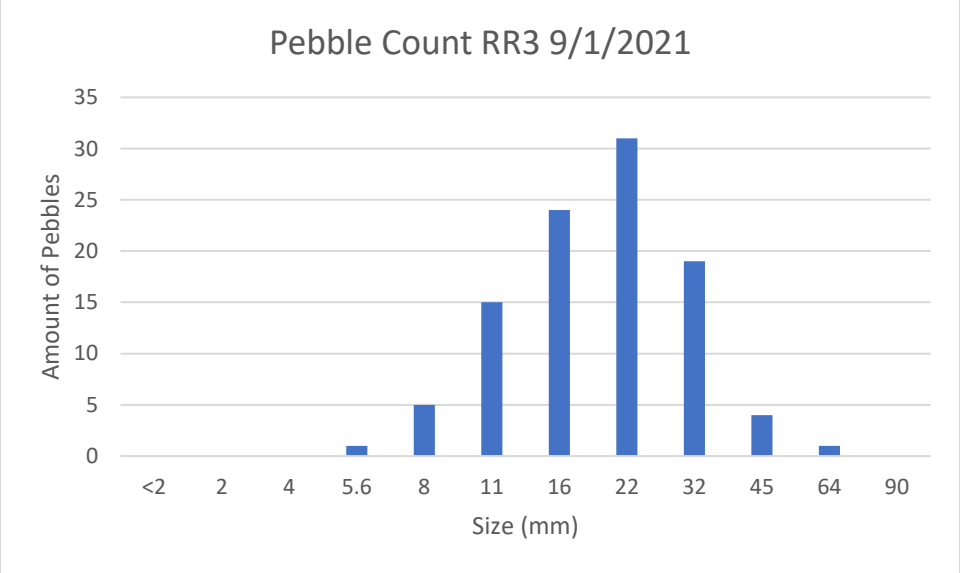

Figure 73: Pebble Count of Rift Rap 3

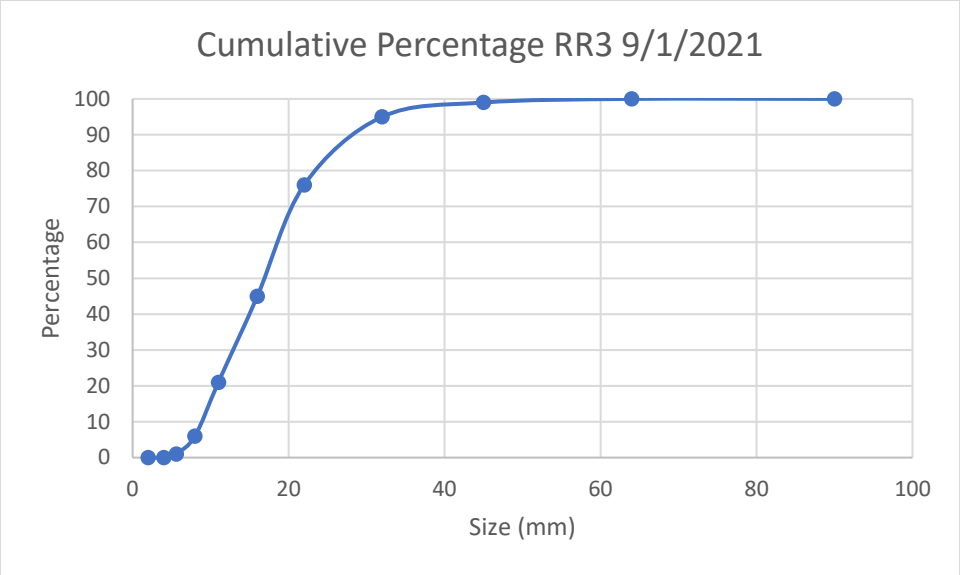

Figure 74: Cumulative Percentage of Rift Rap 3

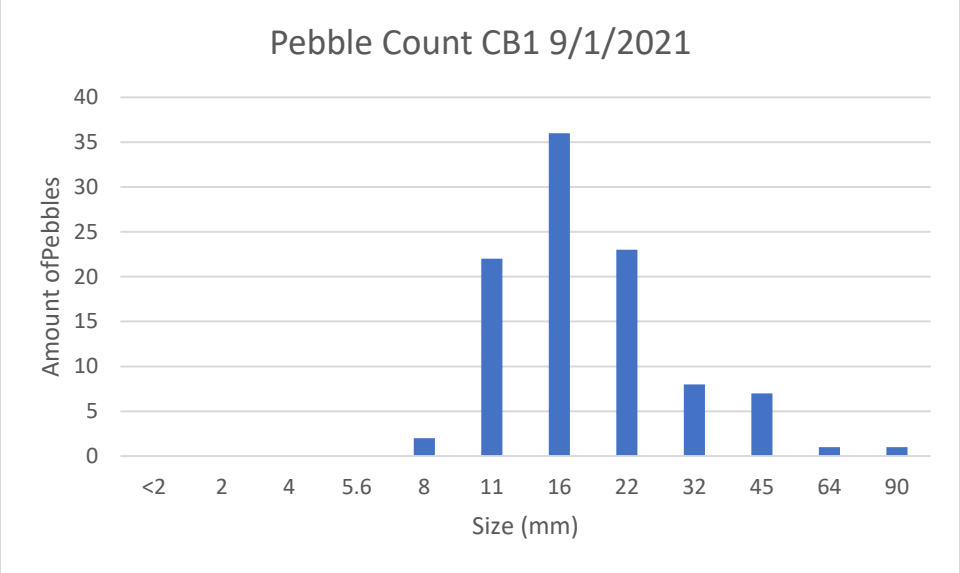

Figure 75: Pebble Count of Central Bar 1

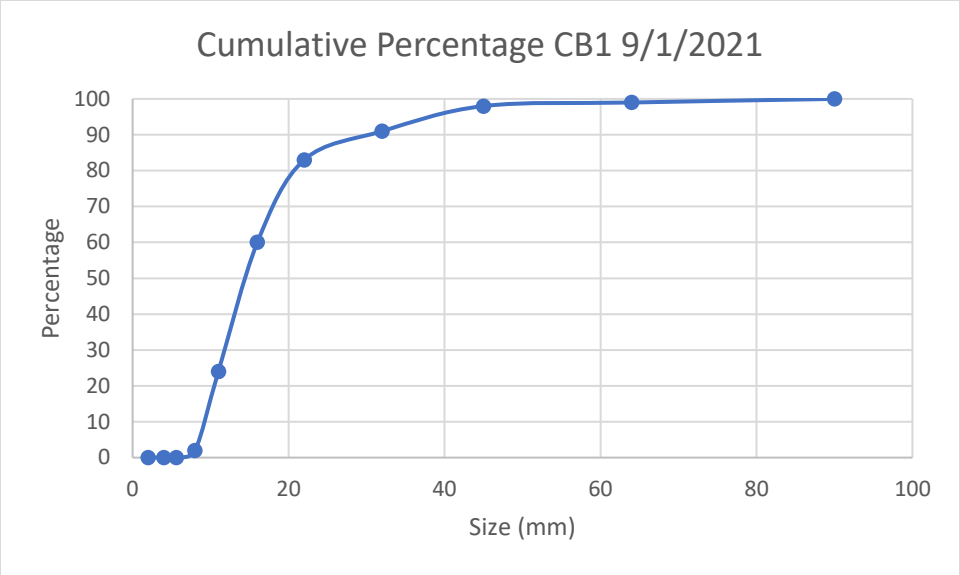

Figure 76: Cumulative Percentage of Central Bar 1

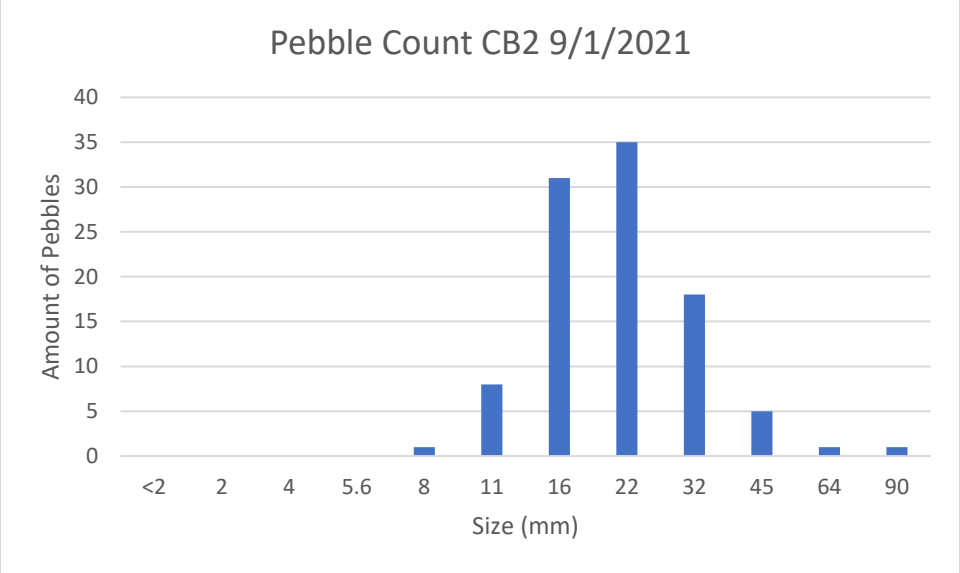

Figure 77: Pebble Count of Central Bar 2

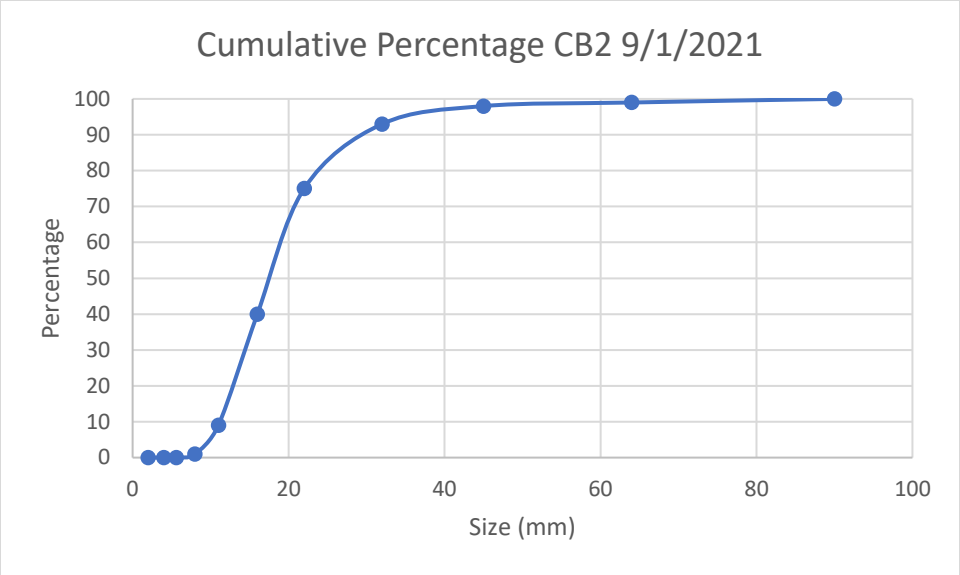

Figure 78: Cumulative Percentage of Central Bar 2

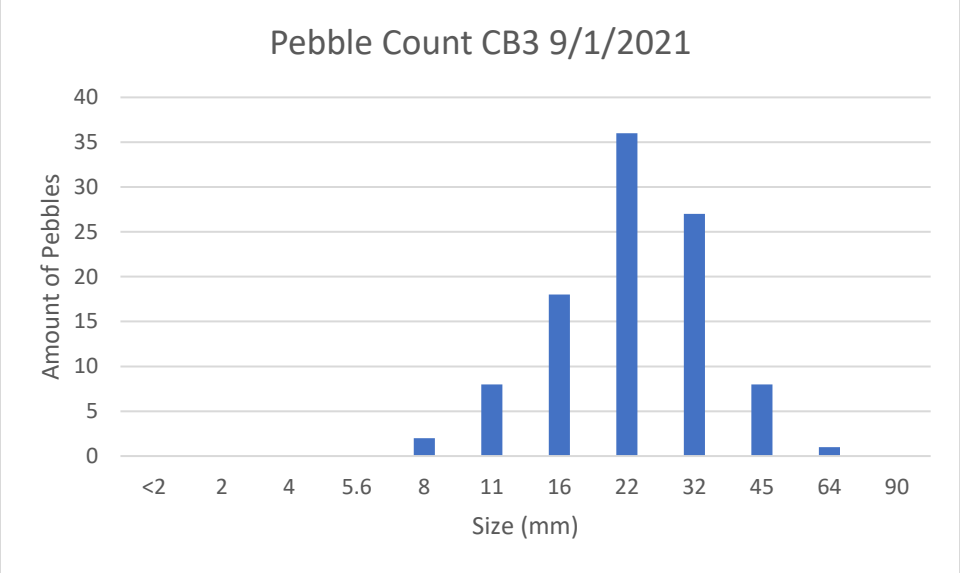

Figure 79: Pebble Count of Central Bar 3

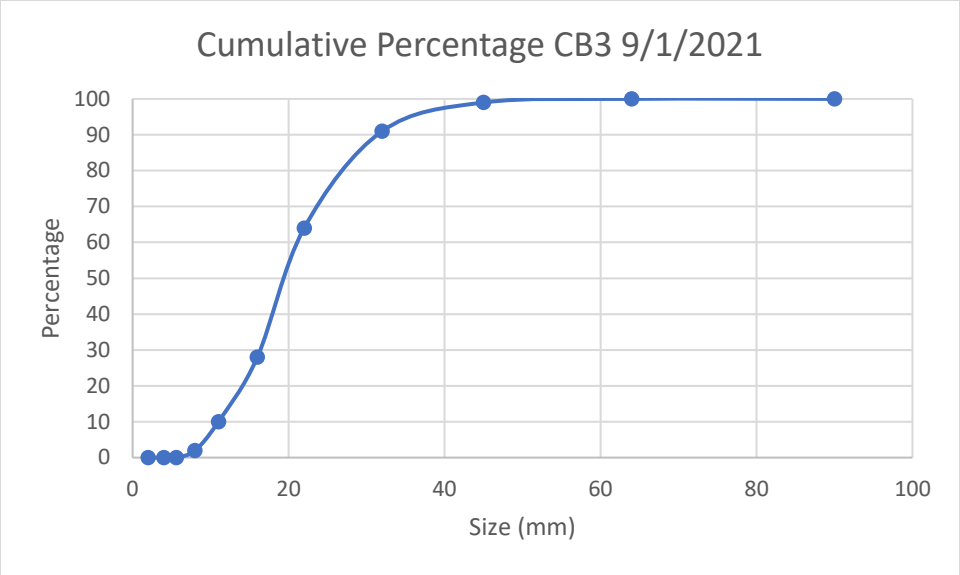

Figure 80: Cumulative Percentage of Central Bar 3

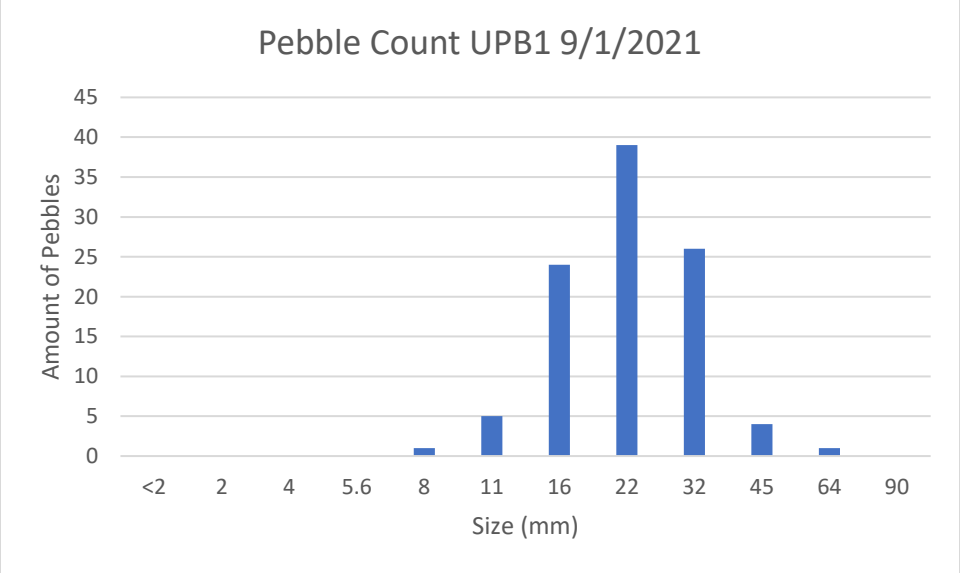

Figure 81: Pebble Count of Upper Point Bar 1

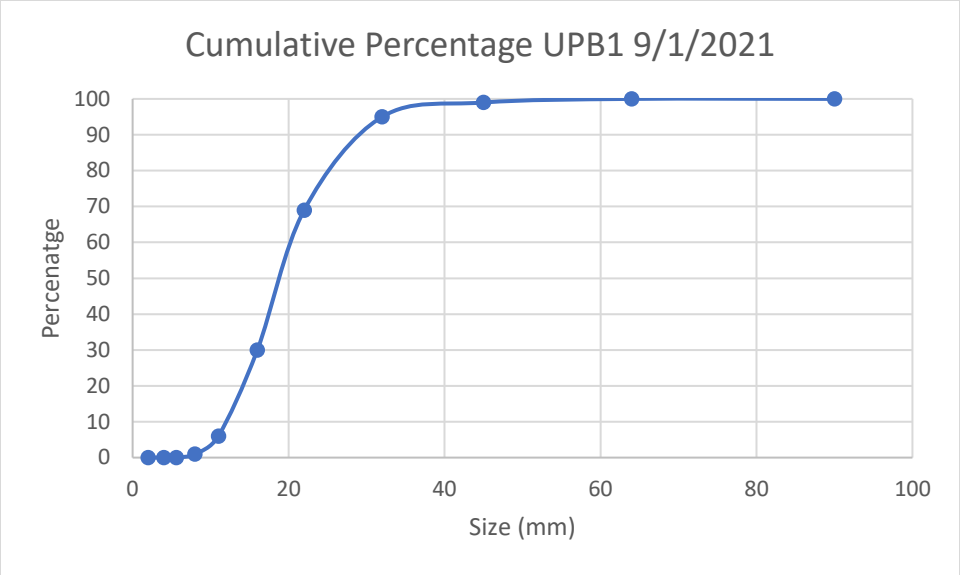

Figure 82: Cumulative Percentage of Upper Point Bar 1

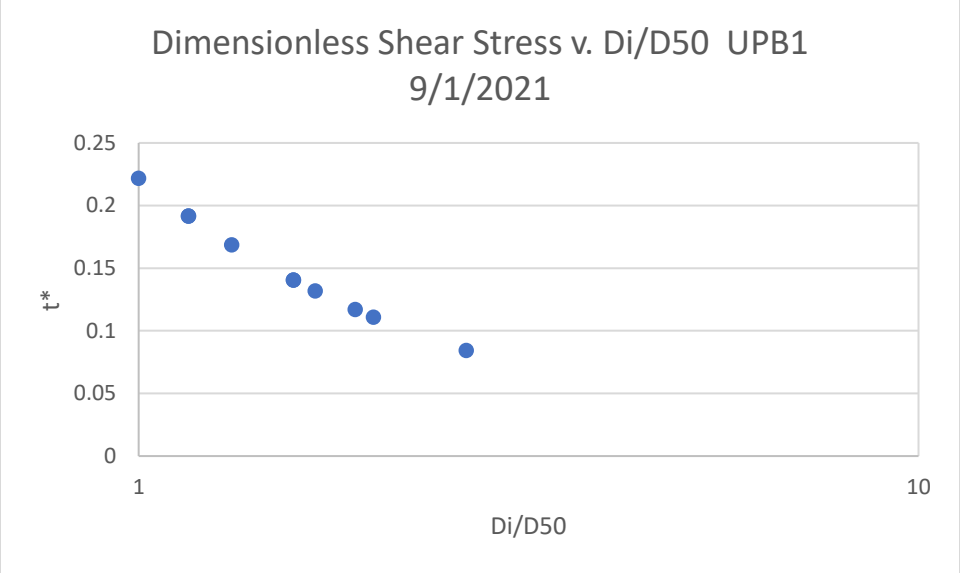

Figure 83: Dimensionless Shear Stress of Upper Point Bar 1

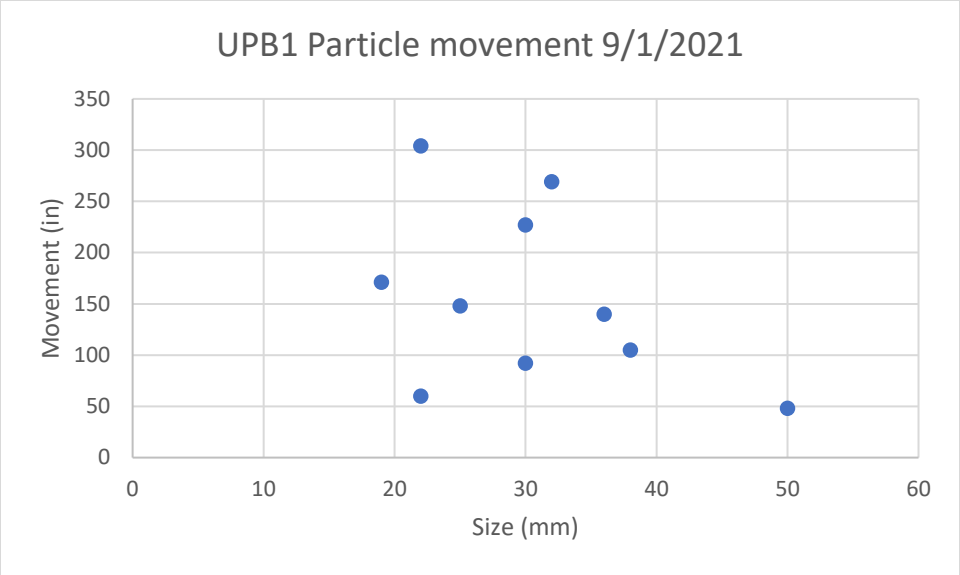

Figure 84: Particle Movement of Upper Point Bar 1 after Storm

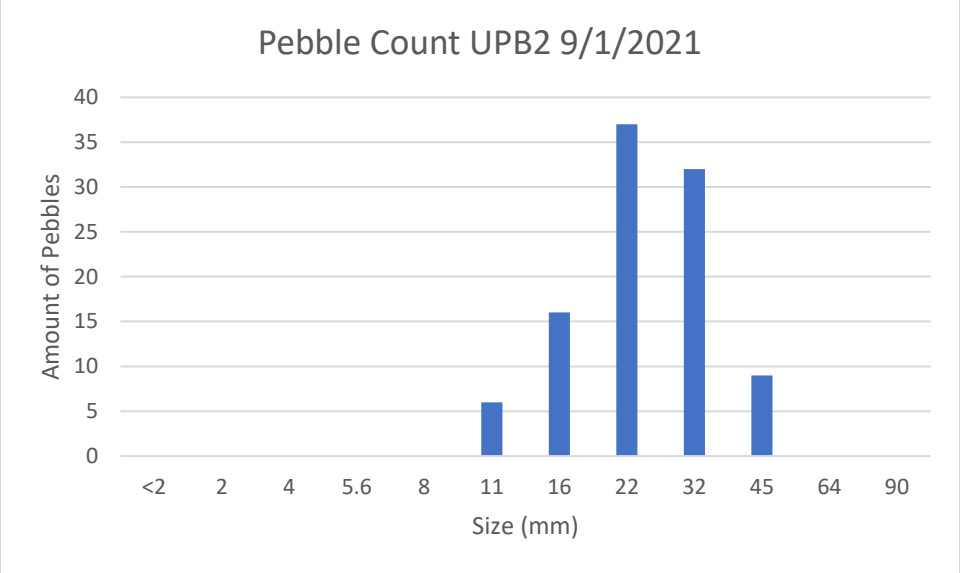

Figure 85: Pebble Count of Upper Point Bar 2

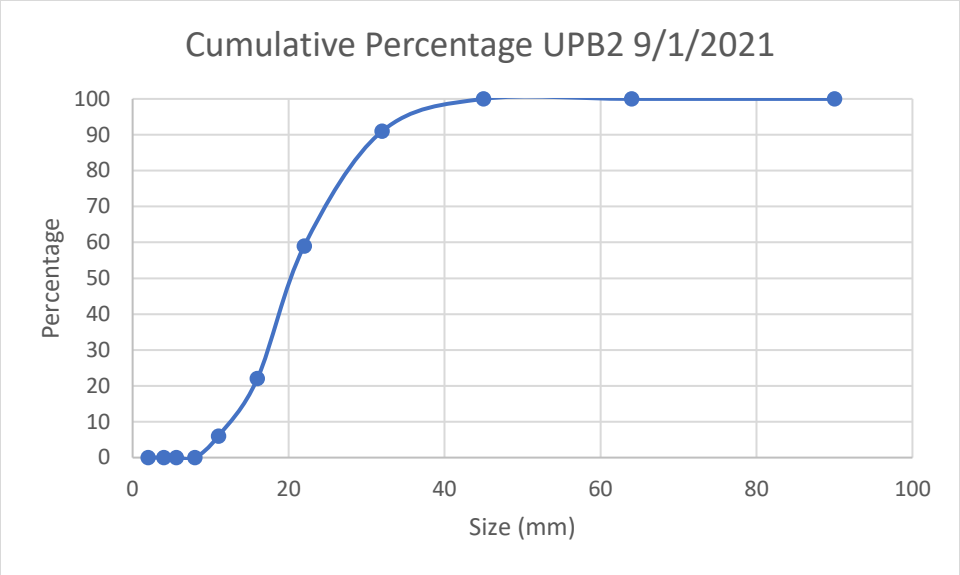

Figure 86: Cumulative Percentage of Upper Point Bar 2

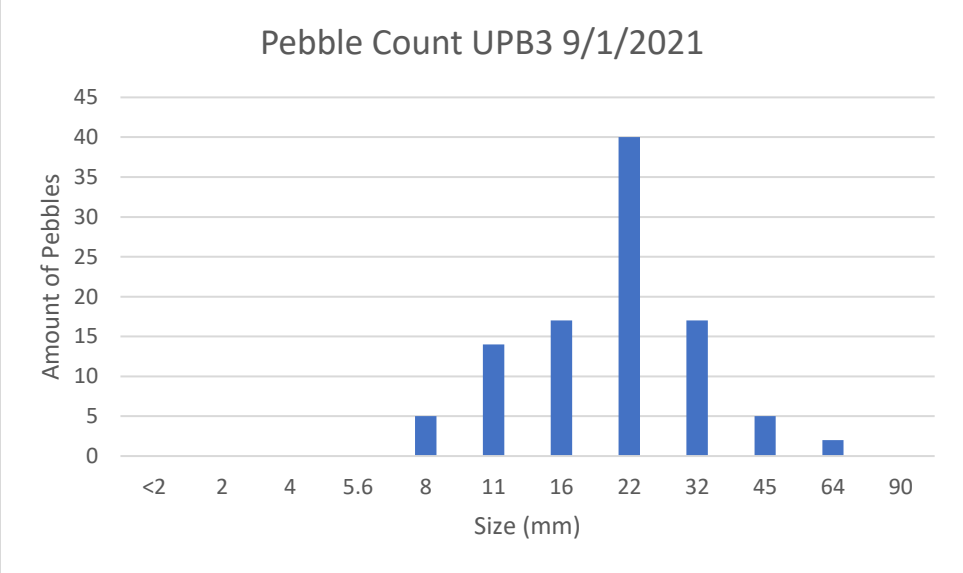

Figure 87: Pebble Count of Upper Point Bar 3

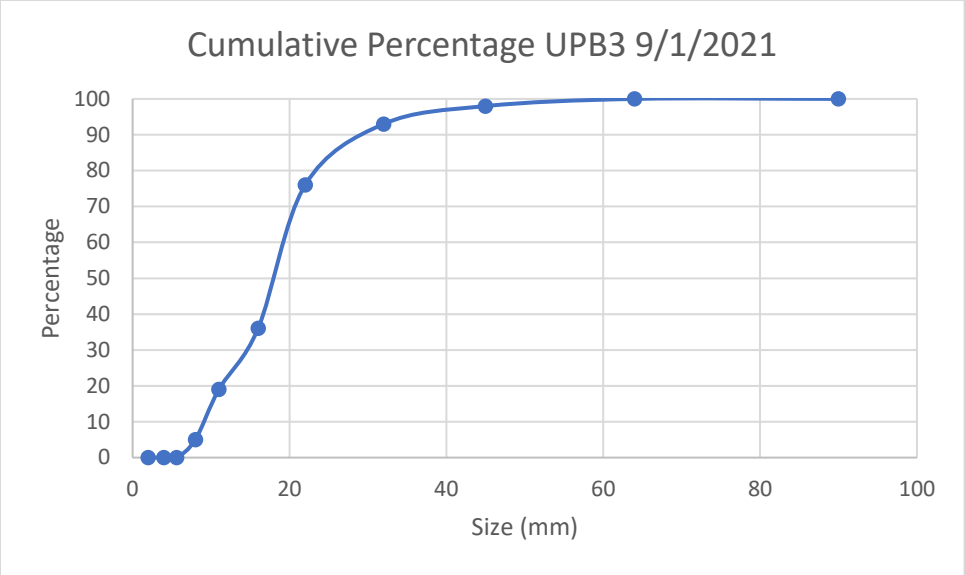

Figure 88: Cumulative Percentage of Upper Point Bar 3

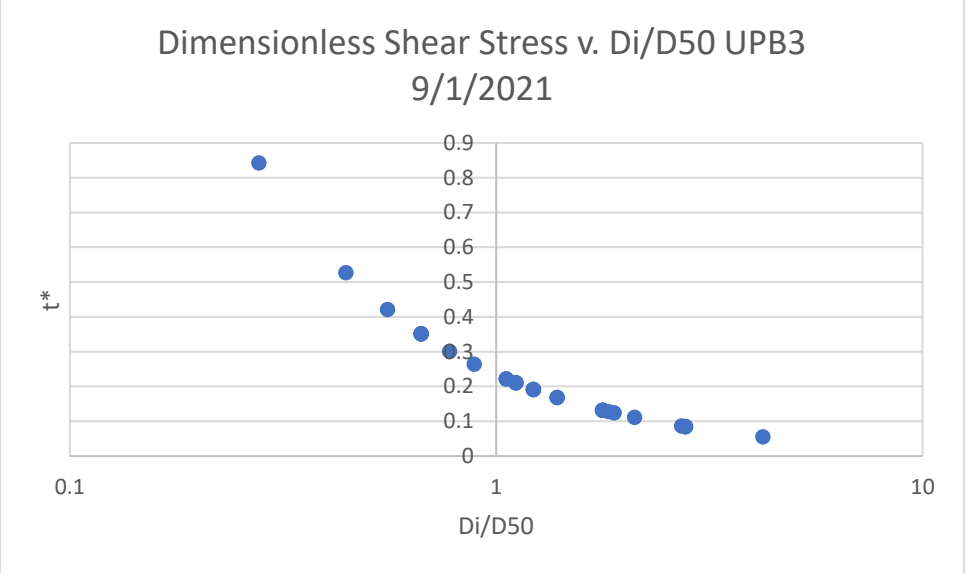

Figure 89: Dimensionless Shear Stress of Upper point Bar 3

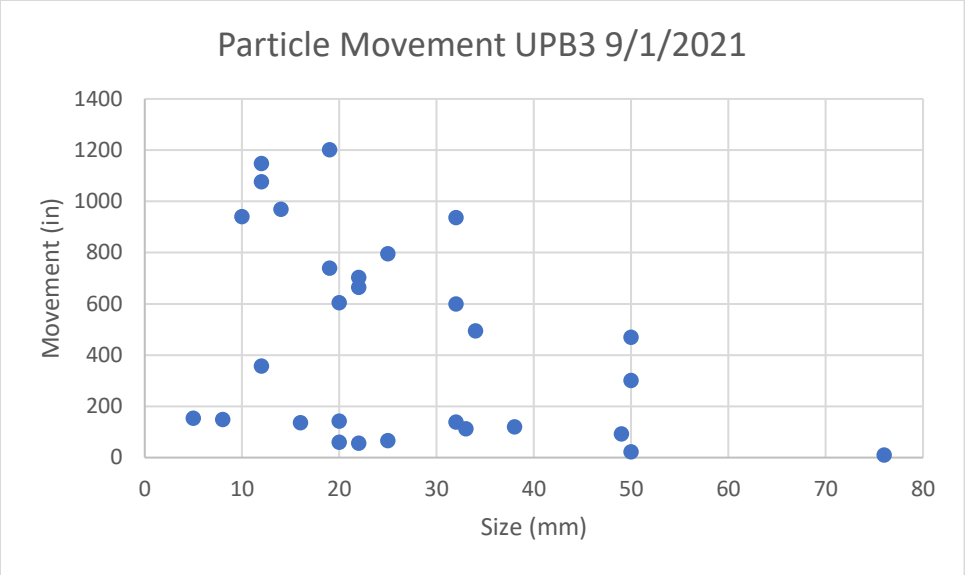

Figure 90: Particle Movement of Upper Point Bar 3 after Storm

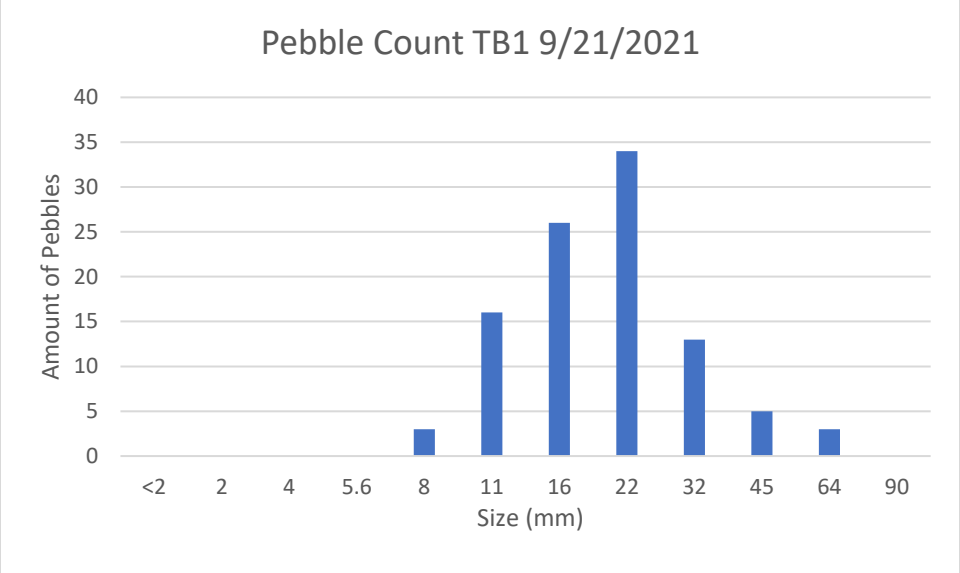

Figure 91: Pebble Count of Tree Bar 1

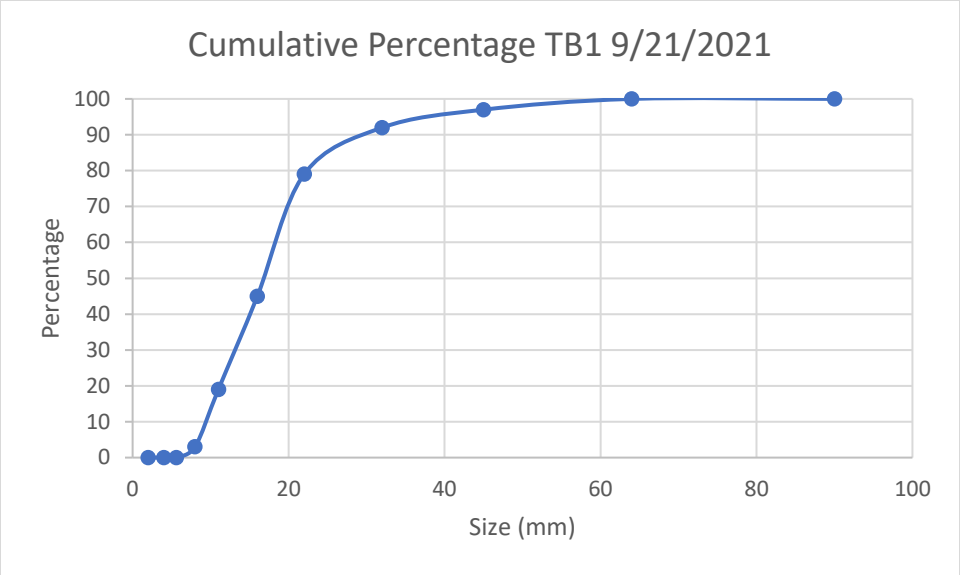

Figure 92: Cumulative Percentage of Tree Bar 1

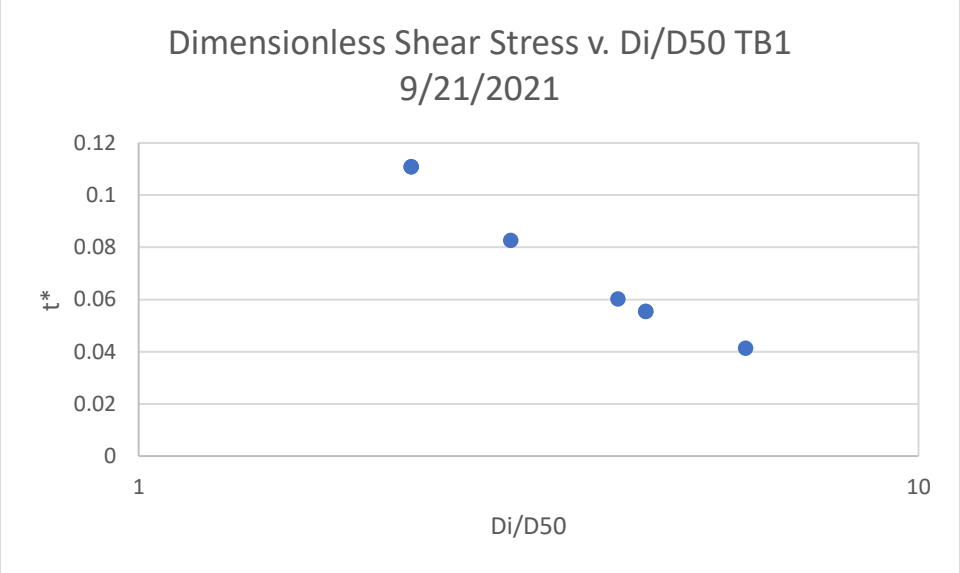

Figure 93: Dimensionless Shear Stress of Tree Bar 1

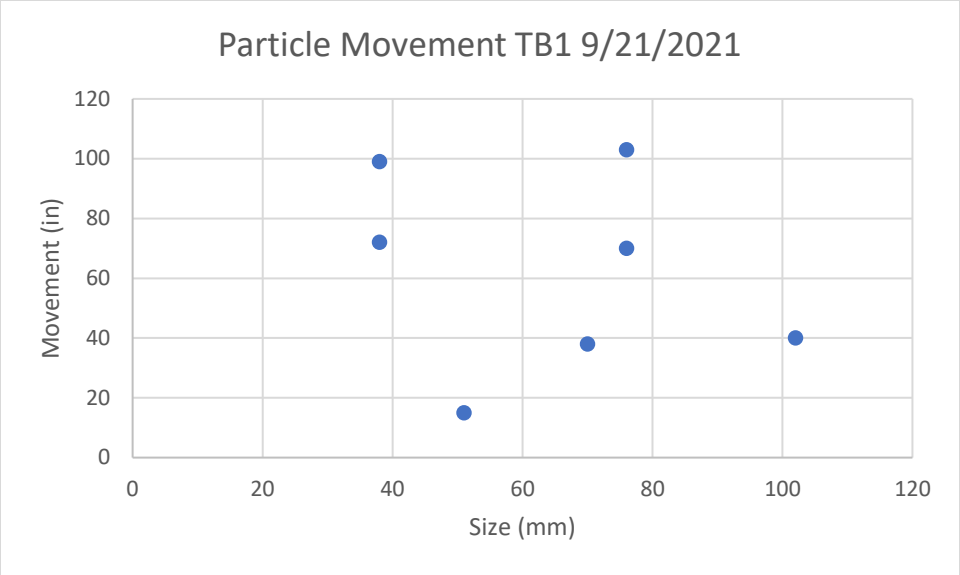

Figure 95: Particle Movement of Tree Bar 1 after Storm

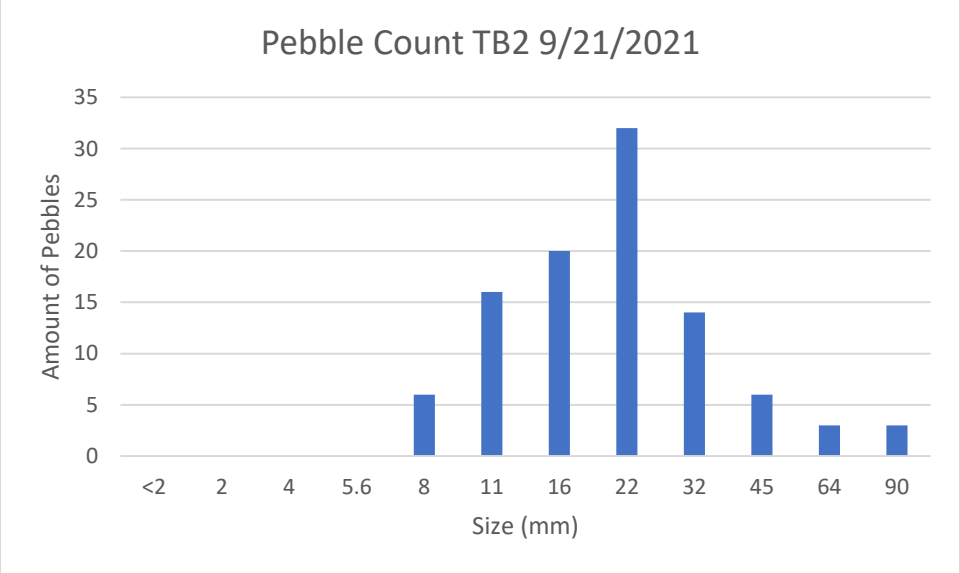

Figure 96: Pebble Count of Tree Bar 2

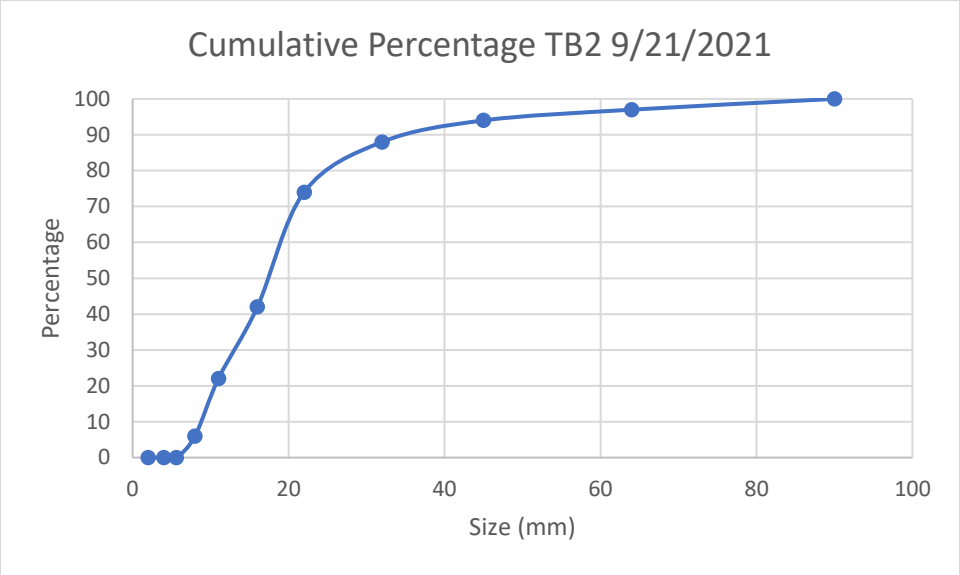

Figure 97: Cumulative Percentage of Tree Bar 2

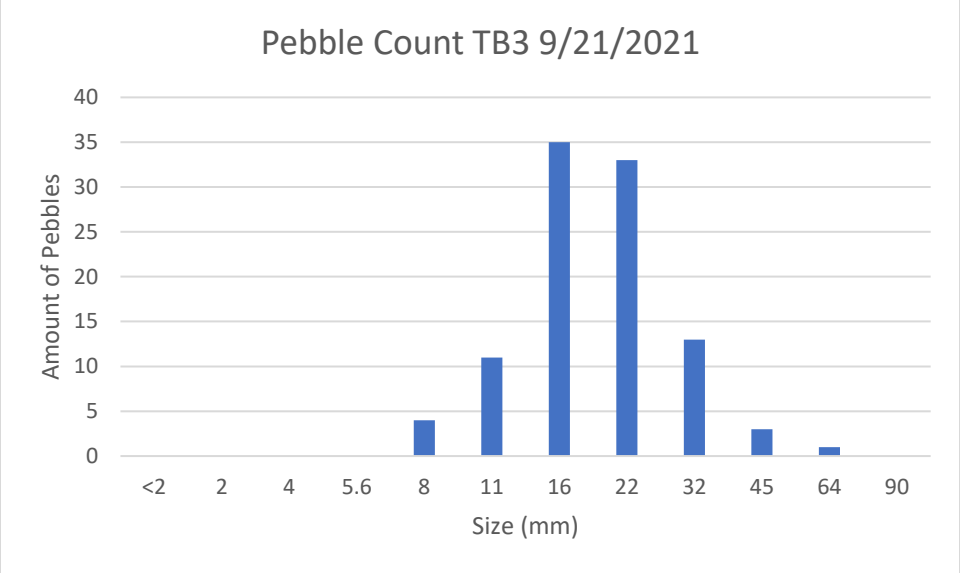

Figure 98: Pebble Count of Tree Bar 3

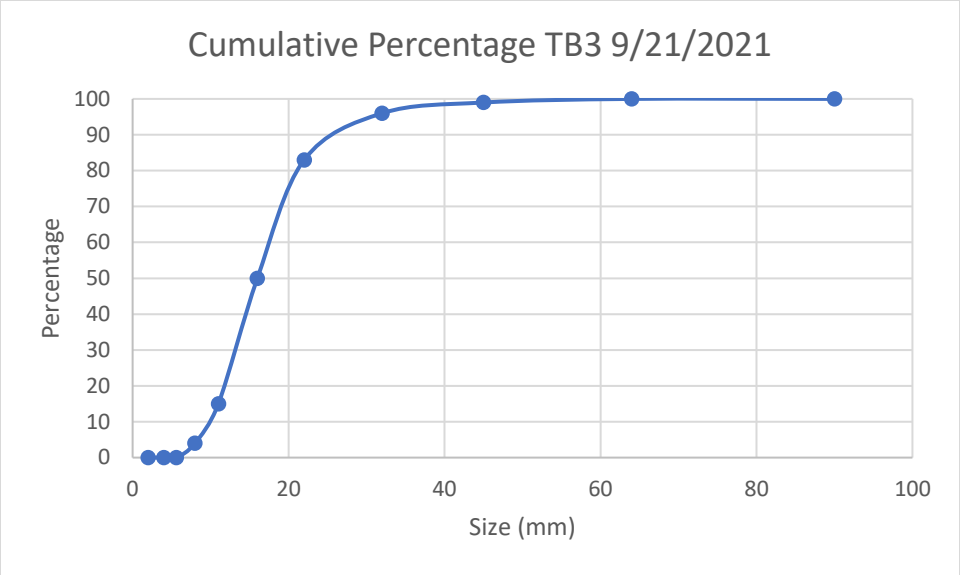

Figure 99: Cumulative Percentage of Tree Bar 3

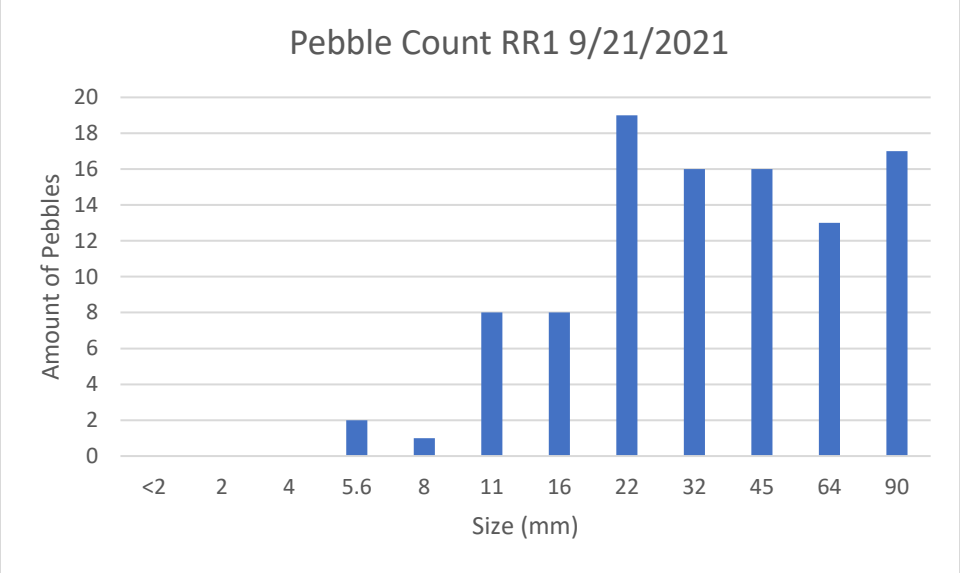

Figure 100: Pebble Count of Rift Rap 1

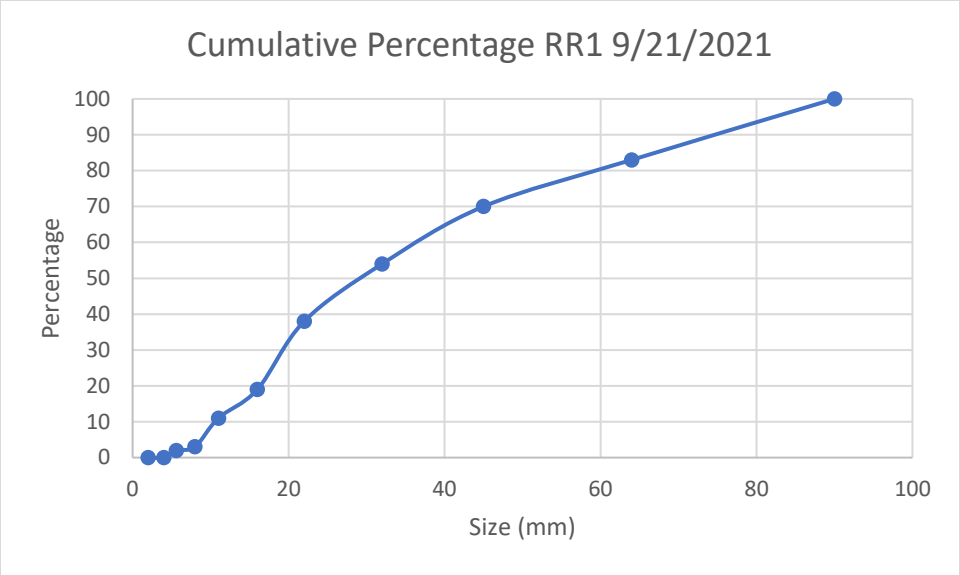

Figure 101: Cumulative Percentage of Rift Rap 1

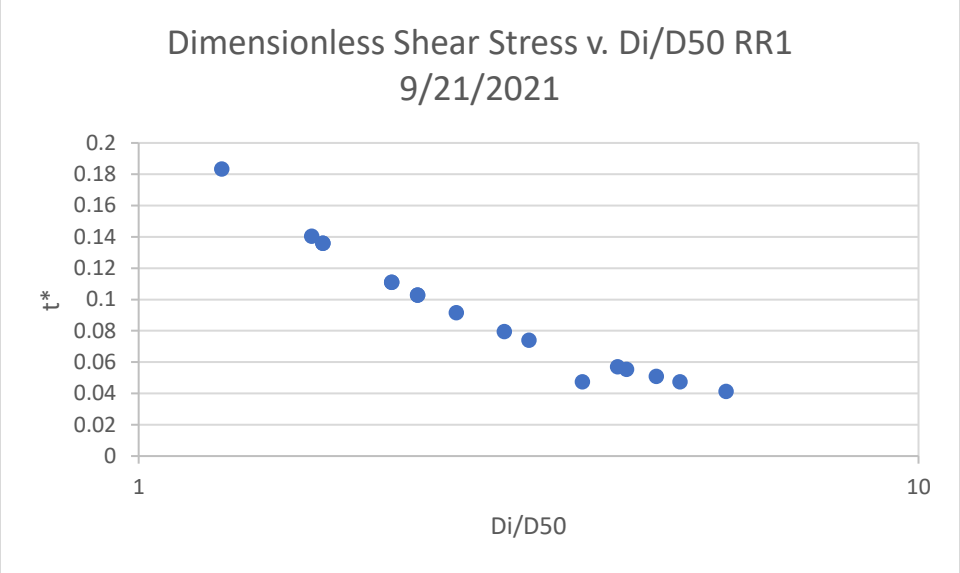

Figure 102: Dimensionless Shear Stress of Rift Rap 1

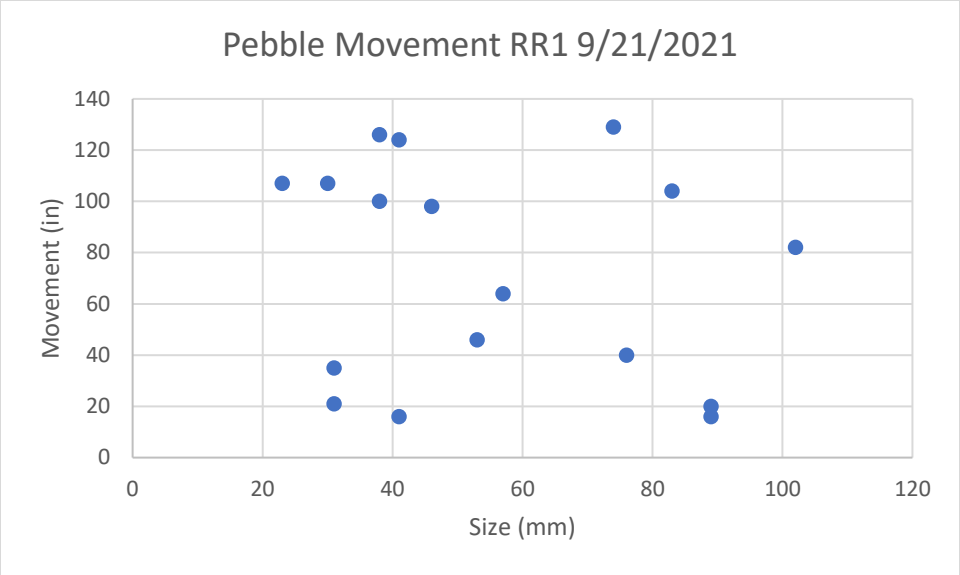

Figure 103: Pebble Movement of Rift Rap 1 after Storm

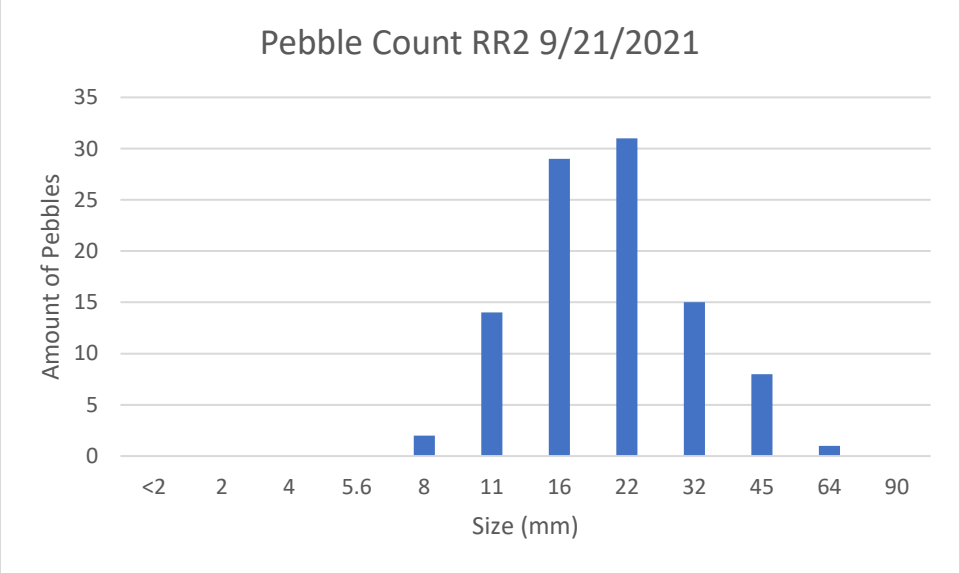

Figure 104: Pebble Count of Rift Rap 2

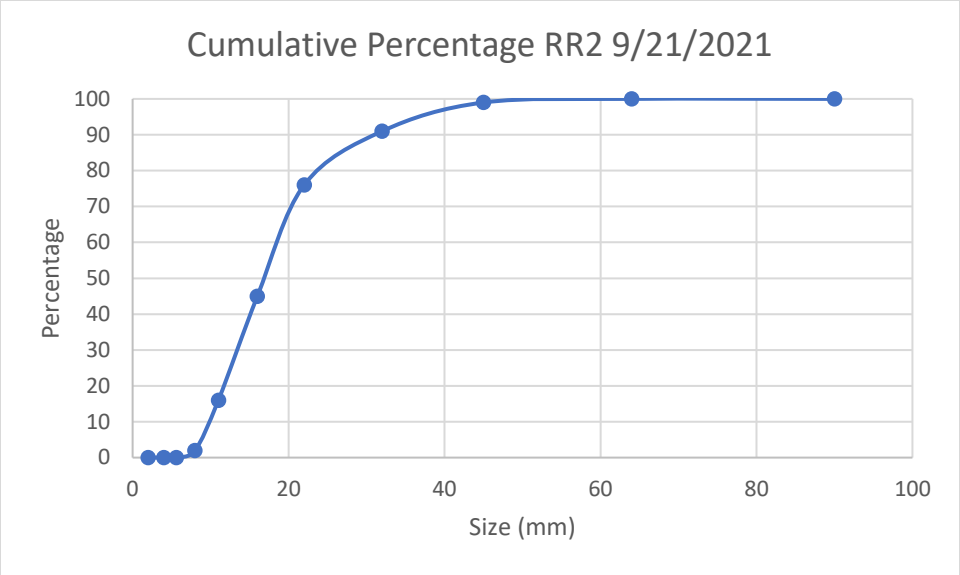

Figure 105: Cumulative Percentage of Rift Rap 2

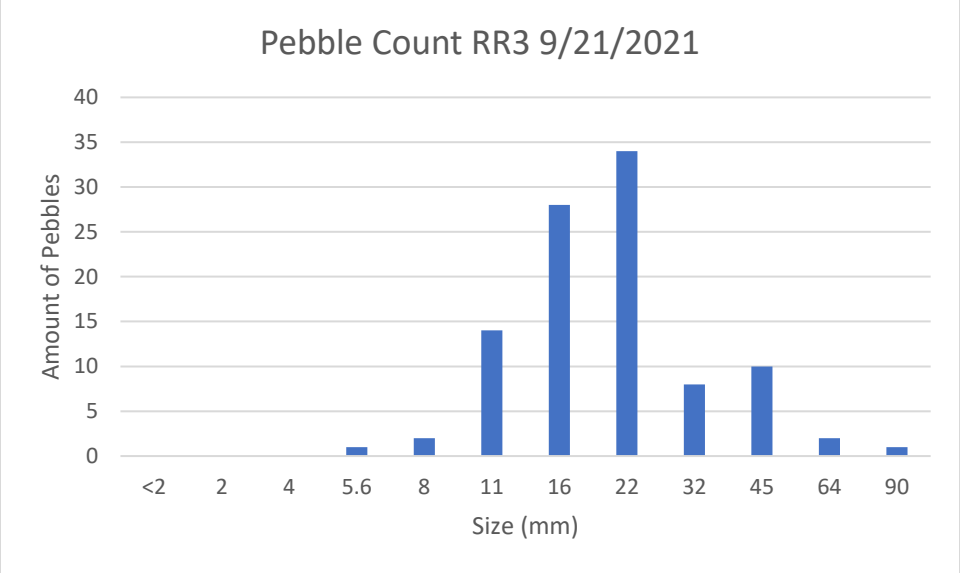

Figure 106: Pebble Count of Rift Rap 3

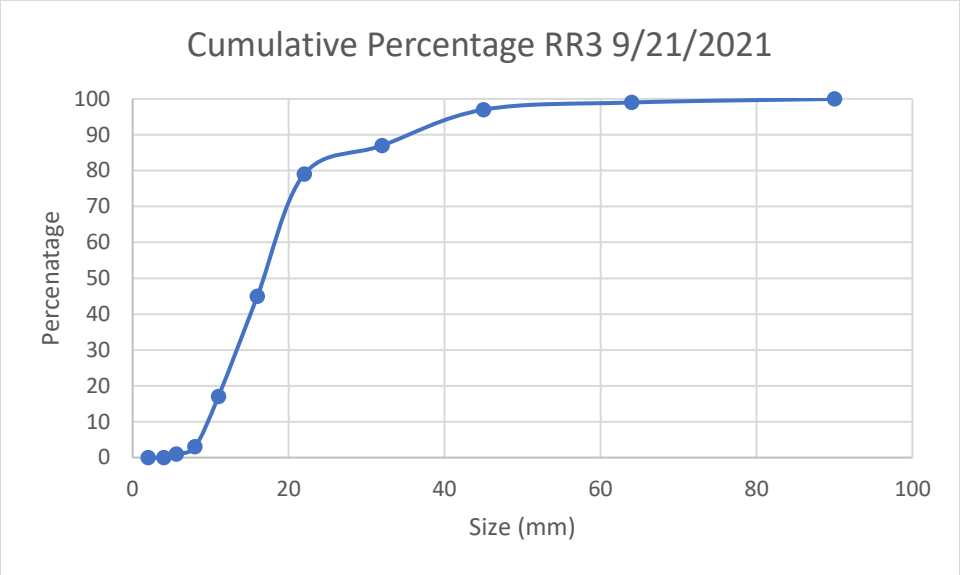

Figure 107: Cumulative Percentage of Rift Rap 3

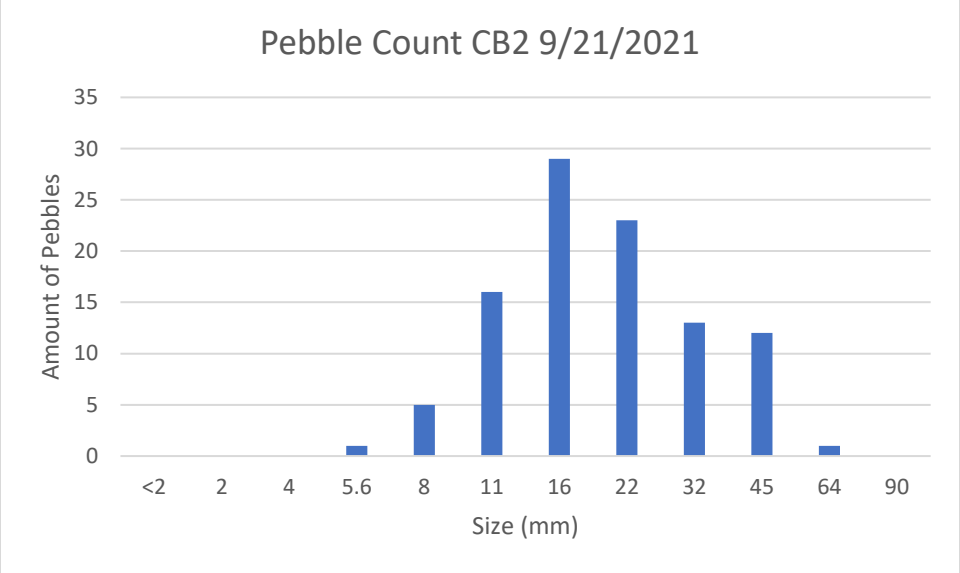

Figure 108: Pebble Count of Central Bar 2

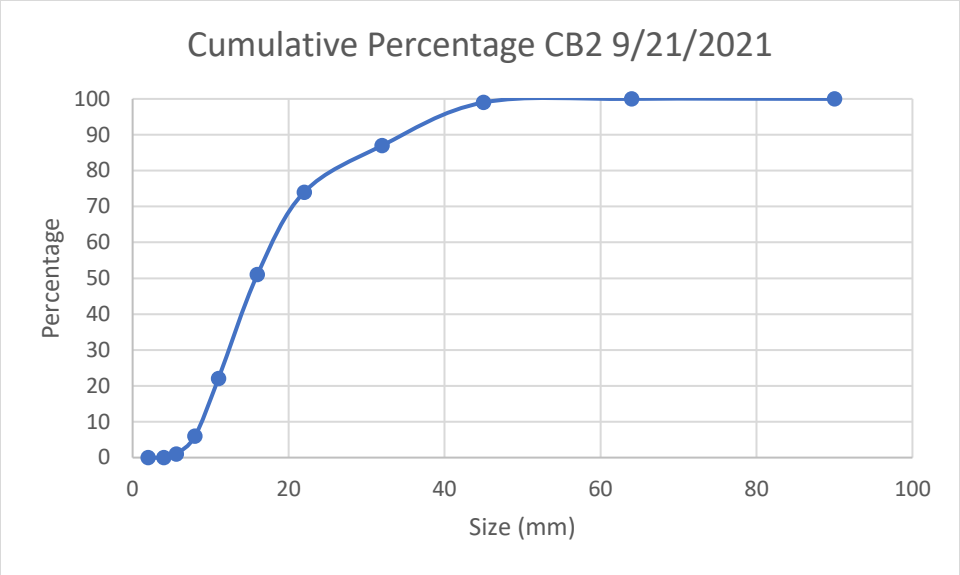

Figure 109: Cumulative Percentage of Central Bar 2

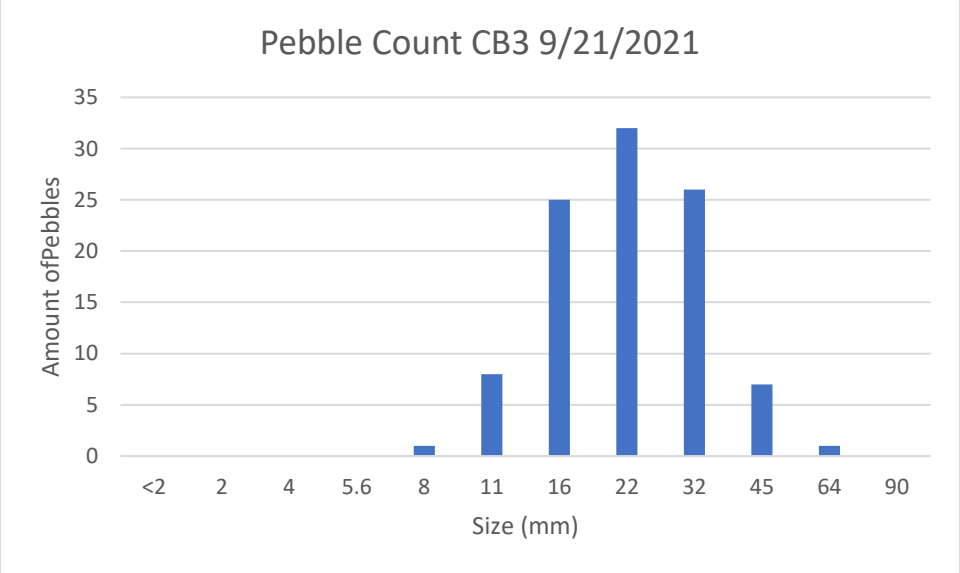

Figure 110: Pebble Count of Central Bar 3

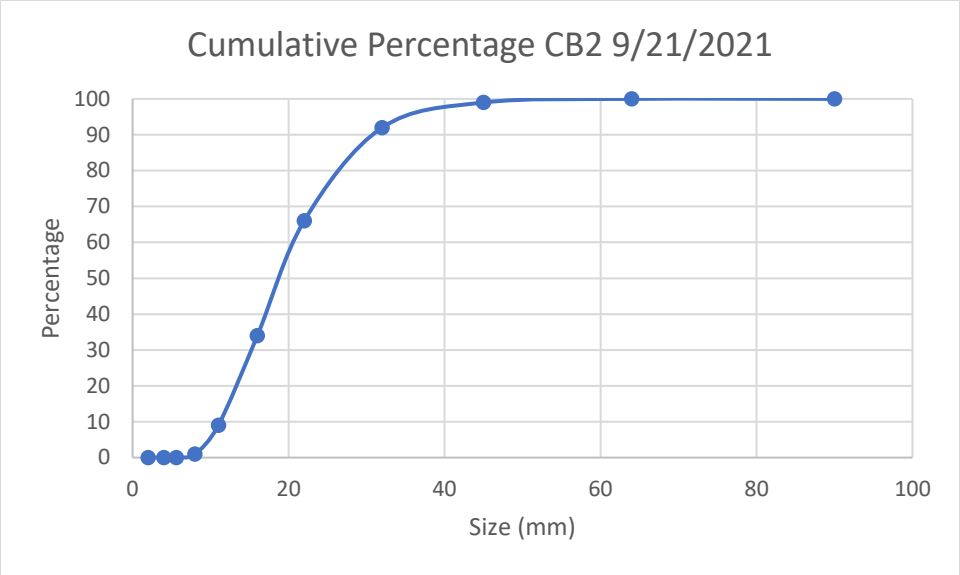

Figure 111: Cumulative Percentage of Central Bar 2

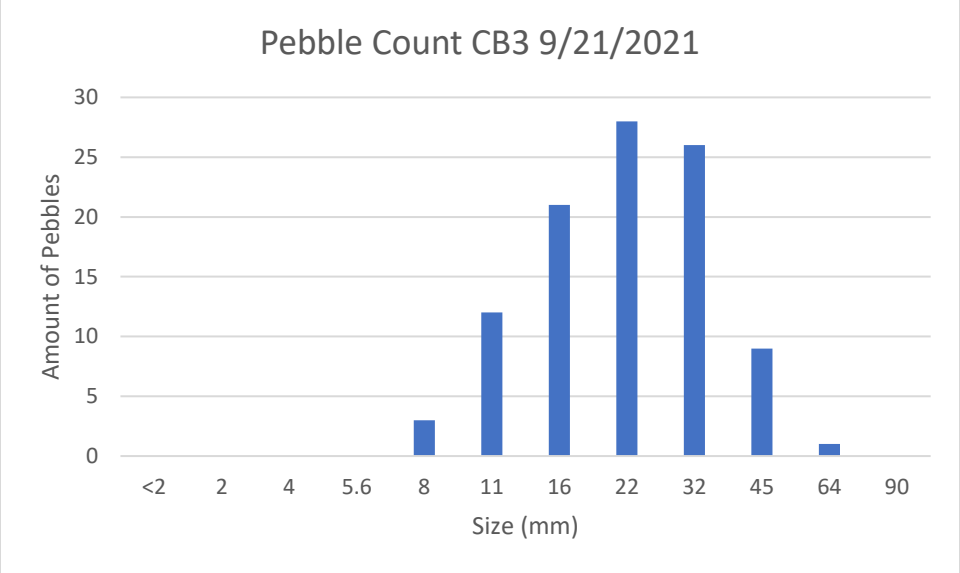

Figure 112: Pebble Count of Central Bar 3

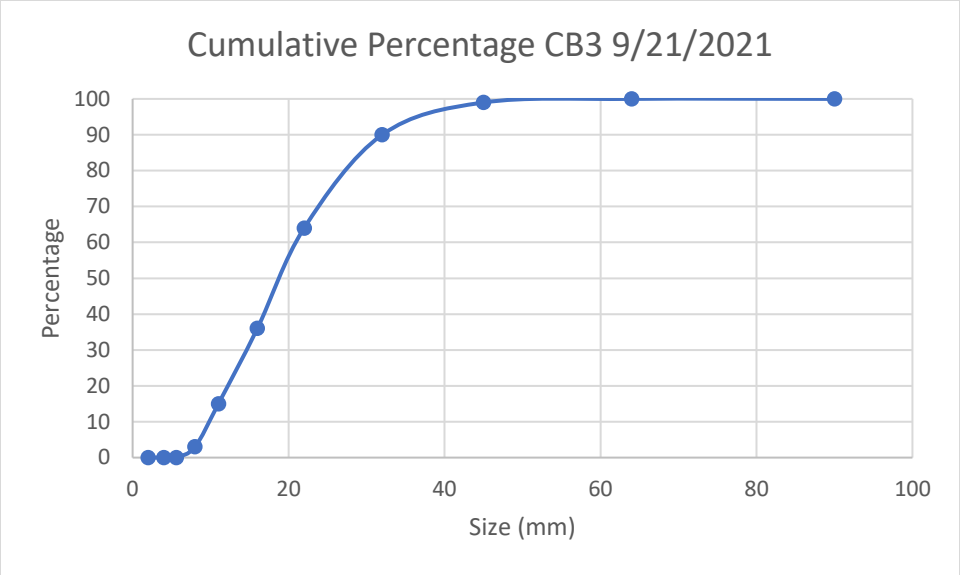

Figure 113: Cumulative Percentage of Central Bar 3

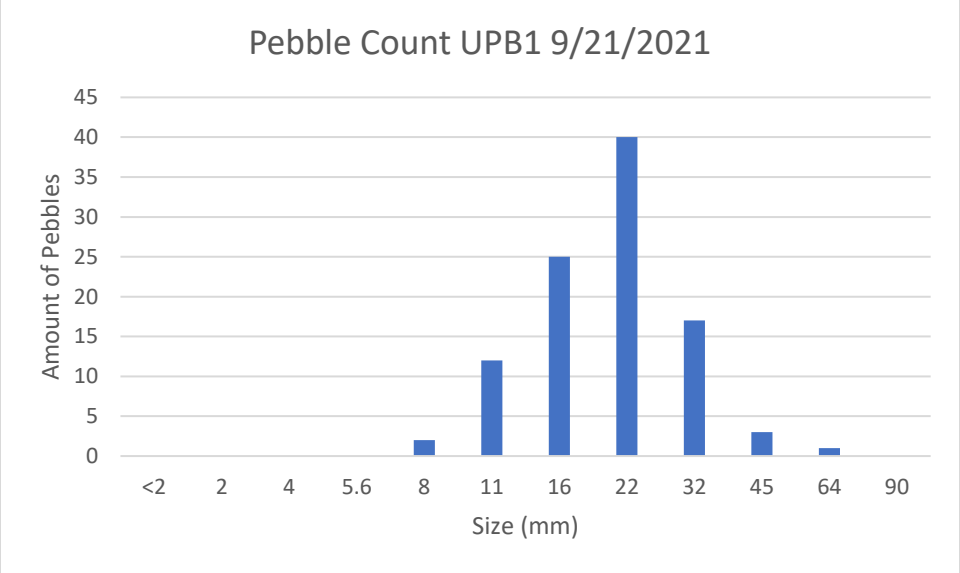

Figure 114: Pebble Count of Upper Point Bar 1

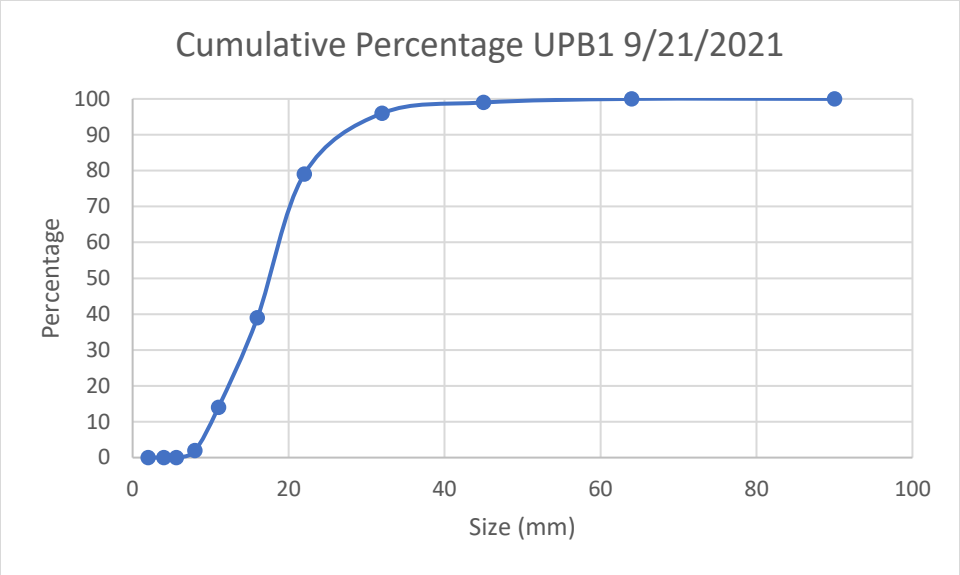

Figure 115: Cumulative Percentage of Upper Point Bar 1

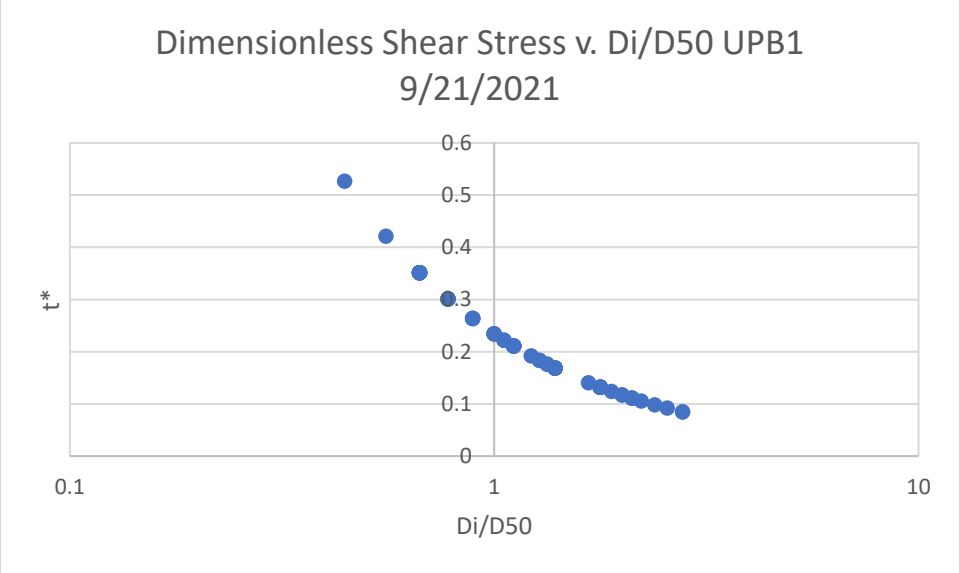

Figure 116: Dimensionless Shear Stress of Upper Point Bar 1

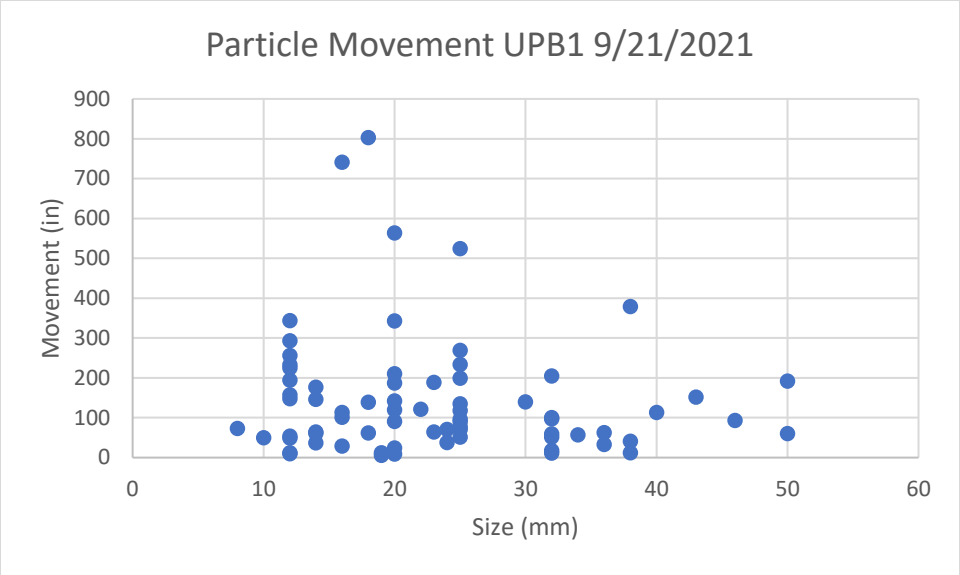

Figure 117: Particle Movement of Upper Point Bar 1

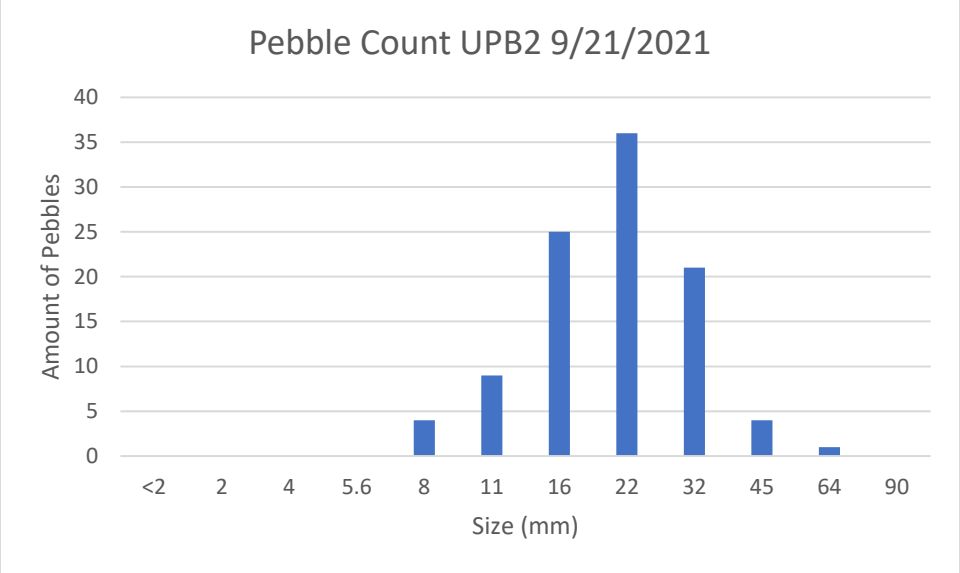

Figure 118: Pebble Count of Upper Point Bar 2

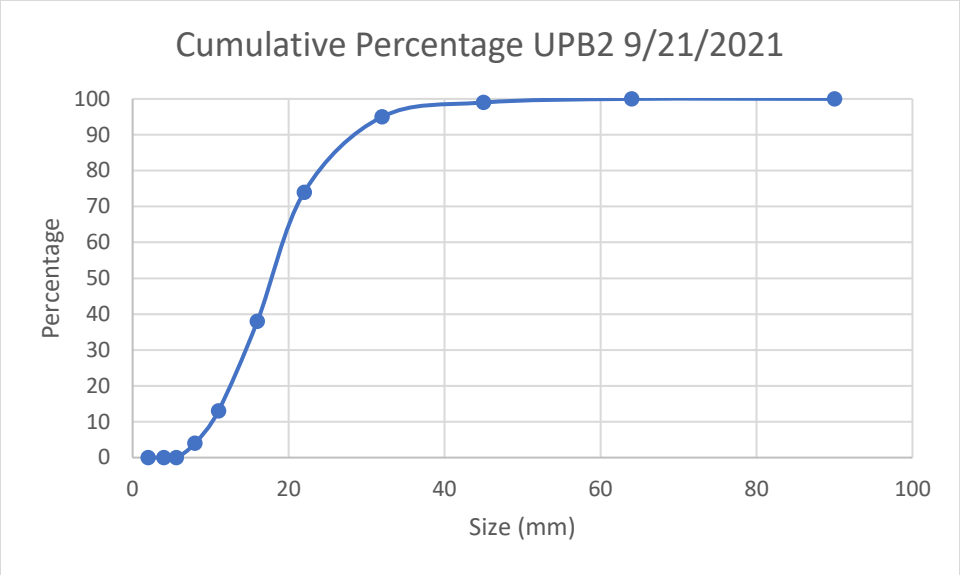

Figure 119: Cumulative Percentage of Upper Point Bar 2

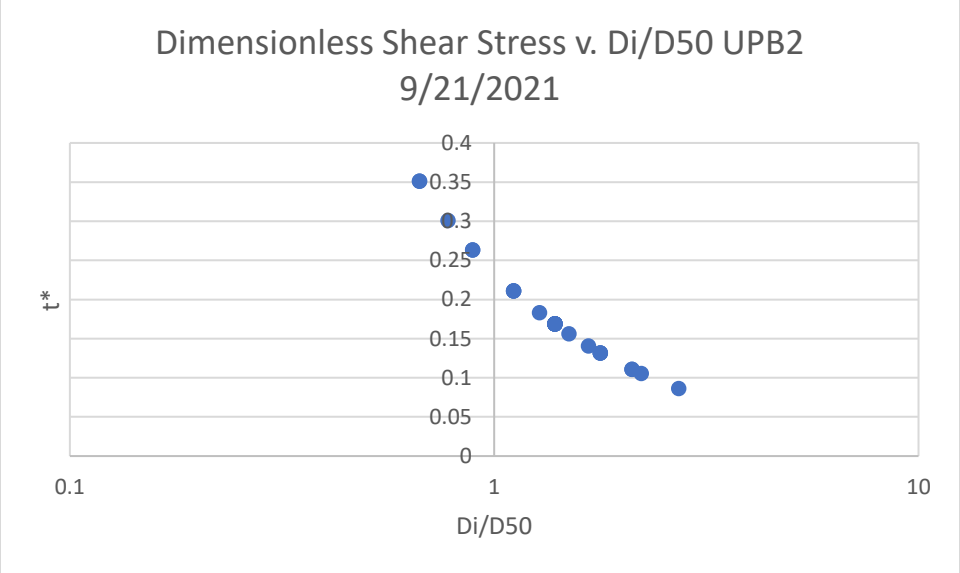

Figure 120: Dimensionless Shear Stress of Upper Point Bar 2

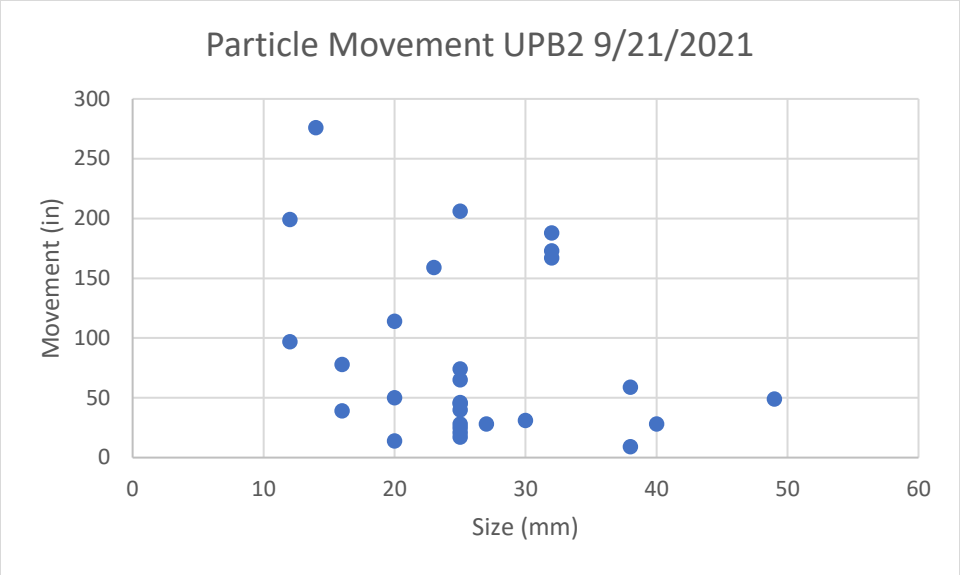

Figure 121: Particle Movement of Upper Point Bar 2

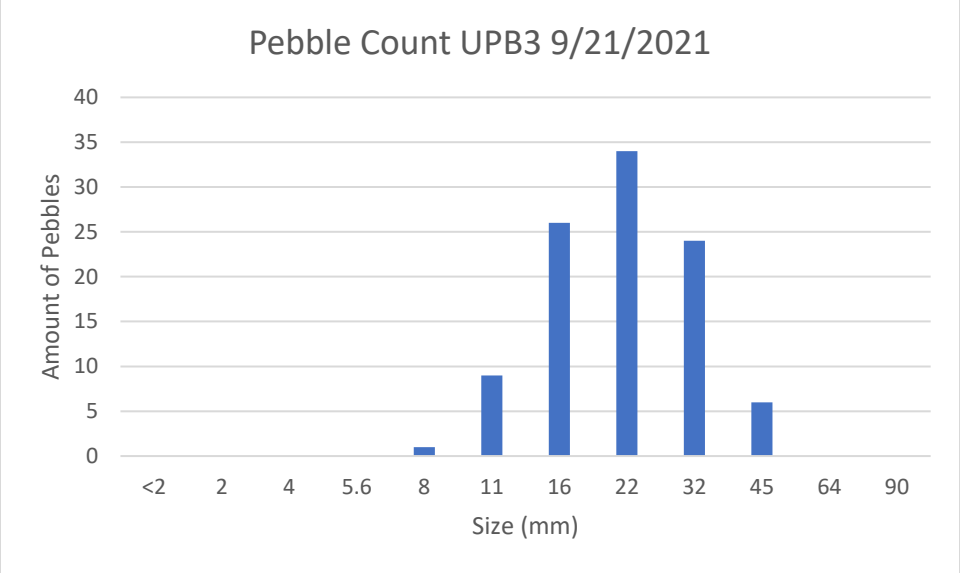

Figure 122: Pebble Count of Upper Point Bar 3

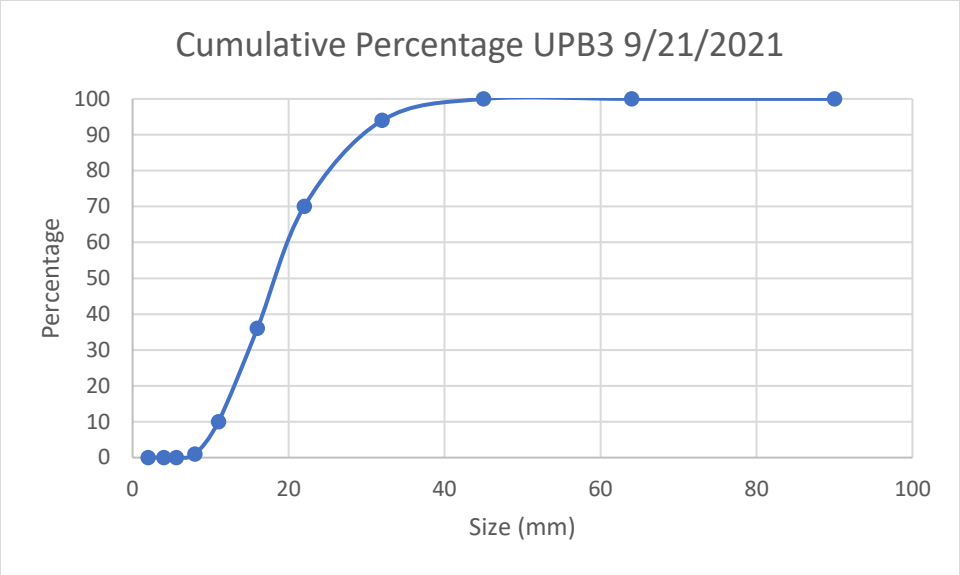

Figure 123: Cumulative Percentage of Upper Point Bar 3

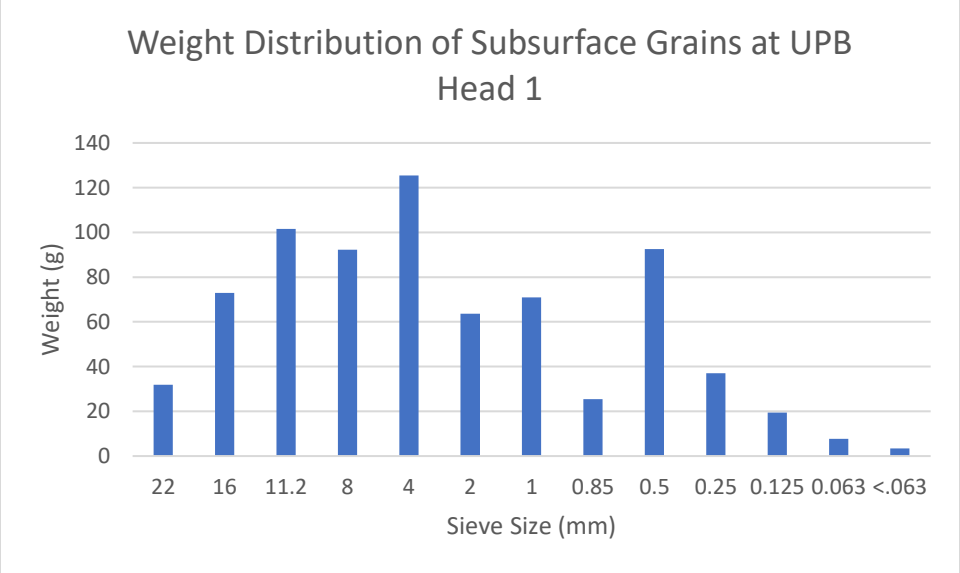

Figure 124: Subsurface Grains of Upper Point Bar

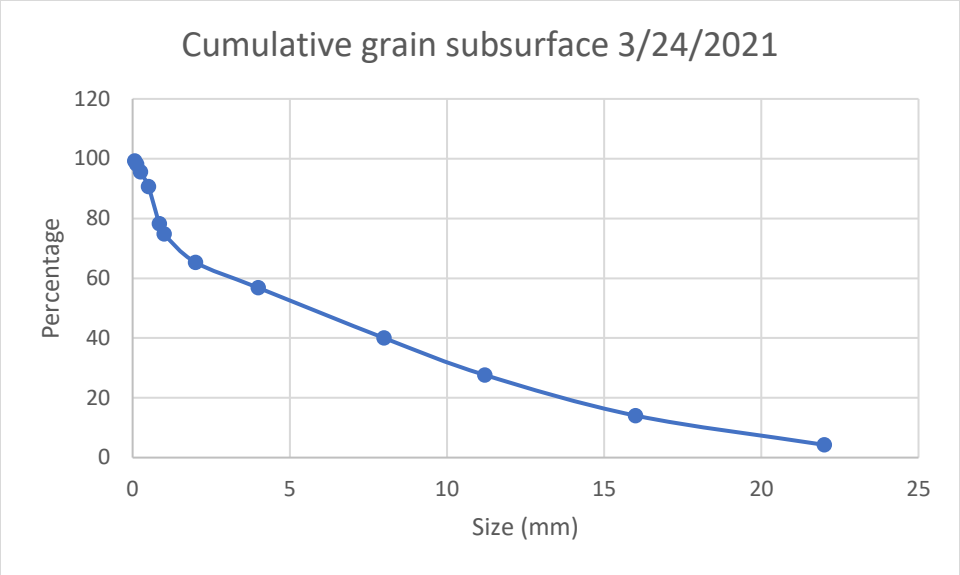

Figure 125: Cumulative Grain Subsurface

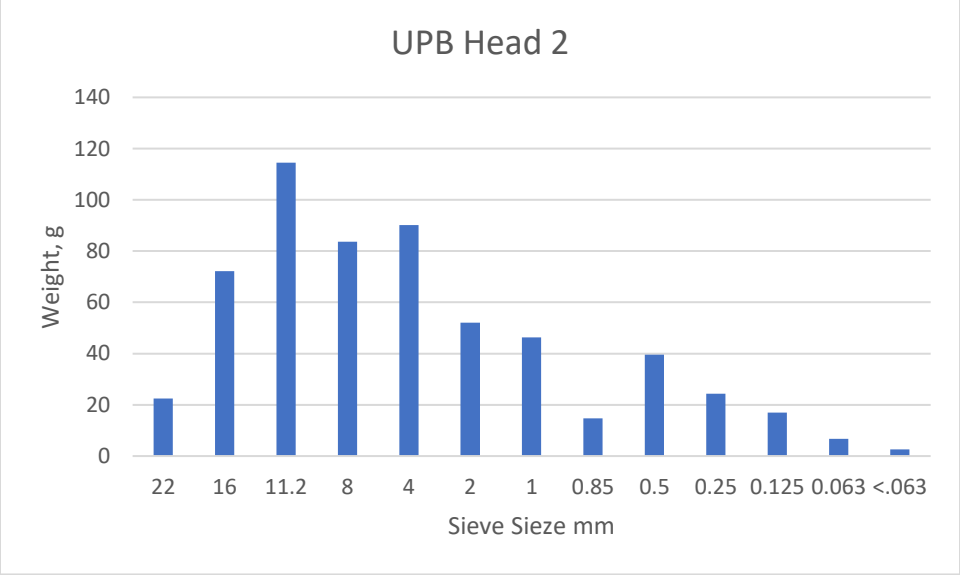

Figure 126: Subsurface Grains of Upper Point Bar

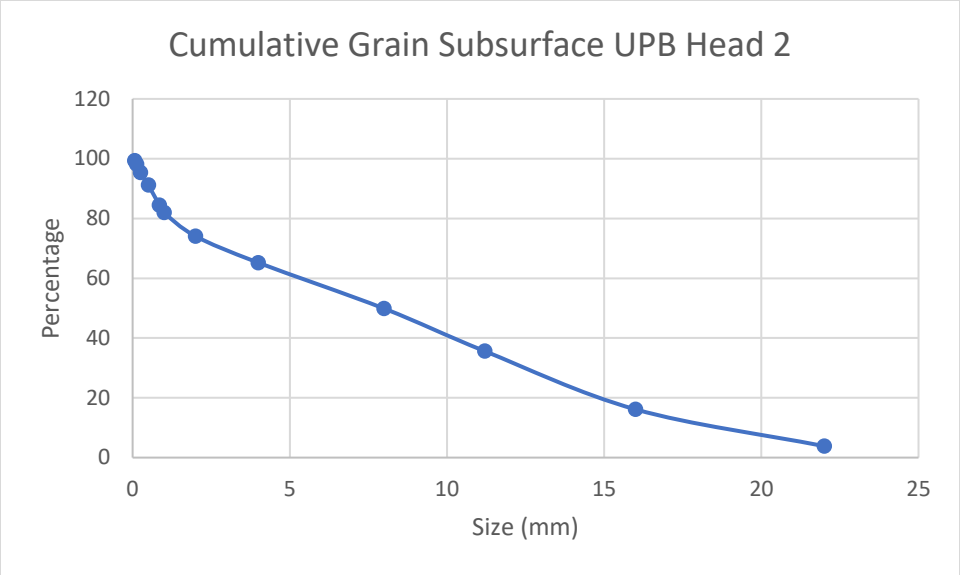

Figure 127: Cumulative Grain Subsurface

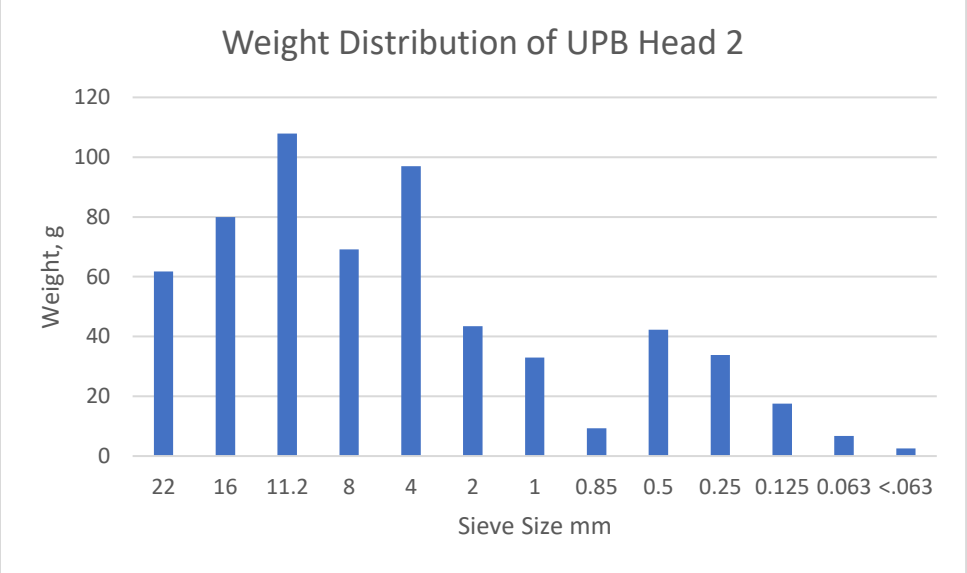

Figure 128: Weight Distribution of Upper Point Bar

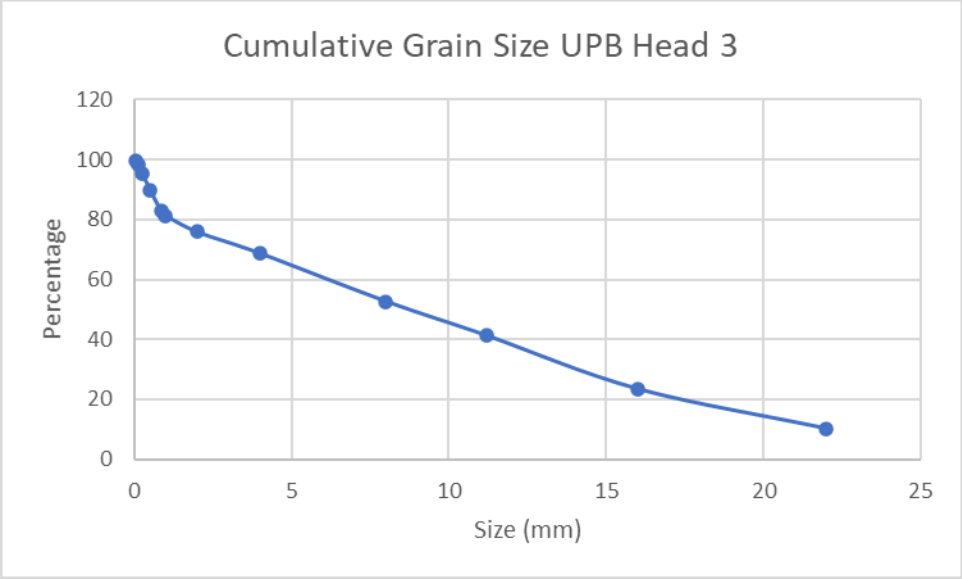

Figure 129: Cumulative Grain Size of Upper Point Bar

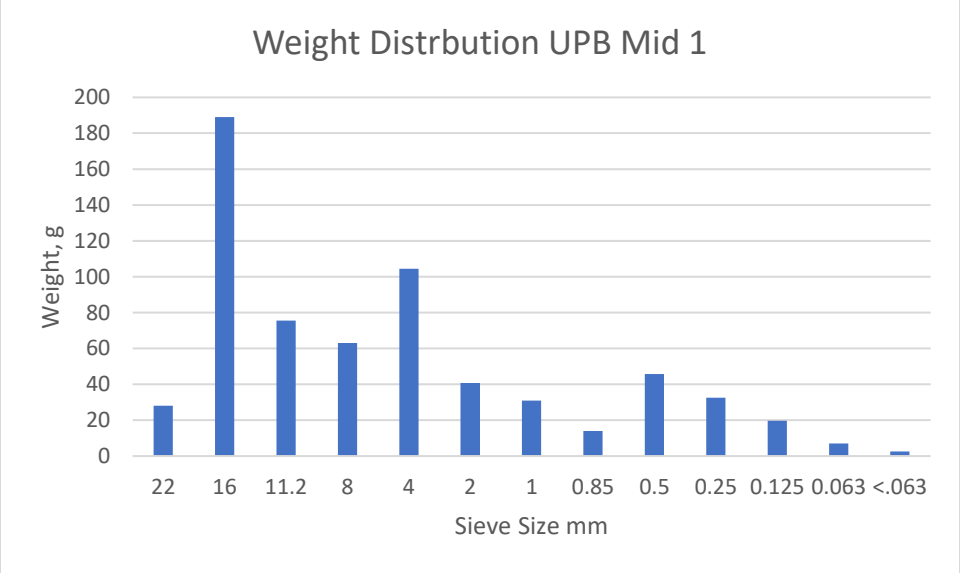

Figure 130: Weight Distribution of UPB MId

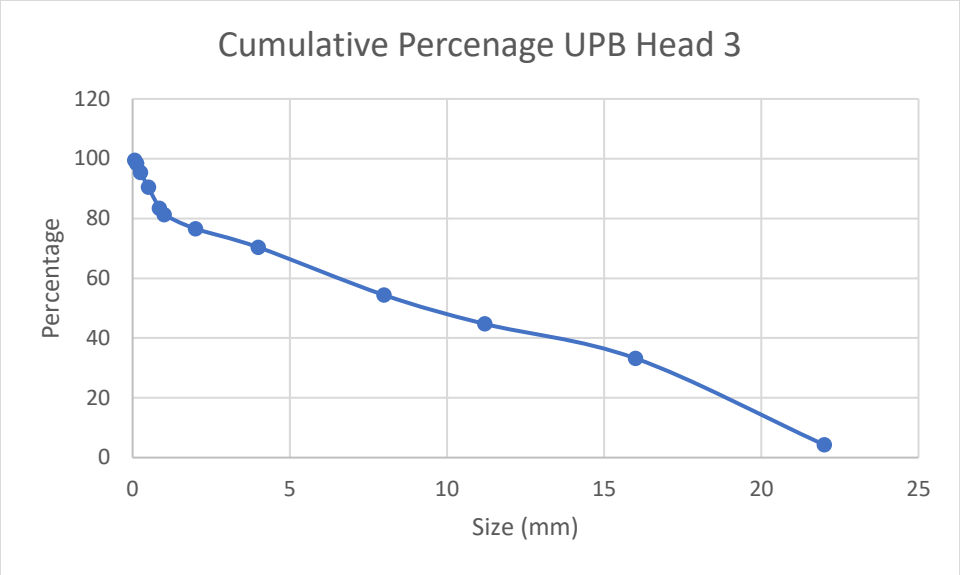

Figure 131: Cumulative Percentage of UPB Head

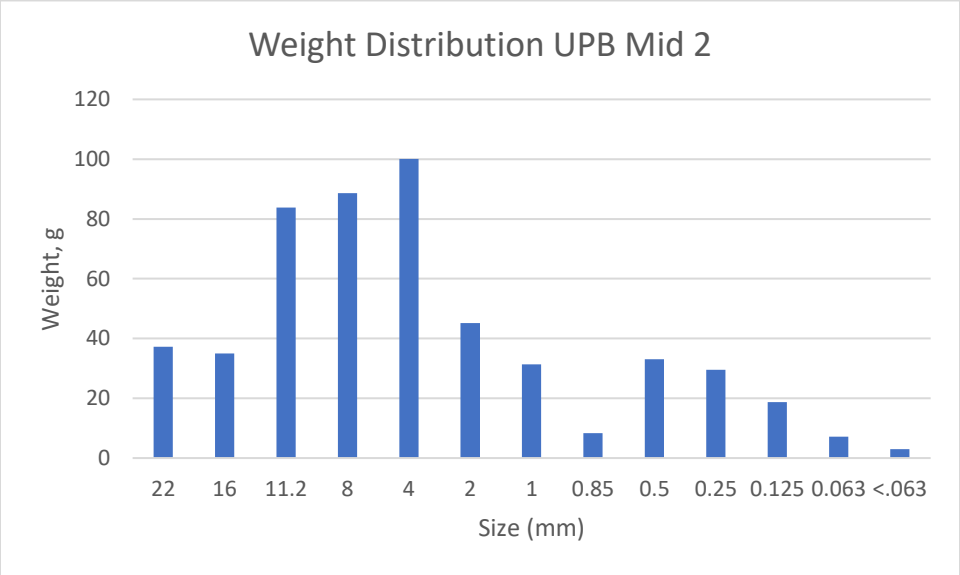

Figure 132: Weight Distribution of UPB Mid

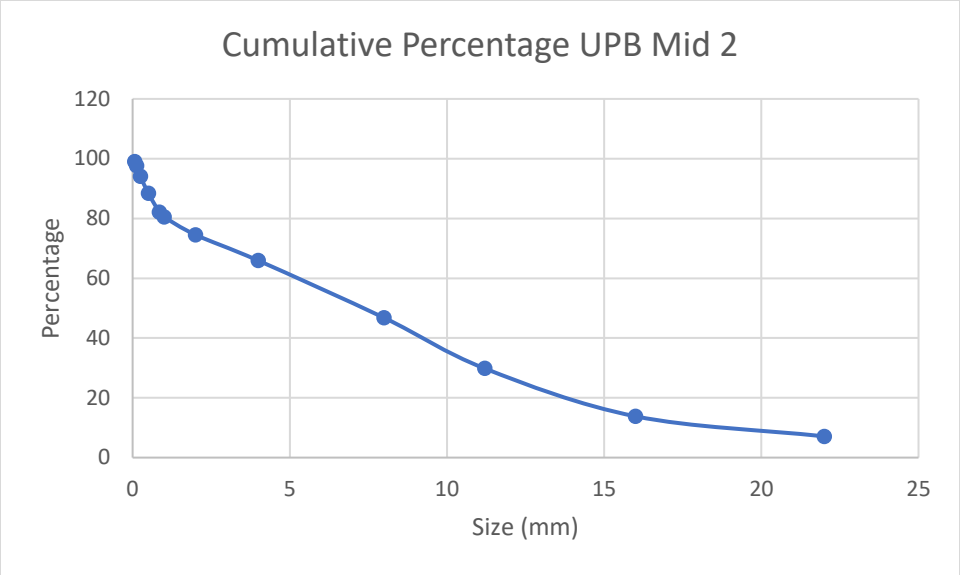

Figure 133: Cumulative Percentage of UPB MId

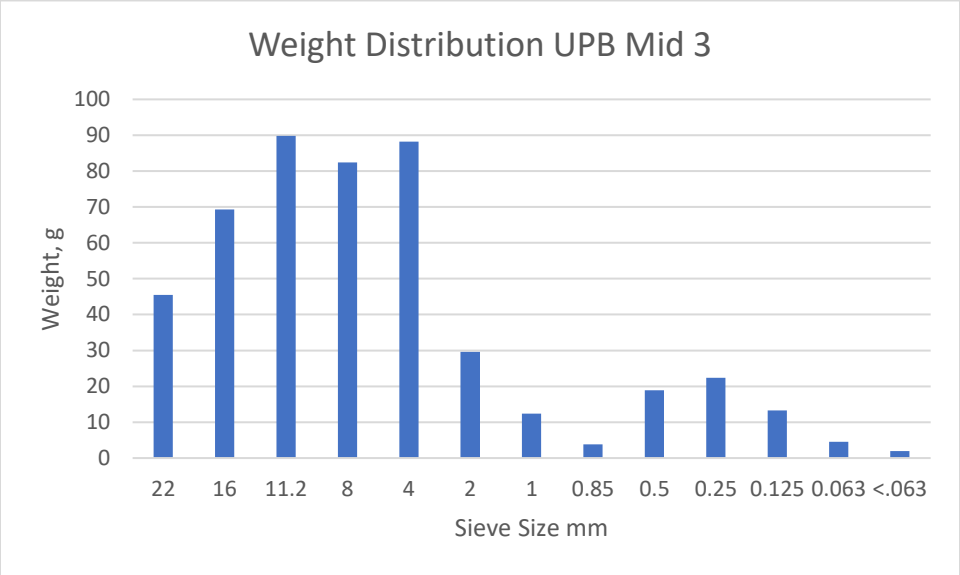

Figure 134: Weight Distribution of UPB Mid

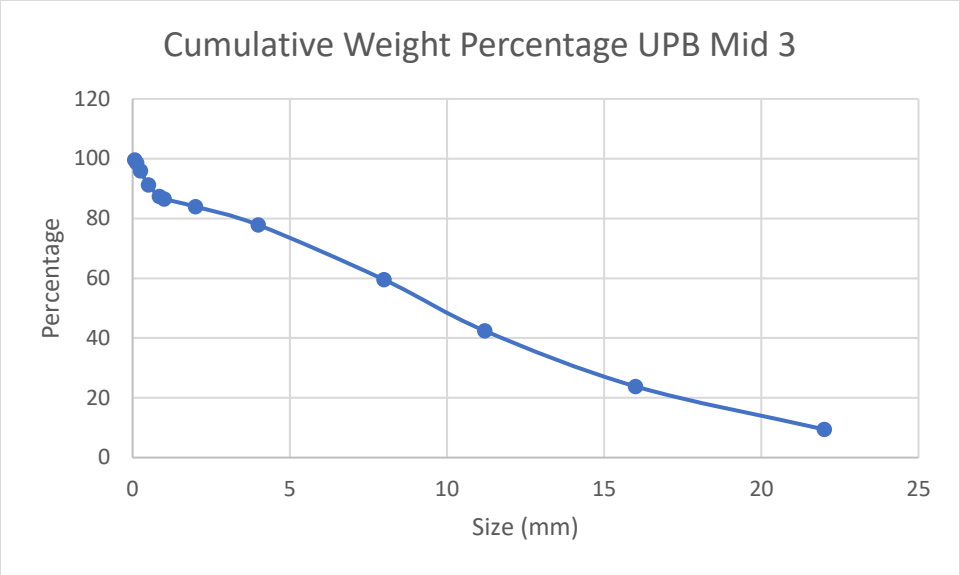

Figure 135: Cumulative Percentage UPB Mid

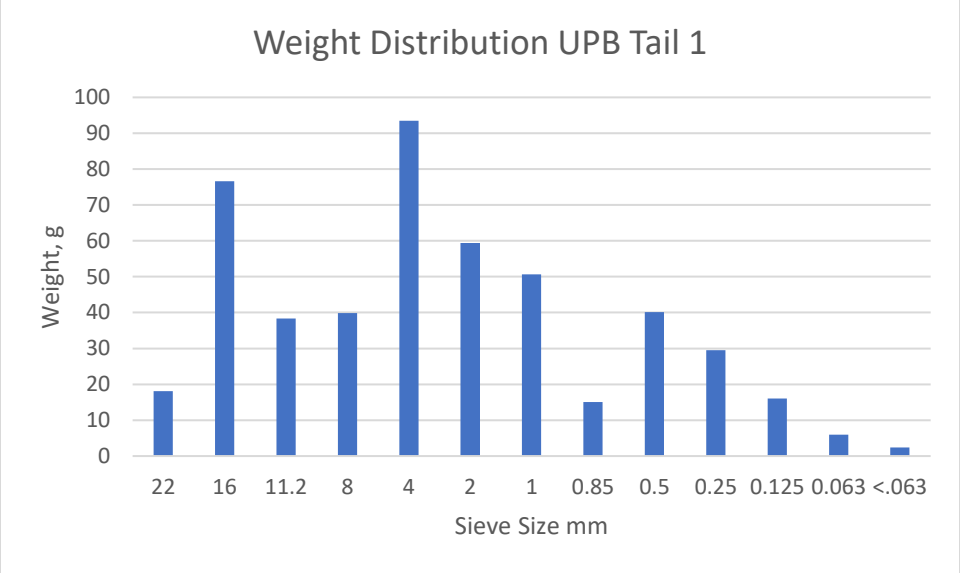

Figure 136: Weight Distribution of UPB Tail

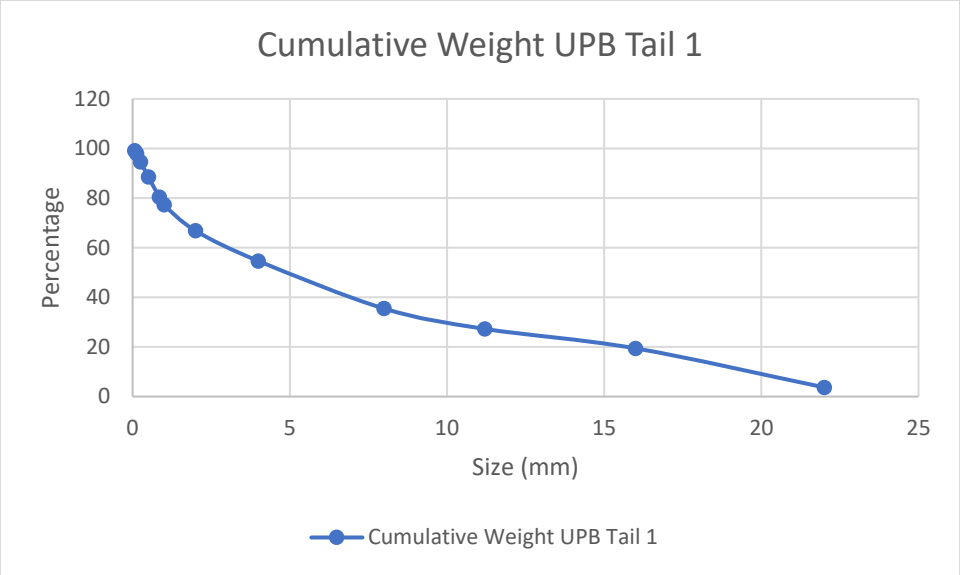

Figure 137: Cumulative Weight UPB Tail

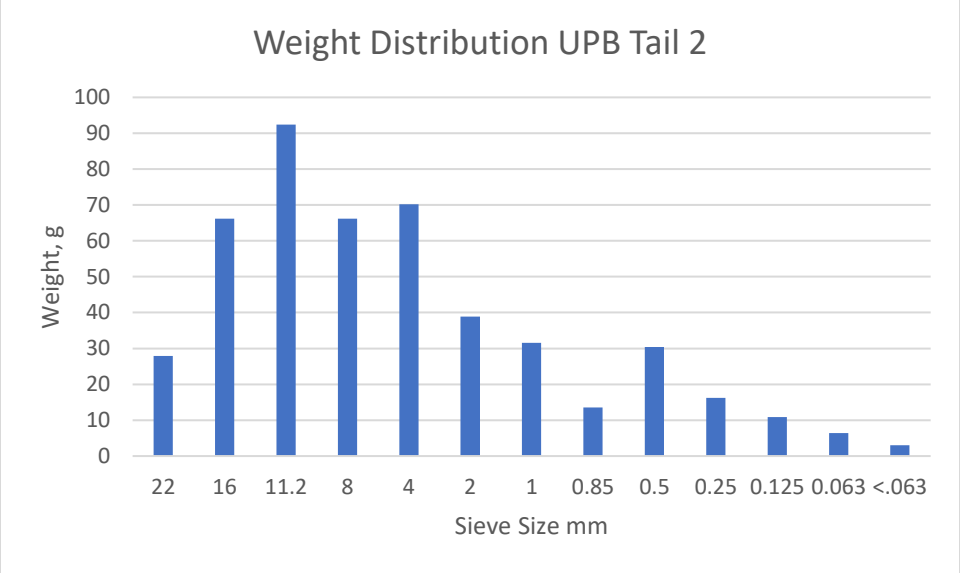

Figure 138: Weight Distribution of UPB Tail

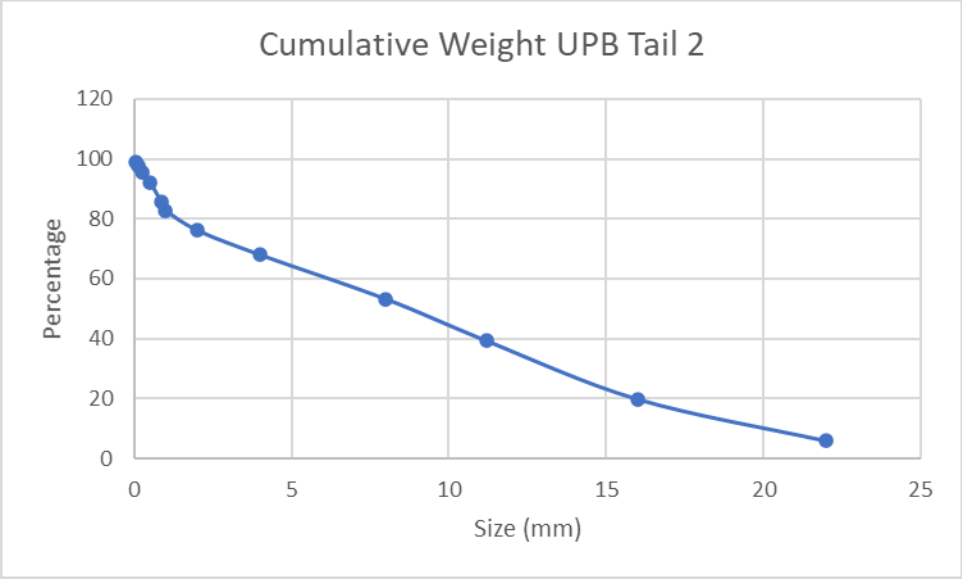

Figure 139: Cumulative Weight UPB Tail

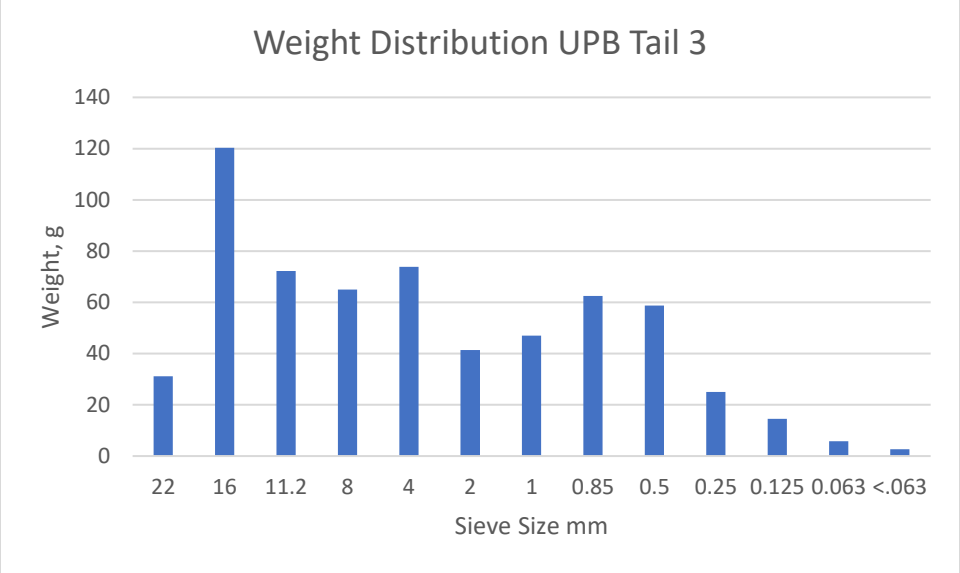

Figure 140: Weight Distribution of UPB Tail

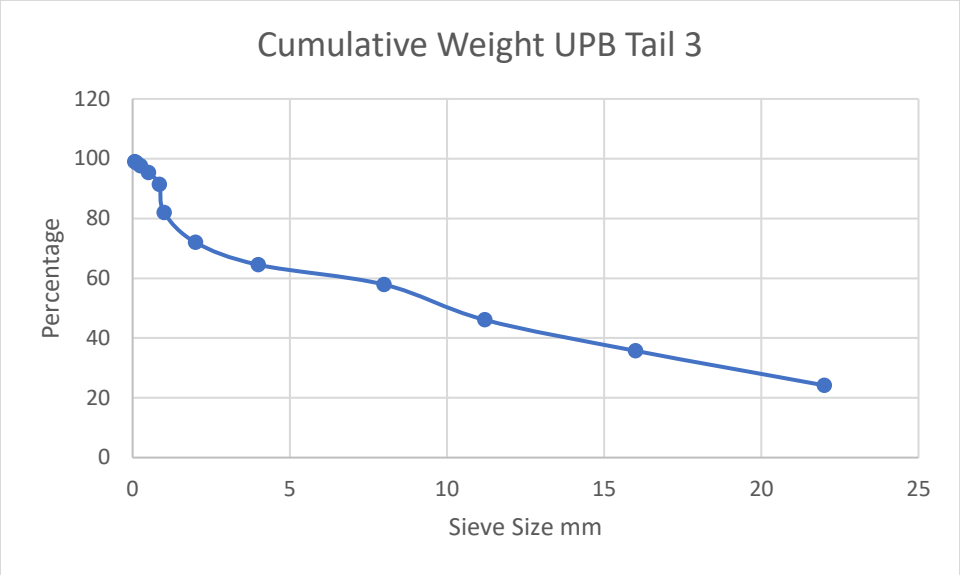

Figure 141: Cumulative Weight UPB Tail

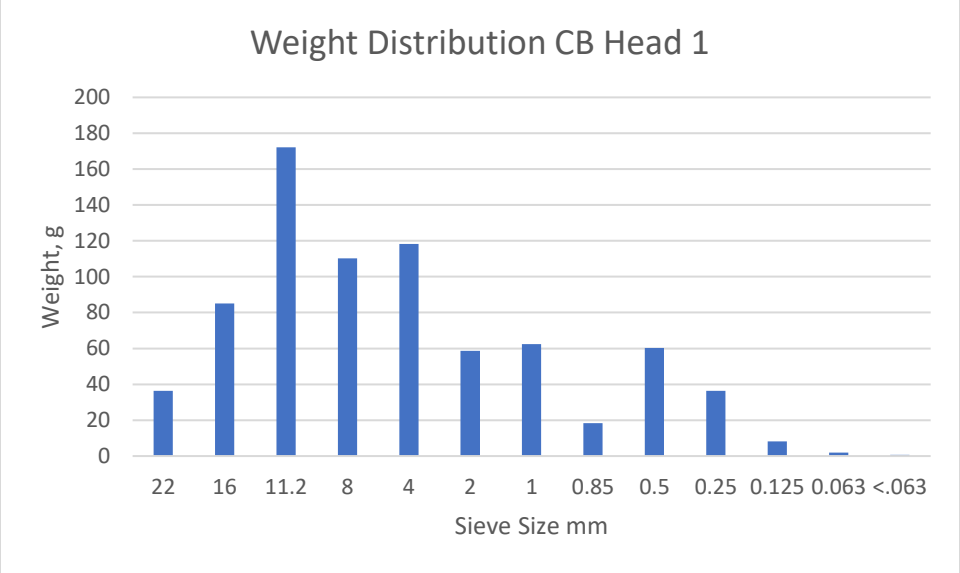

Figure 142: Weight Distribution of CB Head

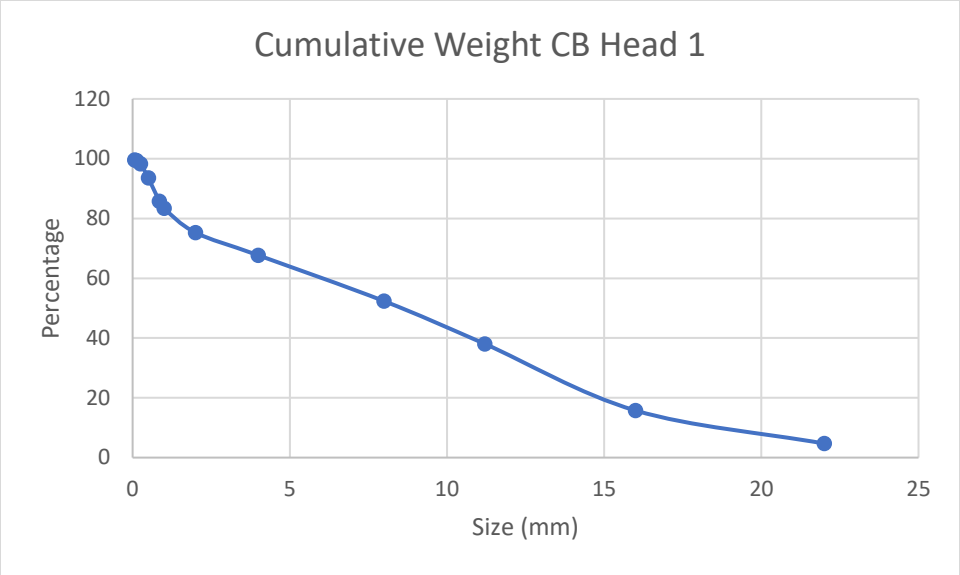

Figure 143: Cumulative weight of CB Head

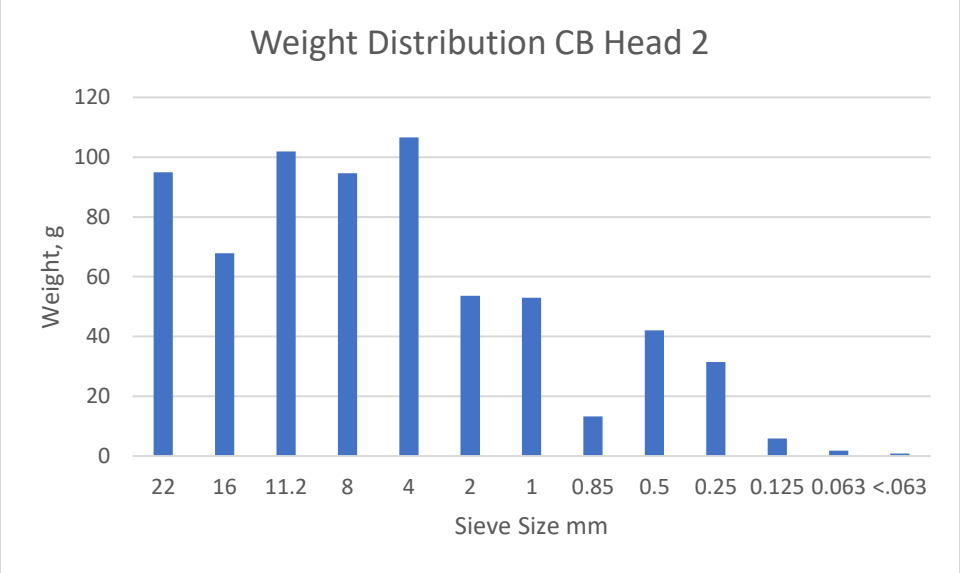

Figure 144: Weight Distribution of CB Head

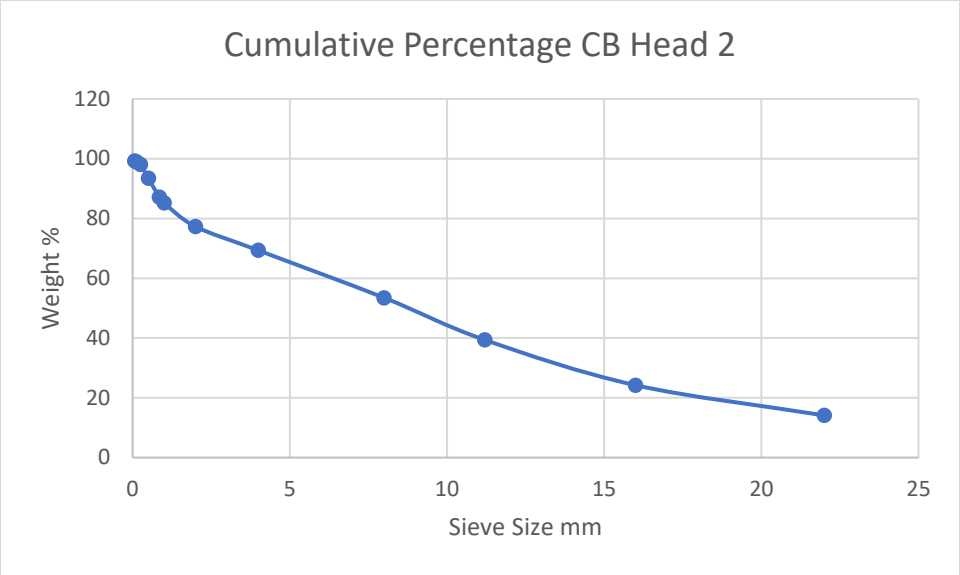

Figure 145: Cumulative Percentage of CB Head

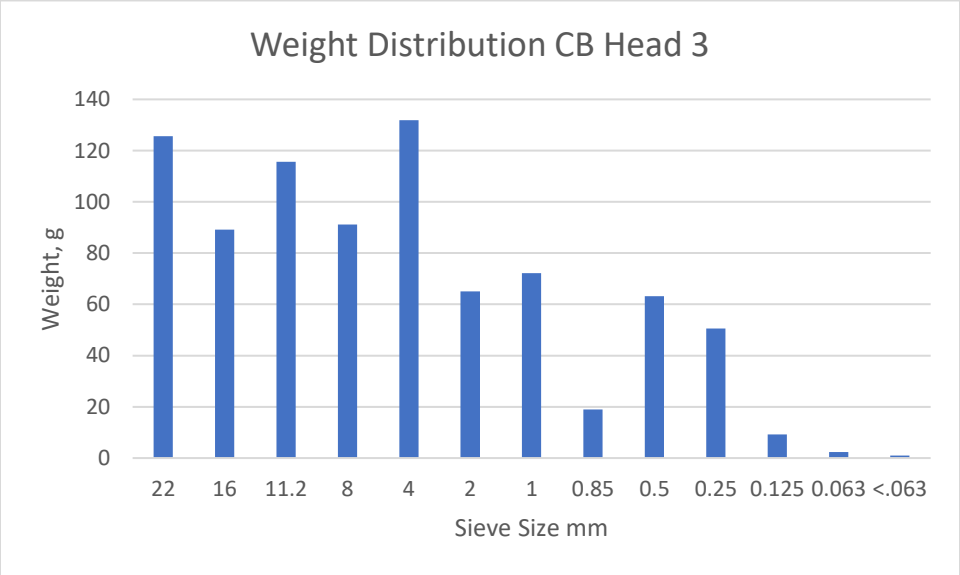

Figure 146: Weight Distribution of CB Head

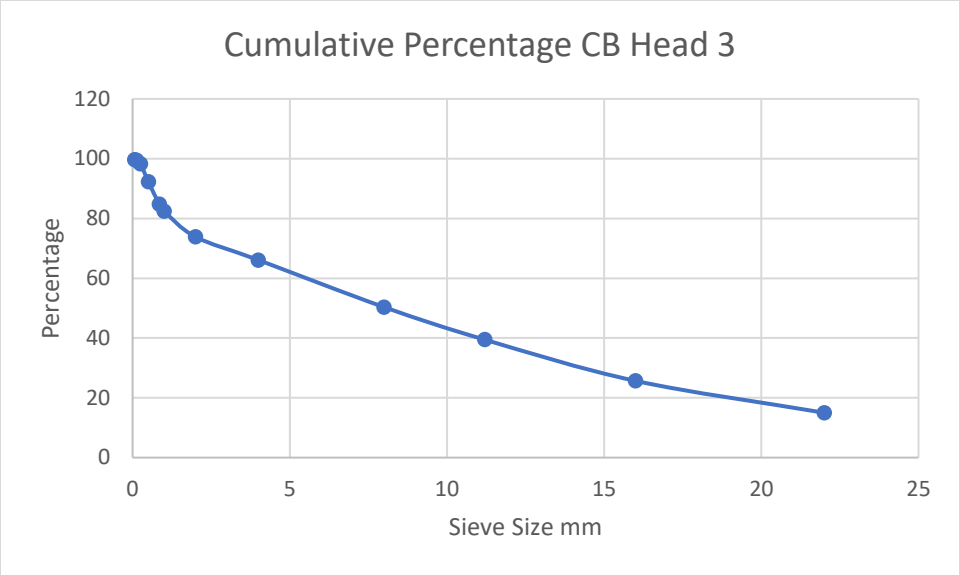

Figure 147: Cumulative Percentage of CN Head

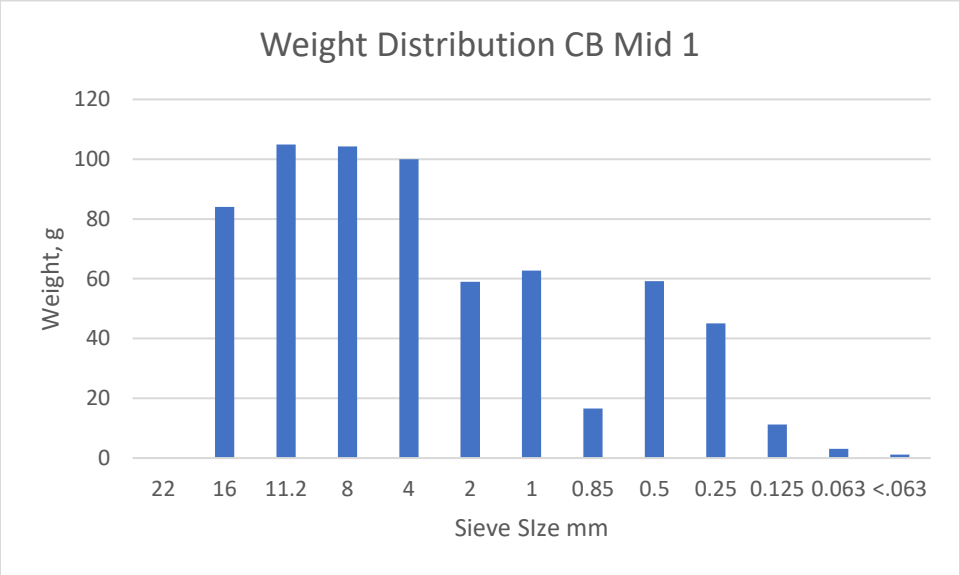

Figure 148: Weight Distribution of CB Mid

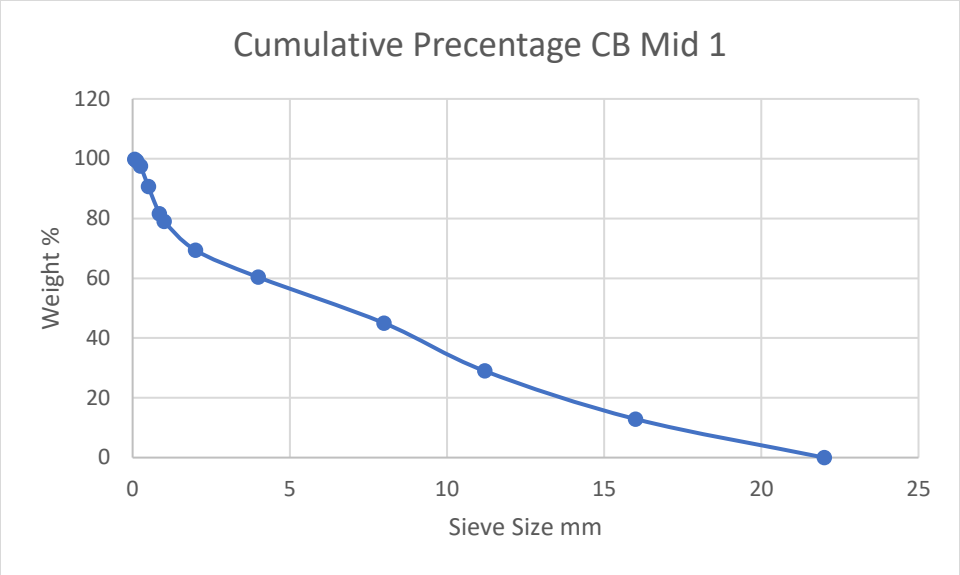

Figure 149: Cumulative Percentage of CB Mid

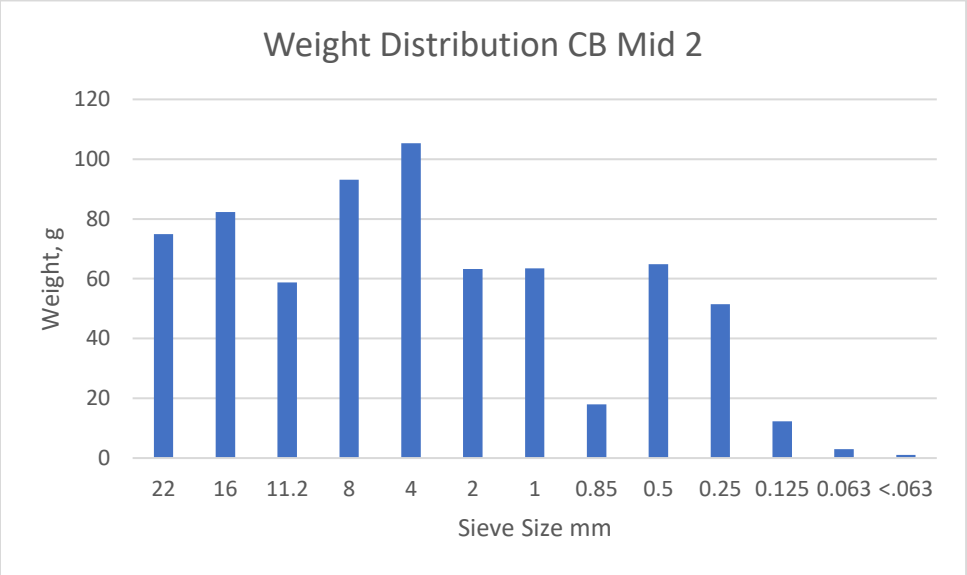

Figure 150: Weight Distribution of CB Mid

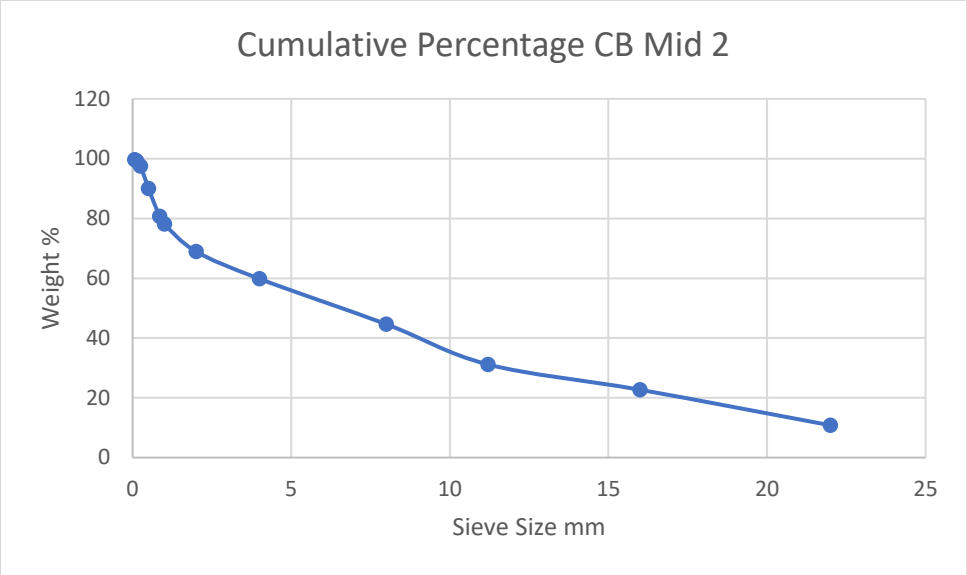

Figure 151: Cumulative Percentage of CB Mid

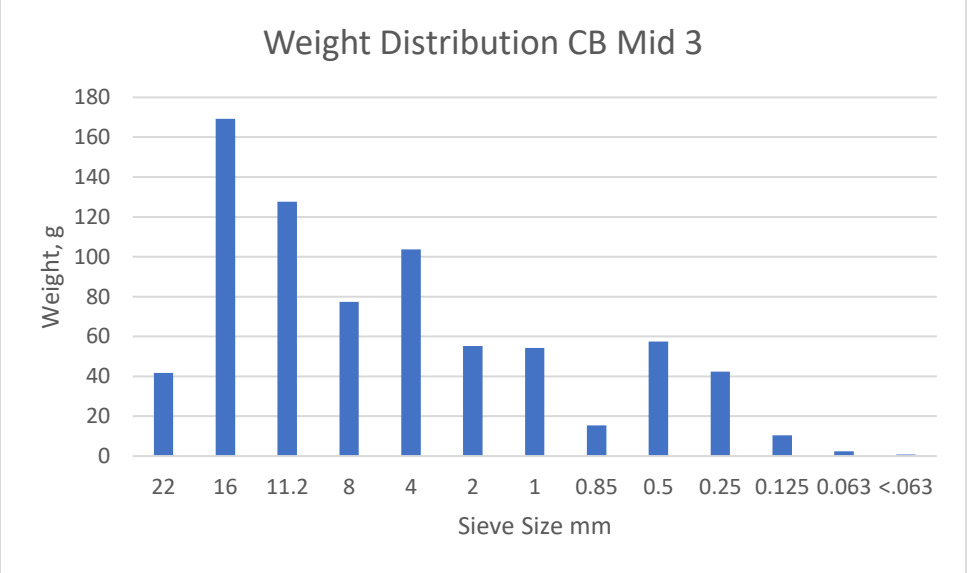

Figure 152: Weight Distribution of CB Mid

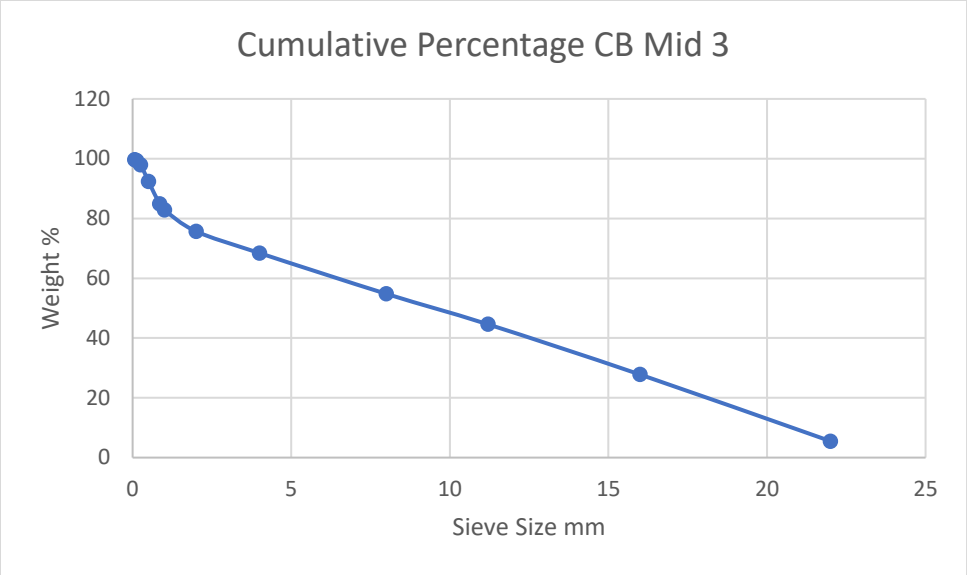

Figure 153: Cumulative Percentage CB Mid

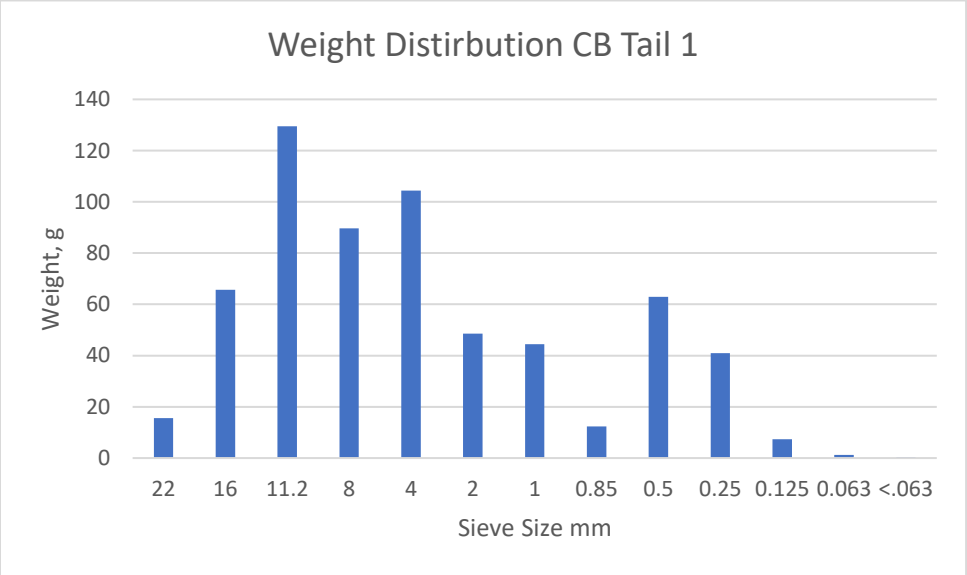

Figure 154: Weight Distribution CB Tail

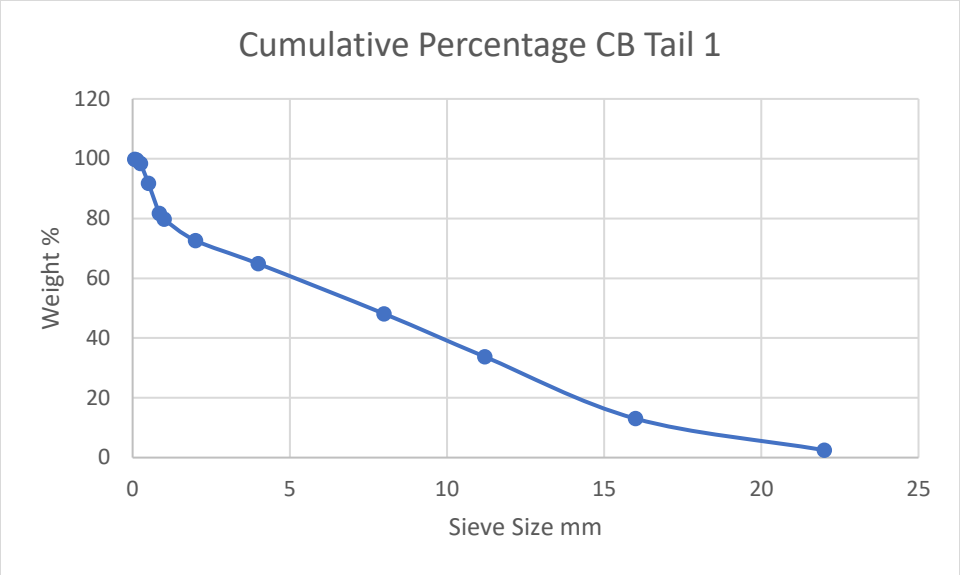

Figure 155: Cumulative Percentage CB Tail

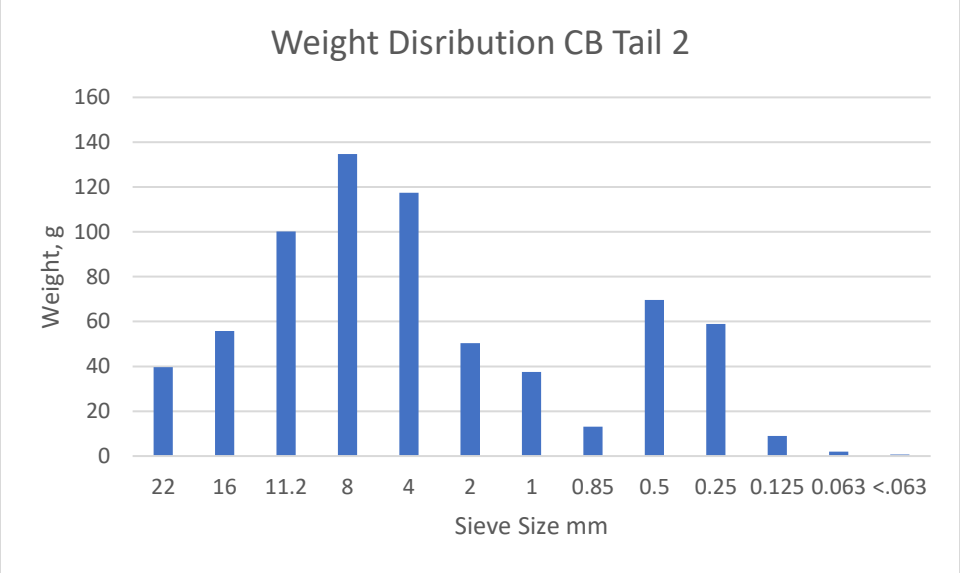

Figure 156: Weight Distribution of CB Tail

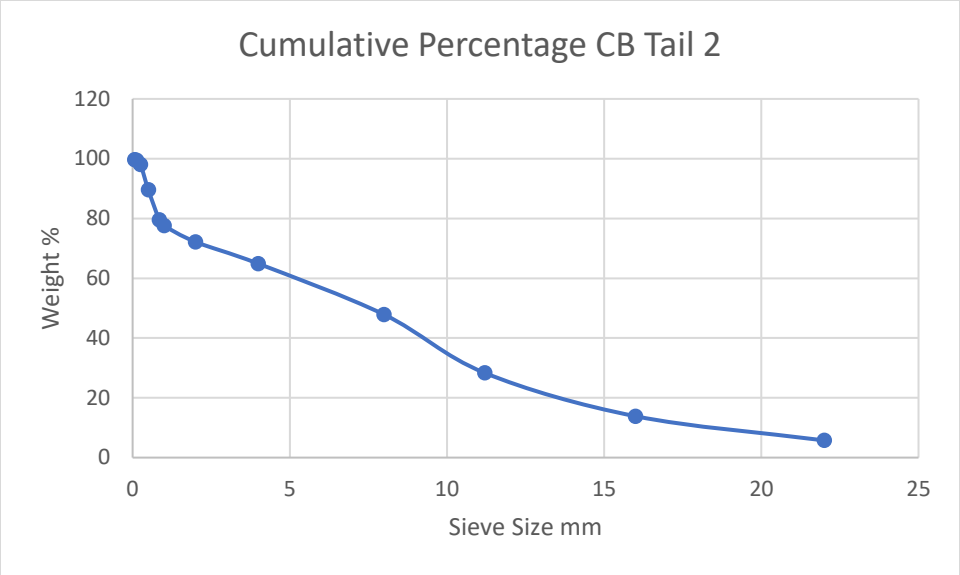

Figure 157: Cumulative Percentage of CB Tail

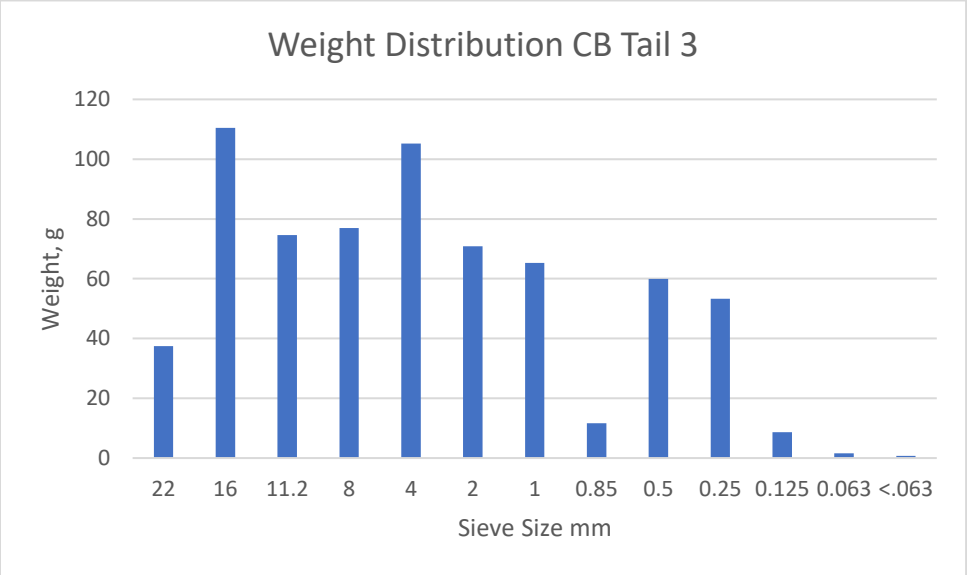

Figure 158: Weight Distribution of CB Tail

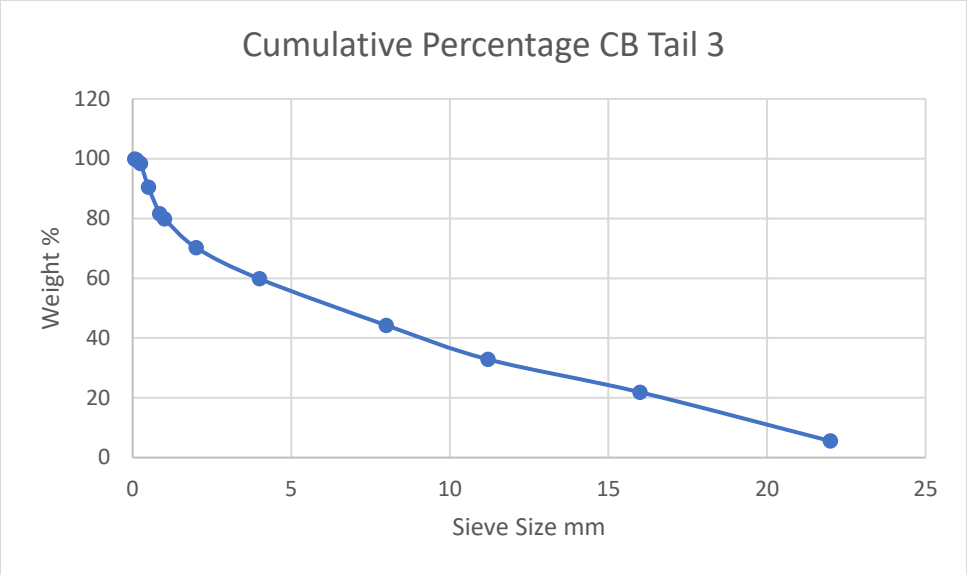

Figure 159: Cumulative Percentage of CB Tail

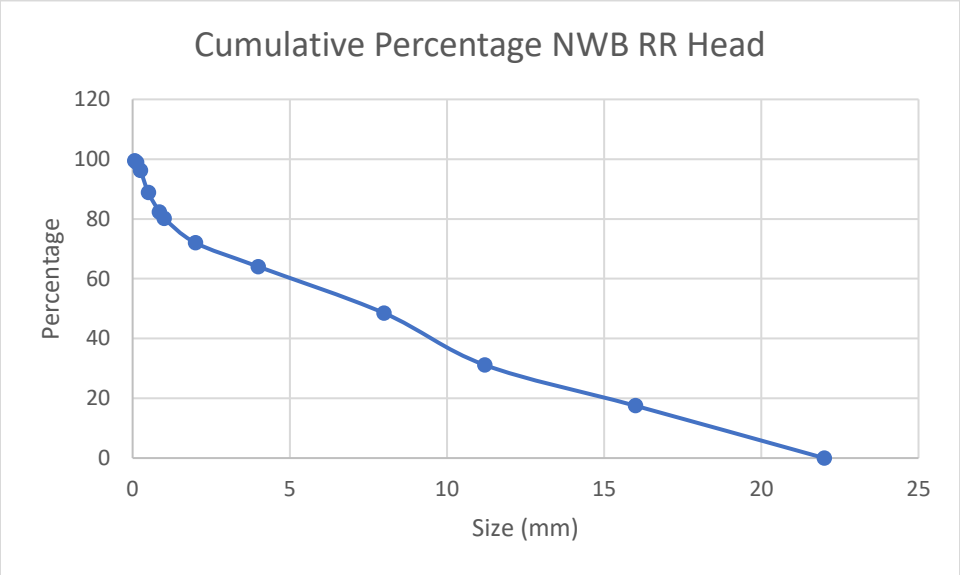

Figure 160: Cumulative Percentage of NWB RR Head

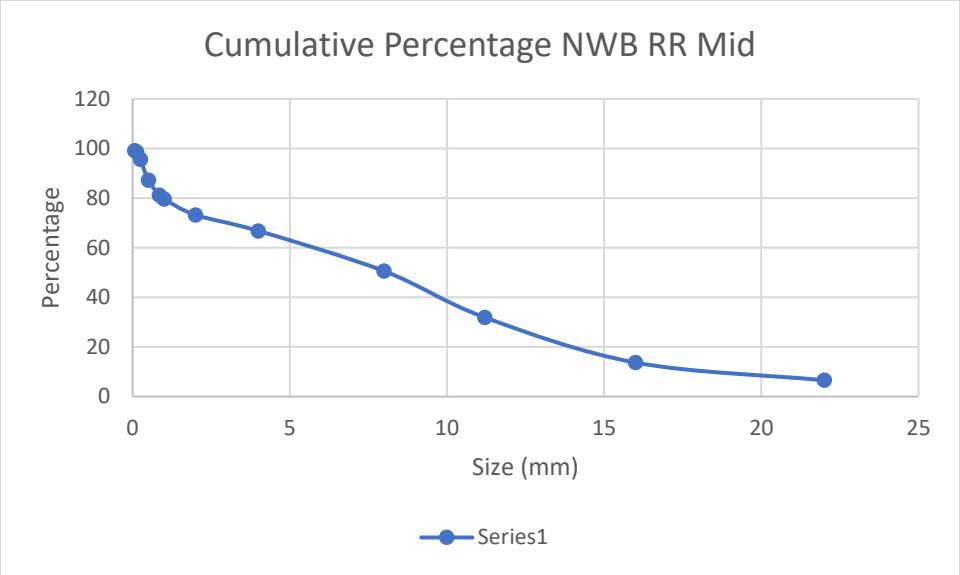

Figure 161: Cumulative Percentage of NWB RR Mid

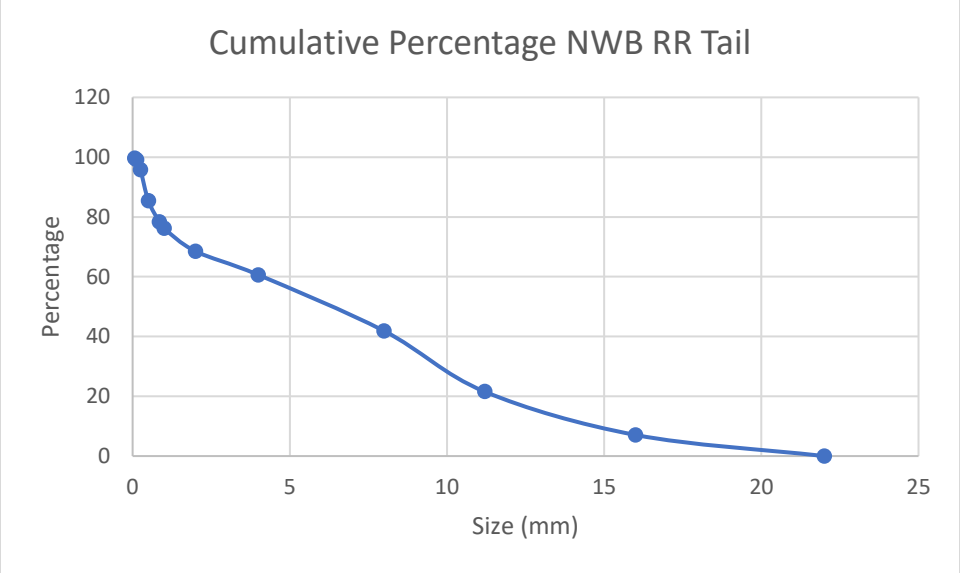

Figure 162: Cumulative Percentage NWB RR Tail

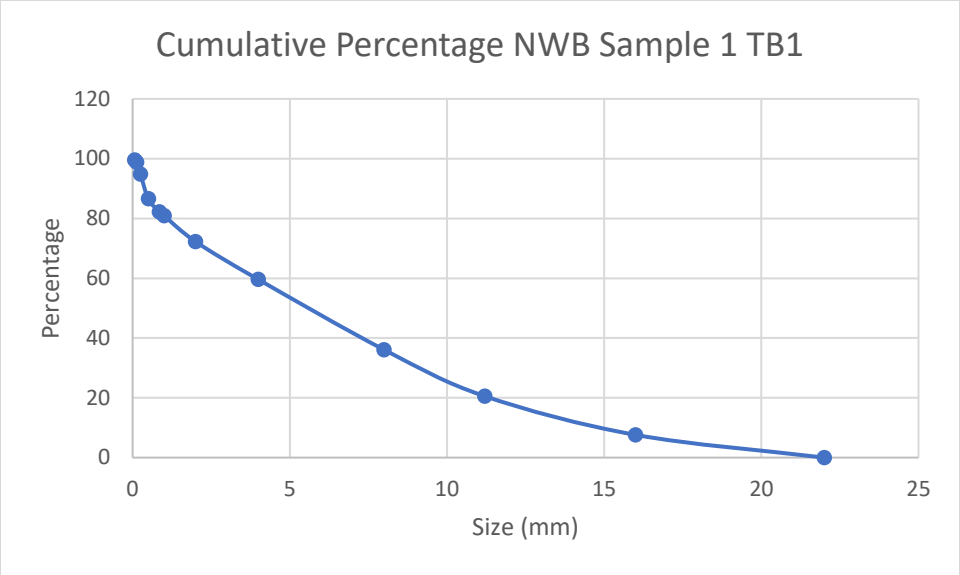

Figure 163: Cumulative Percentage NWB Sample 1 TB1

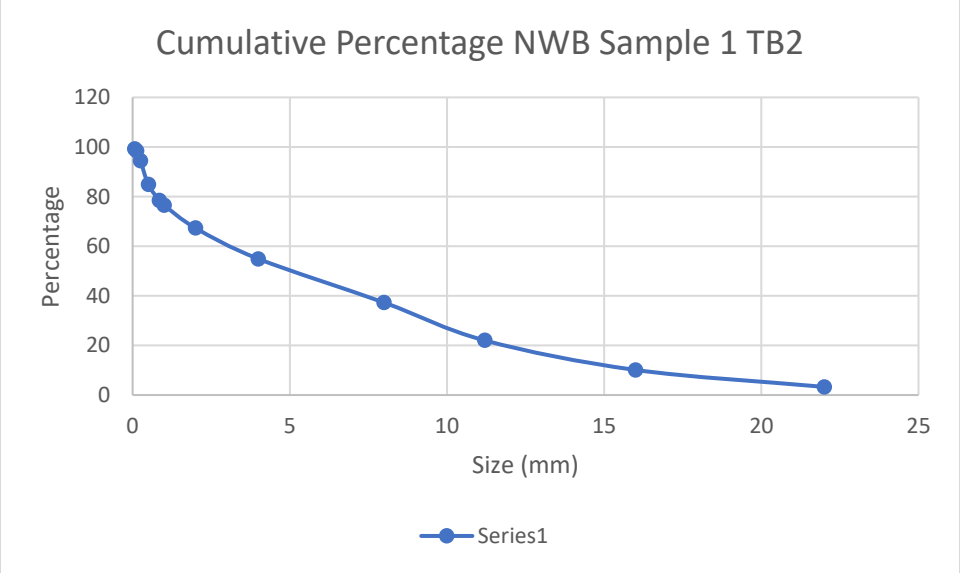

Figure 164: Cumulative Percentage of NWB Sample 1 TB2

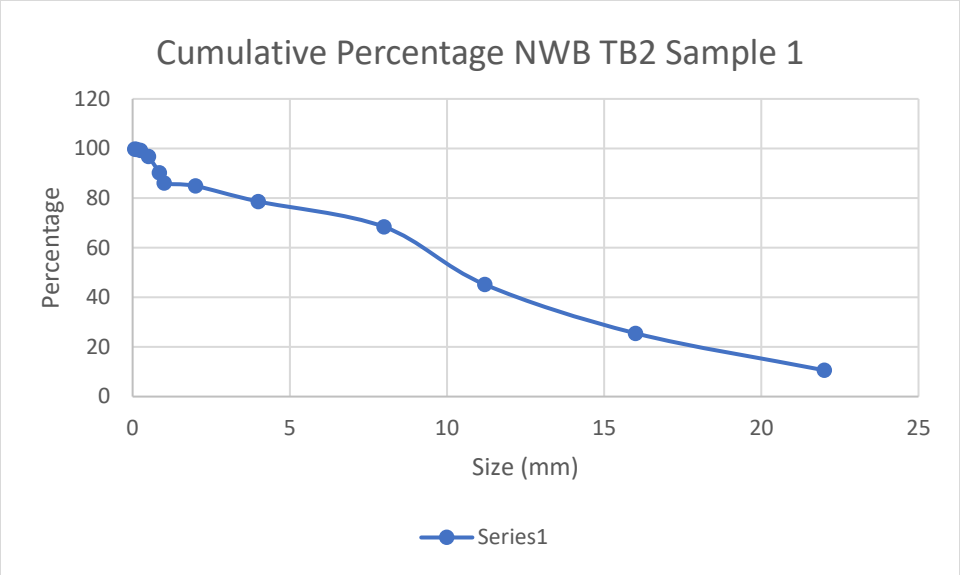

Figure 165: Cumulative Percentage of NWB TB2 Sample 1

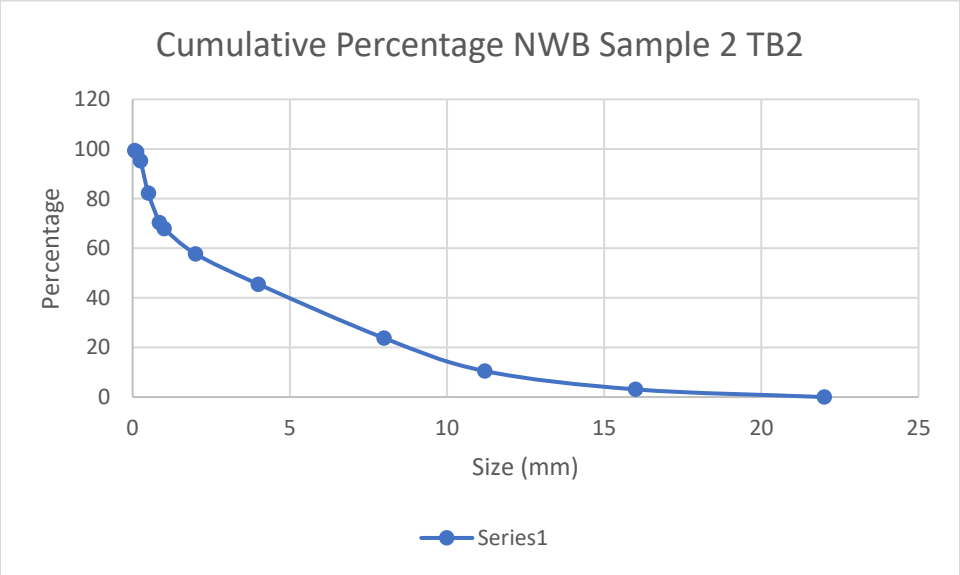

Figure 166: Cumulative Percentage of NWB Sample 2 TB2

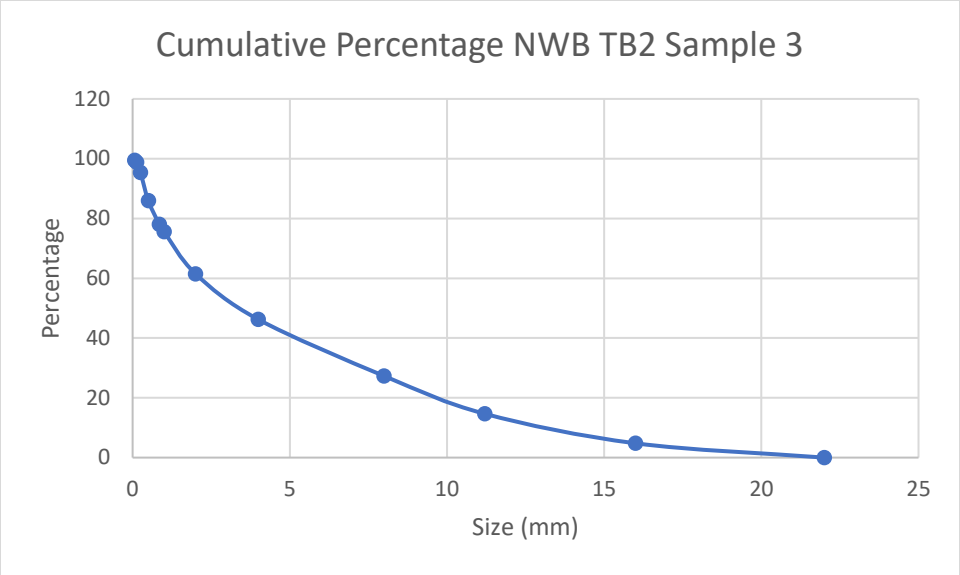

Figure 167: Cumulative Percentage NWB TB2 Sample 3

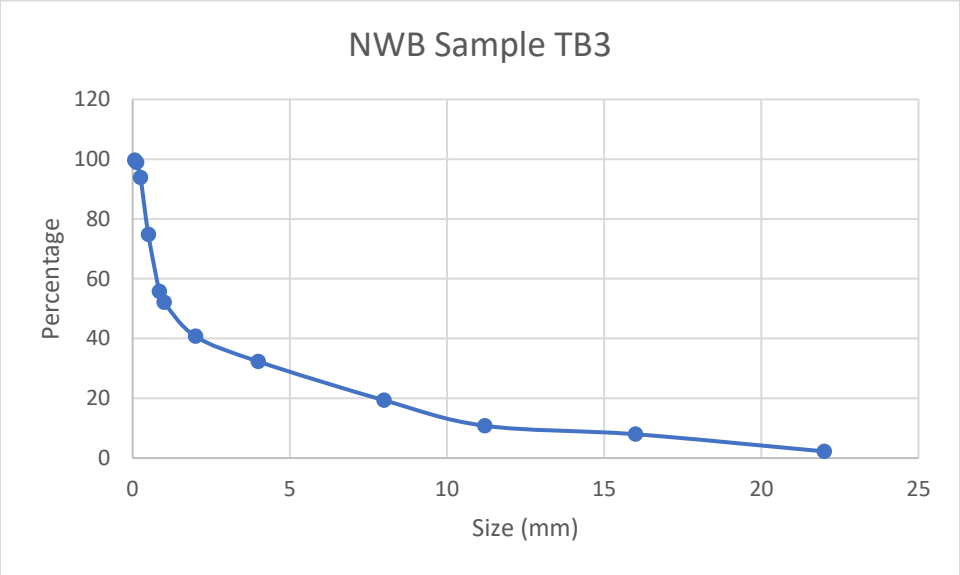

Figure 168: NWB Sample TB3

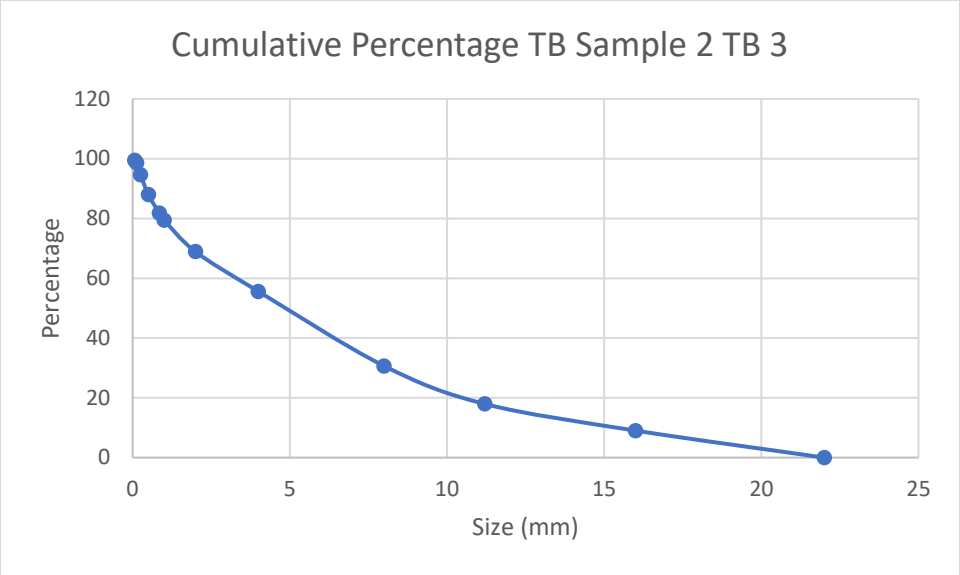

Figure 169: Cumulative Percentage of TB Sample 2 TB 3

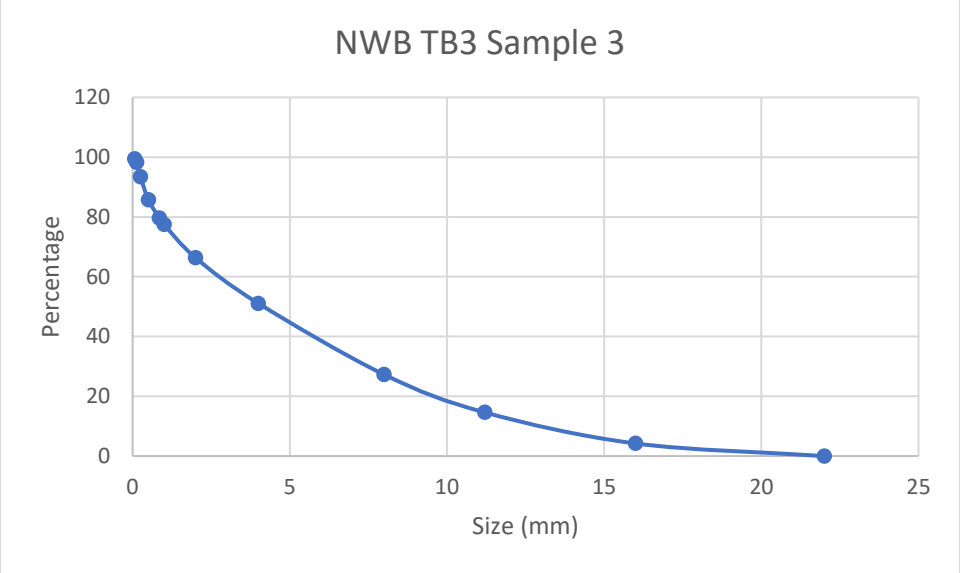

Figure 170: Cumulative Percentage of NWB TB3 Sample 3

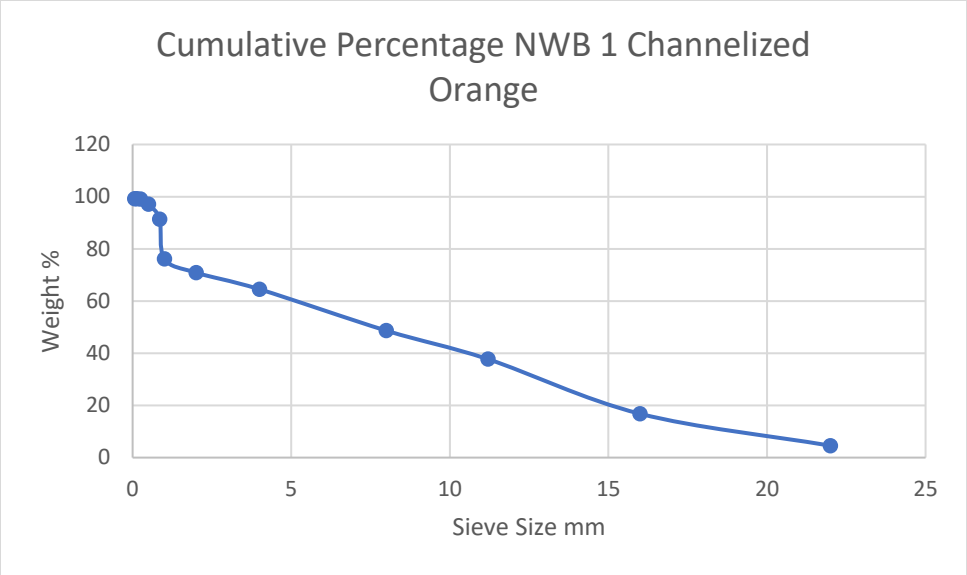

Figure 171: Cumulative Percentage Graph

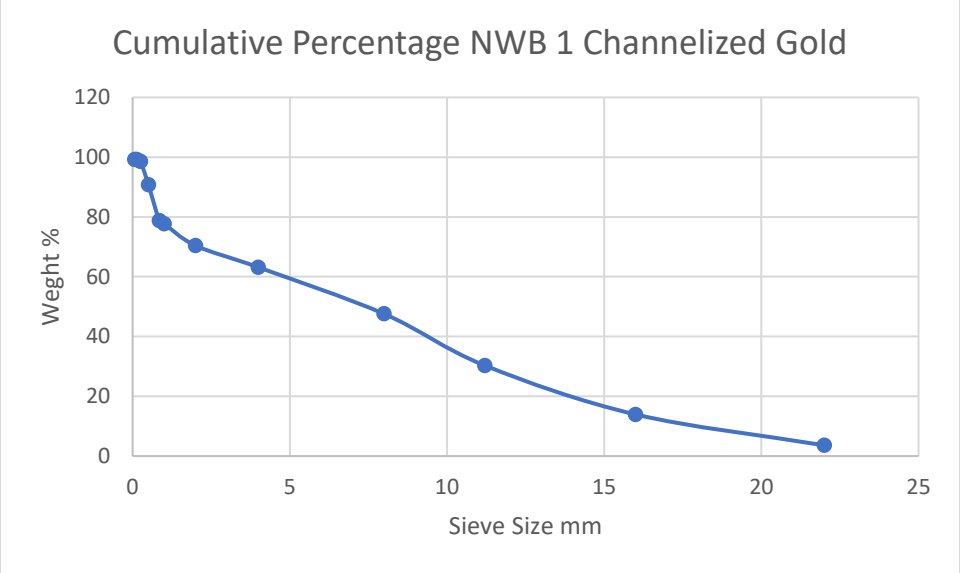

Figure 172: Cumulative Percentage Graph

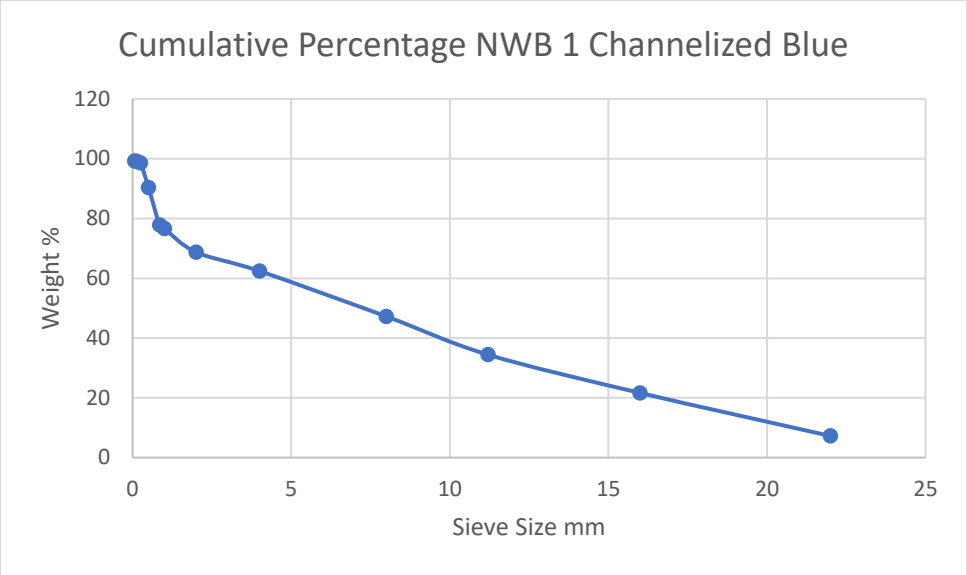

Figure 173: Cumulative Percentage Graph

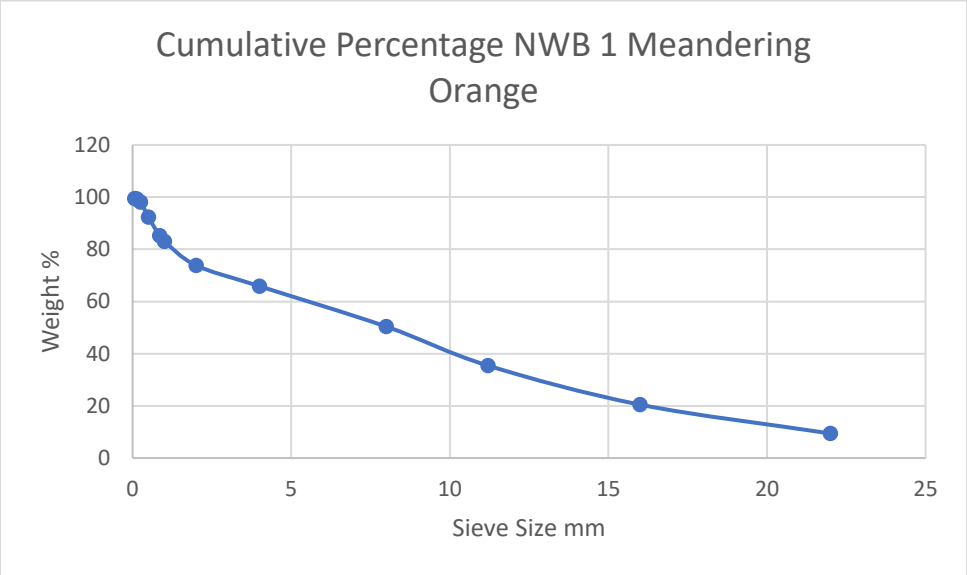

Figure 174: Cumulative Percentage Graph

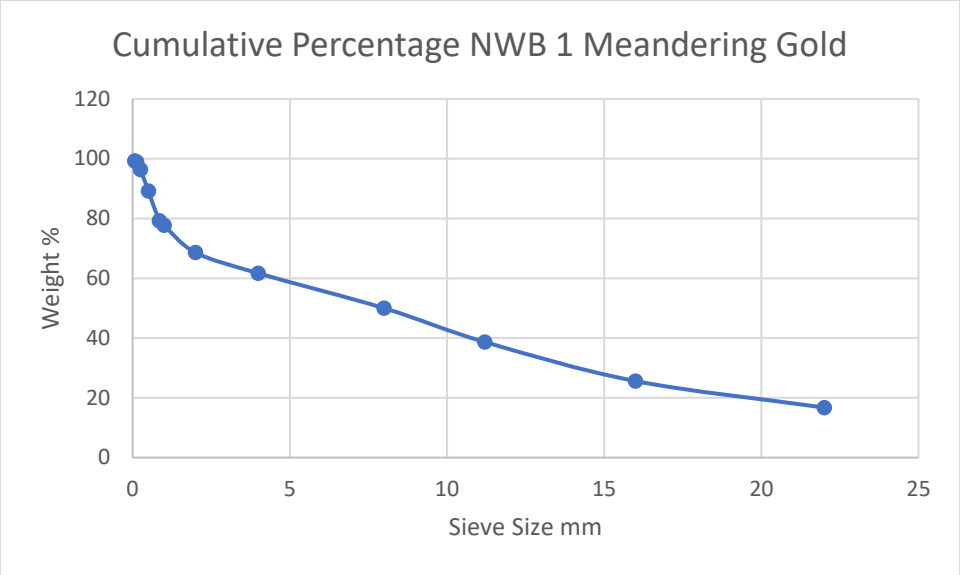

Figure 175: Cumulative Percentage Graph

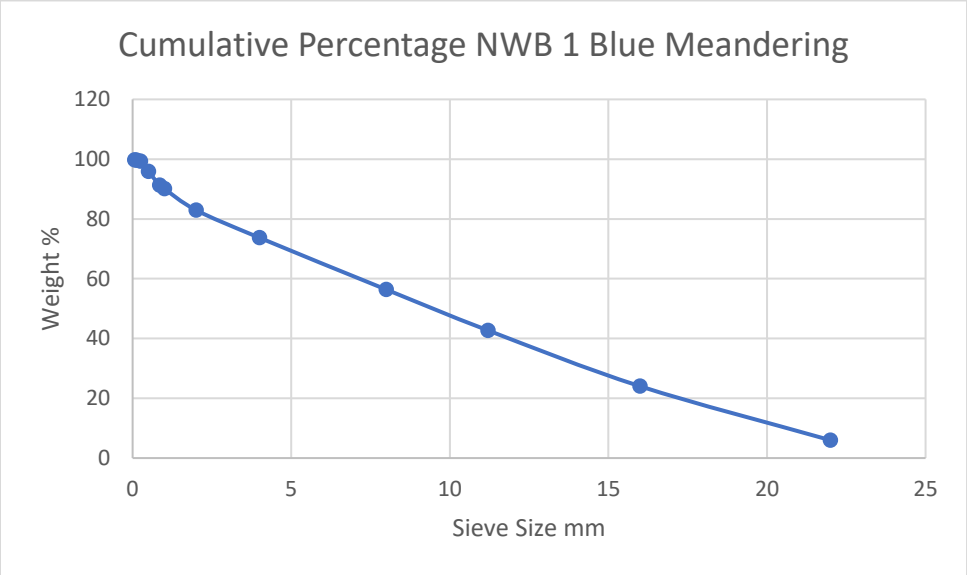

Figure 176: Cumulative Percentage Graph

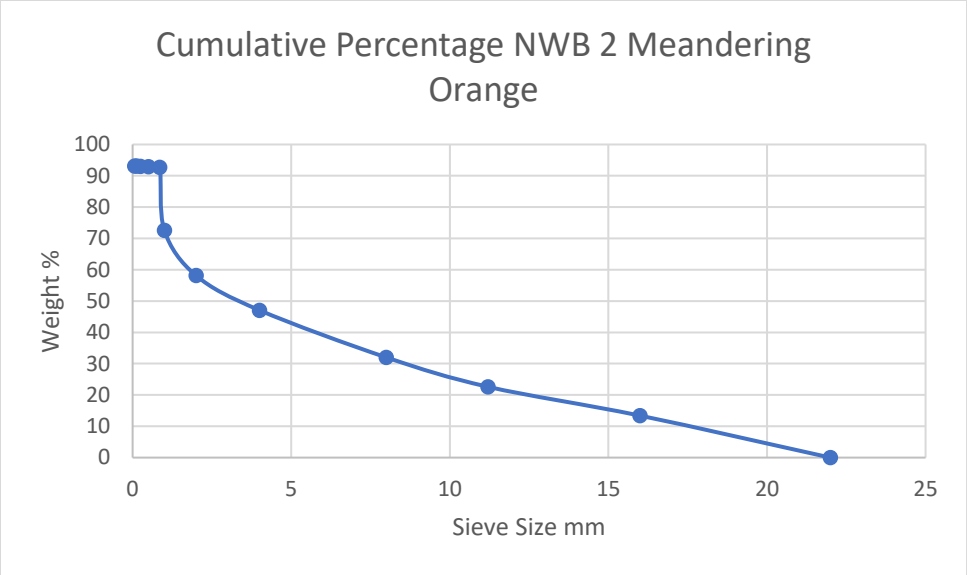

Figure 177: Cumulative Percentage Graph

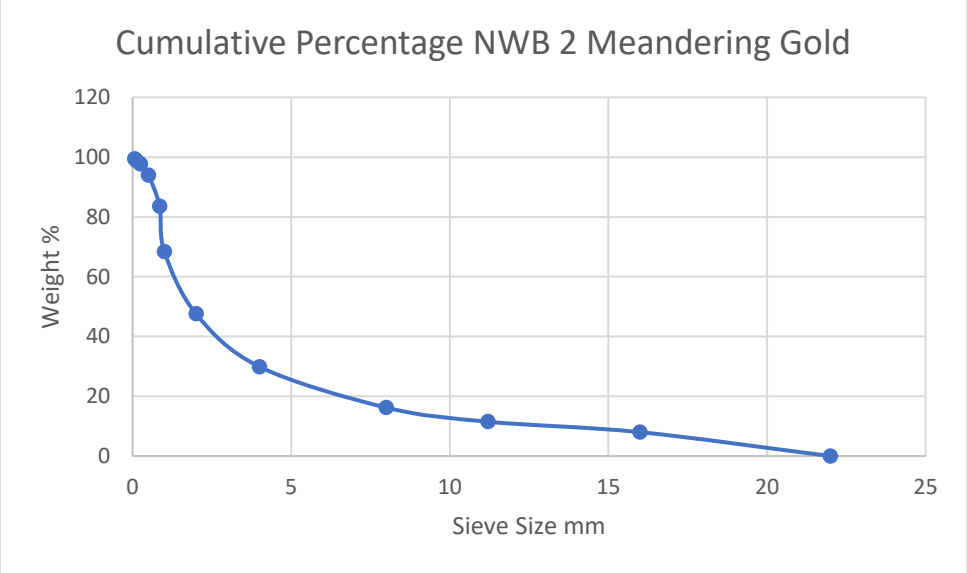

Figure 178: Cumulative Percentage Graph

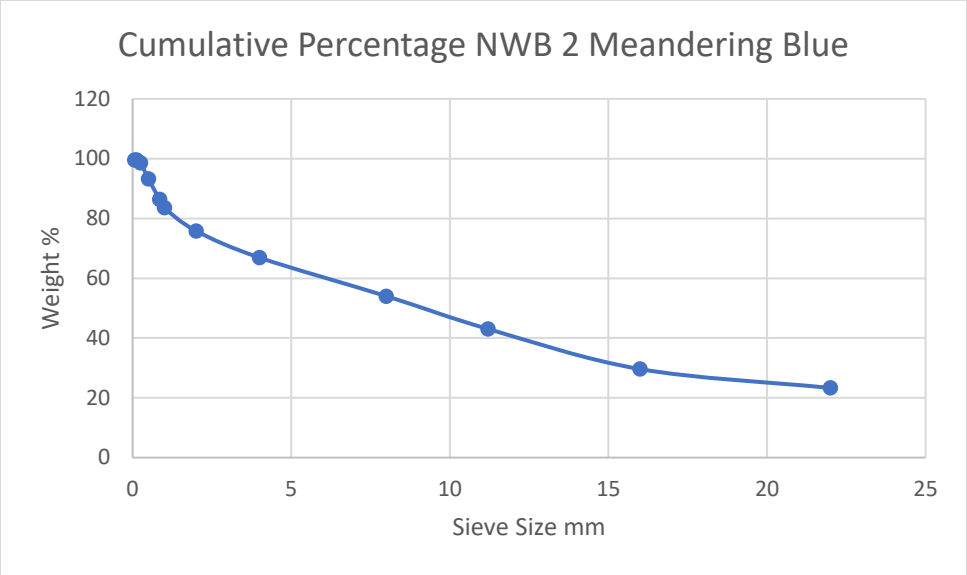

Figure 179: Cumulative Percentage Graph

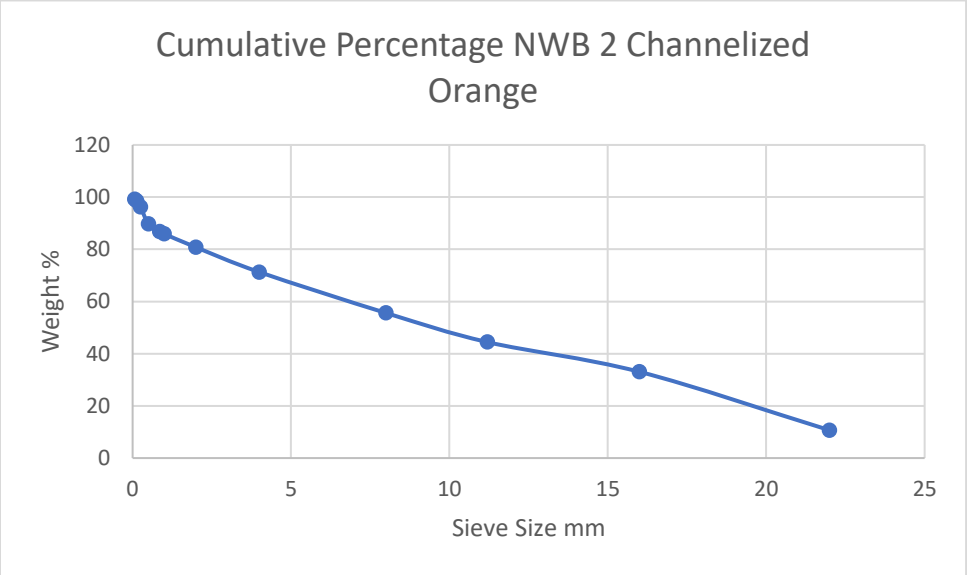

Figure 180: Cumulative Percentage Graph

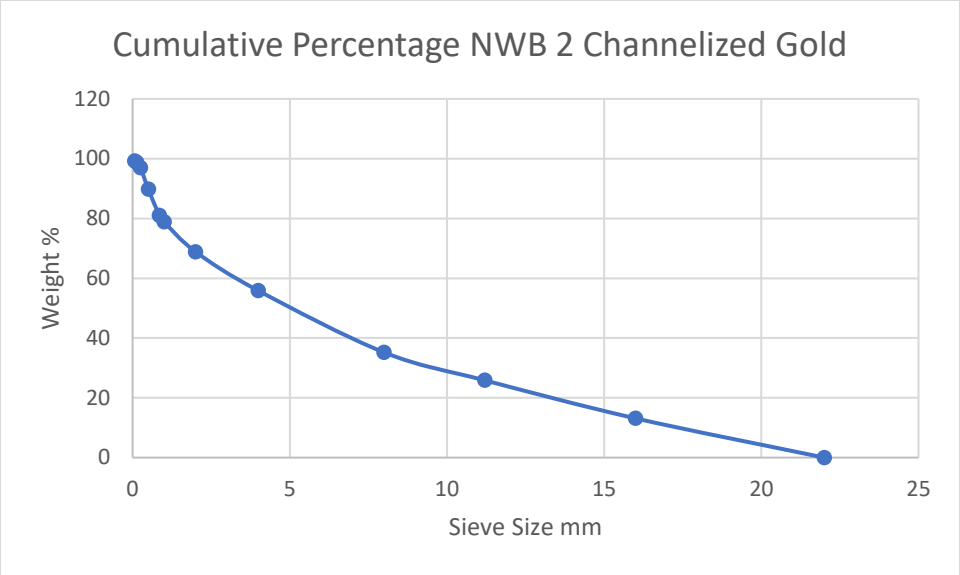

Figure 181: Cumulative Percentage Graph

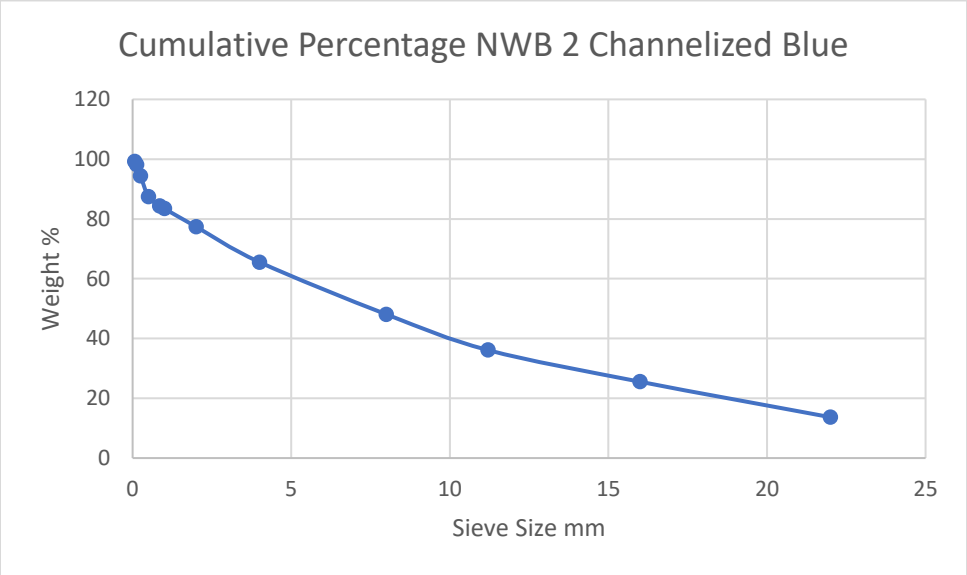

Figure 182: Cumulative Percentage